



International Nuclear Energy Research Initiative

Fiscal Year 2011 Annual Report

I.NERI

Disclaimer

This document was prepared as an account of work sponsored by an agency of the United States Government. Neither the United States Government nor any of its employees makes any warranty, expressed or implied, or assumes any legal liability or responsibility for the accuracy, completeness, or usefulness of any information, apparatus, product, or process disclosed, or represents that its use would not infringe upon privately owned rights. Reference herein to any specific commercial product, process, or service by trade name, trademark, manufacturer, or otherwise, does not necessarily constitute or imply its endorsement, recommendations, or favoring by the United States Government. The views and opinions expressed by the authors herein do not necessarily state or reflect those of the United States Government, and shall not be used for advertising or product endorsement purposes.

Available to DOE, DOE contractors, and the public from the

U.S. Department of Energy
Office of Nuclear Energy
1000 Independence Avenue, S.W.
Washington, D.C. 20585

Foreword

Fiscal year (FY) 2011 marks the ten-year anniversary of the founding of the International Nuclear Energy Research Initiative, or I-NERI. Designed to foster international partnerships that address key issues affecting the future global use of nuclear energy, I-NERI is perhaps even more relevant today than at its establishment. In the face of increasing energy demands coupled with clean energy imperatives, we must clear the hurdles to expanding the role of nuclear power in our energy portfolio. And in an increasingly global society, the importance of international cooperation in these efforts has escalated.

For ten years, I-NERI has been a vehicle for establishing bilateral agreements with our partners in the global nuclear community. These agreements have resulted in collaborative research and development that investigates next-generation nuclear systems and fuel cycles, helping to determine tomorrow's solutions to today's challenges. For ten years, I-NERI has upheld U.S. visibility in the worldwide nuclear community and served as a foundation for mutual cooperation not only in technical advancement but also in enhanced safety and security.

This year we celebrate dual milestones with not only ten successful years but also a grand total of 100 I-NERI collaborative research projects initiated through the program—as well as six new projects that were recently authorized. This annual report provides abstracts of these new projects and findings of projects ongoing or completed in FY 2011. I look forward to another productive decade as U.S. researchers, arm in arm with their international partners, bring nuclear power into the next generation.



Peter B. Lyons
Assistant Secretary, Office of Nuclear Energy
U.S. Department of Energy

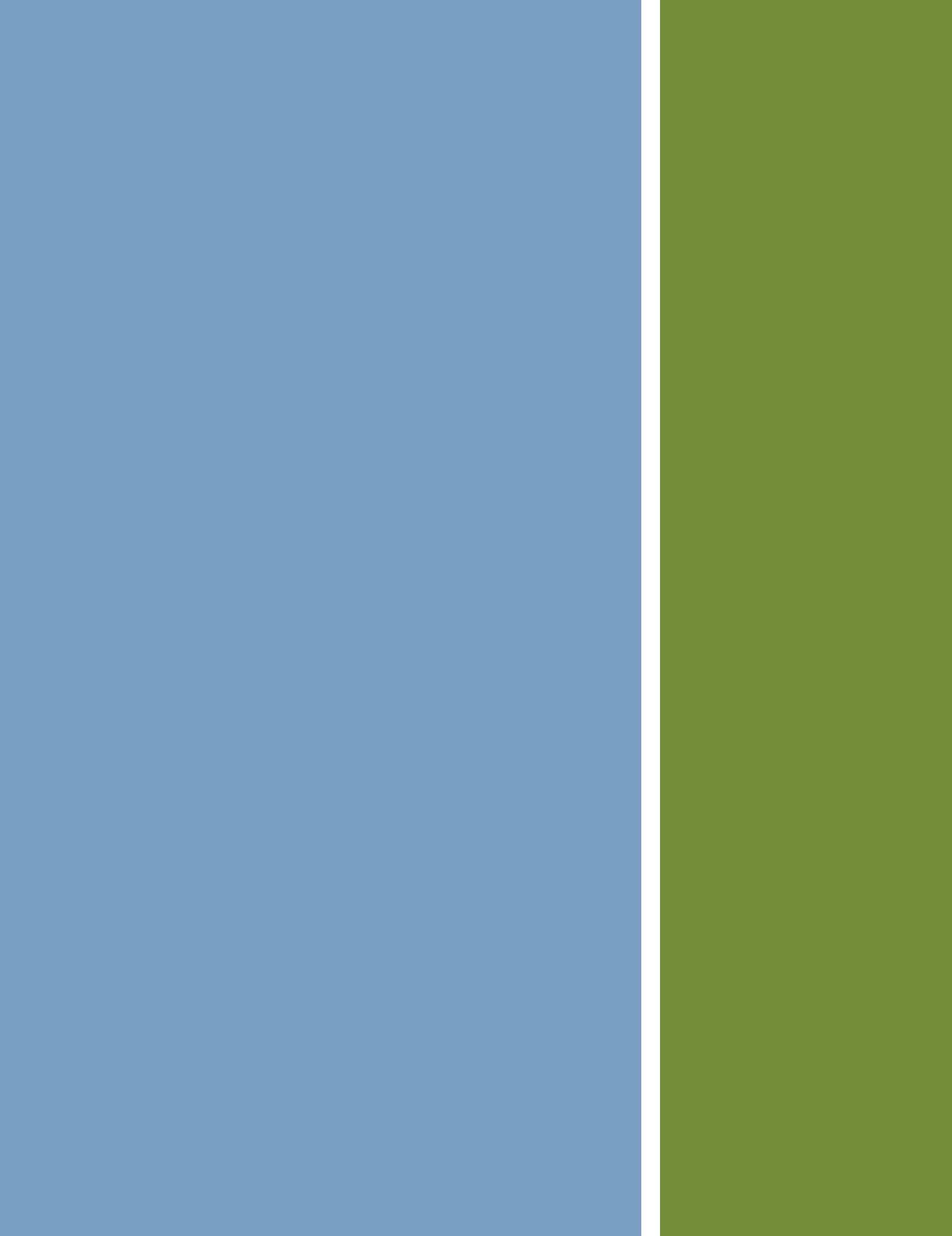


Table of Contents



1. Introduction

1



2. Program Background

5



3. Summary of FY 2011 Accomplishments

17



4. Project Summaries and Abstracts

21



4.1 U.S.-Canada Collaboration

22



4.2 U.S.-European Union Collaboration

26



4.3 U.S.-Republic of Korea Collaboration

48



Appendix I: Acronyms and Initialisms

87



Appendix II: Index of I-NERI Projects

93





1. Introduction

1.1 Overview

The International Nuclear Energy Research Initiative (I-NERI) is a research-oriented collaborative program that supports the advancement of nuclear science and technology in the United States and around the world. I-NERI promotes bilateral scientific and engineering research and development (R&D) with other nations. Innovative research performed under the I-NERI umbrella addresses key issues affecting the future use of nuclear energy and its global deployment. By partnering with international organizations, U.S. researchers gain broader perspectives on issues of global importance and can potentially achieve faster results at reduced cost. A link to the program can be found on the NE website.¹

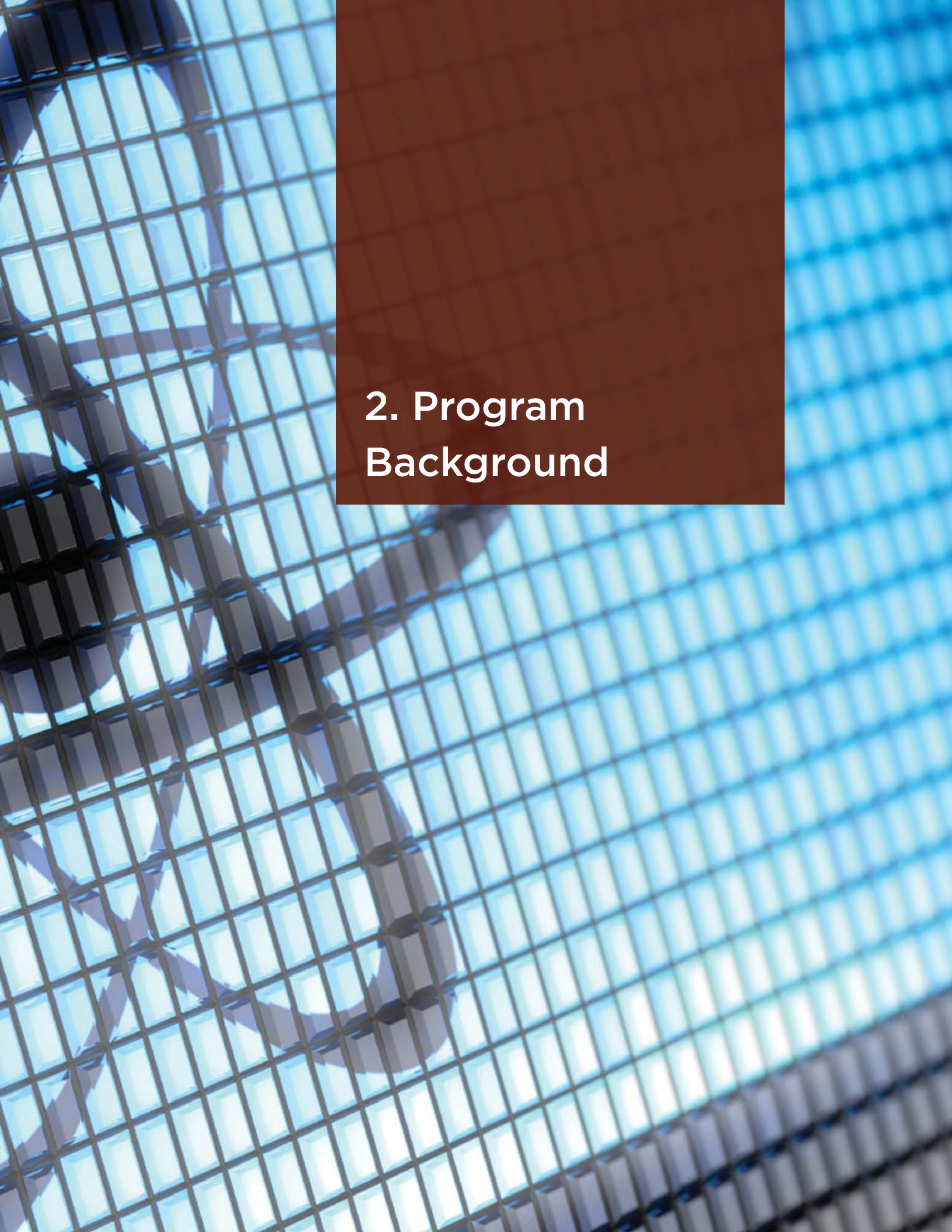
1.2 About This Document

The *I-NERI 2011 Annual Report* provides an update on I-NERI accomplishments achieved during FY 2011, including final activities and findings of completed projects and comprehensive progress summaries of ongoing projects. Following is an overview of each section:

- Section 1 provides an overview of the I-NERI program and this annual report.
- Section 2 goes into greater detail about I-NERI's mission and scope, as well as providing information about program background and the countries and organizations that have participated in the program.
- Section 3 provides a summary of FY 2011 program and project accomplishments.
- Section 4 presents the R&D work scope for current I-NERI collaborative projects between the United States and three partners: Canada, the European Union, and the Republic of Korea. For these partnerships, the report presents summary information for projects that were initiated, ongoing, or completed in FY 2011. Progress summaries of earlier research efforts can be found in previous annual reports, which are accessible through the NE website (see footnote).

¹ <http://www.nuclear.gov/INERI/neINERI1.html>





2. Program Background

2.1 Purpose

The United States is confronting two powerful imperatives that are driving today's resurgence of nuclear power: the escalation of energy demands parallels the increasing urgency to establish a clean energy portfolio to meet these demands. Nuclear power plants presently provide 70 percent of our low-emissions energy supply. However, expanded use of nuclear energy as a power source faces obstacles, such as high costs, proliferation risks, and improved accident resiliency, that require further R&D for resolution. The April 2010 *Nuclear Energy Research and Development Roadmap*² defines four objectives to address existing challenges:

- Develop technologies and other solutions that can improve the reliability, sustain the safety, and extend the life of current reactors.
- Develop improvements in the affordability of new reactors to enable nuclear energy to help meet the Administration's energy security and climate change goals.
- Develop sustainable nuclear fuel cycles.
- Understand and minimize risks of nuclear proliferation and terrorism.

Fortunately, the United States stands with a global nuclear community that shares these challenges. Scientists worldwide are exploring ways to improve today's processes and to discover and implement next-generation methods, ultimately promoting safer and more cost-efficient use of nuclear energy. The United States benefits from collaborations with countries that have mature nuclear systems, while providing useful assistance to those countries with developing technology. As noted in the NE R&D Roadmap: "There is potential to leverage and amplify effective U.S. R&D through collaboration with other nations via multilateral and bilateral agreements."

In an increasingly global society, the importance of international cooperation has escalated beyond the advantages of information sharing. The NE R&D Roadmap also states: "International expansion of the use of nuclear energy raises concerns about the proliferation of nuclear weapons stemming from potential access to special nuclear materials and technologies." Bilateral and multilateral R&D collaborations are key to a common understanding, as well as an integrated approach to nuclear technologies that incorporates their technical development, including safeguards and security technologies and systems, and the maintenance and strengthening of nonproliferation frameworks and protocols.

The International Nuclear Energy Research Initiative (I-NERI), through its bilateral nuclear agreements, promotes targeted cooperative research that is most pertinent to meeting our energy goals. The I-NERI program was established in 2001 with a focus on developing frameworks for international collaboration, along with the associated program planning and project procurement activities. With a mission to sponsor innovative scientific and engineering R&D in cooperation with partnering international countries, the program is designed to foster closer collaboration among international researchers, improve communications, and promote sharing of nuclear research information. The bilateral agreements provide frameworks for these objectives. Cooperative research projects funded through this program further the objectives of NE R&D programs and, ultimately, the NE objectives noted in the 2010 Roadmap.

The program has established the following overall objectives:

- To develop advanced concepts and scientific breakthroughs in nuclear energy and reactor technology in order to address and overcome the principal technical and scientific obstacles to expanding the global use of nuclear energy.
- To promote bilateral and multilateral collaboration with international agencies and research organizations to improve the development of nuclear energy.
- To promote a nuclear science and engineering infrastructure to meet future technical challenges.

Through the I-NERI program, DOE-NE has coordinated wide-ranging scientific discussions among governments, industry, academia, and the worldwide research community regarding the development of advanced reactor concepts and advanced fuel cycles. Figure 1 illustrates key features of the I-NERI program.

² http://www.nuclear.energy.gov/pdfFiles/NuclearEnergy_Roadmap_Final.pdf

VISION

Promote innovative scientific
and engineering R&D through
international cooperation

GOALS/OBJECTIVES

Address potential technical and scientific obstacles
Foster international collaboration to develop nuclear technology
Promote and maintain a nuclear infrastructure

SCOPE OF PROGRAM

Advanced nuclear energy systems

Advanced nuclear fuels/fuel cycles

R&D PRIORITIES

Advanced reactors, systems, and components

Advanced fuels

Alternative energy conversion cycles

Transmutation science and engineering

Design and evaluation methods

Fuel cycle systems analysis

Advanced structural materials

Nuclear hydrogen production

Used nuclear fuel separations, waste forms, and fuel resources technologies

IMPLEMENTATION STRATEGY

Collaborative research efforts

Continuous national laboratory oversight

Program management support

Annual reviews and bilateral meetings

RESULTS

Worldwide partnerships

Innovative technologies

Nuclear infrastructure development

Advances in nuclear engineering

Global nuclear awareness

Leverage of DOE funding

Figure 1. I-NERI program features.

2.2 Research Work Scope

I-NERI project work scopes are jointly developed by the United States and the collaborating country based on terms of the bilateral agreement and current common R&D needs. For the United States, the work scope of I-NERI projects must be directly linked to the scientific and engineering needs of DOE-NE R&D programs. Current I-NERI projects are funded by two principal research programs: Reactor Concepts Research, Development and Demonstration (Reactor Concepts RD&D) and Fuel Cycle Research and Development (FCR&D). This section provides an overview of the work scopes for these NE R&D programs.

Reactor Concepts Research, Demonstration and Development

The mission of the Reactor Concepts RD&D program is to develop new and advanced reactor designs and technologies with broader applicability and improved affordability and competitiveness. RD&D activities address technical, cost, safety, and security challenges associated with the program elements described below.

- **Advanced Reactor Concepts (ARC).** ARC is an expanded version of the Generation IV research program. The program sponsors RD&D that explores advanced reactor technologies and methods that improve the nuclear fuel cycle and nuclear waste management, while offering the potential of reduced capital and operating costs, better performance, enhanced safety, and reduced proliferation risk. Focus areas include advanced thermal and fast neutron spectrum systems.
- **Next Generation Nuclear Plant (NGNP).** The NGNP will demonstrate the technical viability of high-temperature gas-cooled reactor (HTGR) technology for the dual production of hydrogen as a fuel and high-temperature process heat for industrial use. DOE provides support through R&D ranging from fundamental nuclear phenomena to the development of advanced fuels that could improve the economic and safety performance of these advanced reactors.
- **Small Modular Reactor (SMR) Advanced Concepts R&D.** SMRs can potentially improve the affordability of nuclear power with streamlined construction and simplified operation, along with design features that enhance safety and security. The program supports RD&D activities that advance the understanding and demonstration of these innovative reactor technologies and concepts.
- **Light Water Reactor Sustainability (LWRS).** Over the next three decades, most currently operating nuclear power plants will reach the ends of their operating licenses. Even with the expected addition of new nuclear generating capacity, existing reactors must continue operating beyond 60 years to help meet the nation's expanding electricity requirements. This program supports acquiring the scientific understanding needed to develop and demonstrate technologies that support safe and economical long-term operation of existing reactors, as well as new technologies that enhance performance. Extending the life of the current fleet requires fundamental science to predict and measure changes in materials, systems, structures, and components as they age in environments associated with continued long-term operation of existing reactors.
- **Advanced Modeling and Simulation.** Two major initiatives are developing the advanced modeling and simulation that will provide the validated tools necessary to enable fundamental change in how the United States designs and manages its current fleet of nuclear facilities and those yet being developed. The Consortium for Advanced Simulation of Light Water Reactors (CASL) is a DOE-sponsored energy innovation hub that brings together industry, universities, and the national laboratories to create a virtual model with advanced predictive and simulation capabilities for the current generation of reactors. The Nuclear Energy Advanced Modeling and Simulation (NEAMS) program is a longer-term initiative that is developing a suite of integrated codes and cross-cutting numerical tools to support the entire range of NE's nuclear energy R&D.

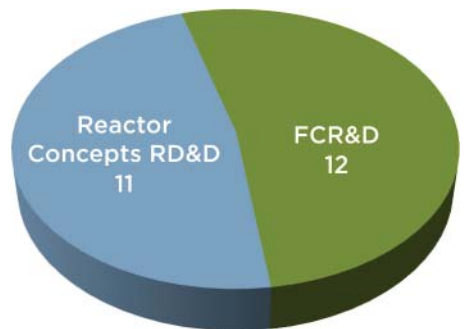


Figure 2. Ongoing projects by program area.

Fuel Cycle Research and Development

One of the four NE R&D objectives delineated in the FY 2010 *Nuclear Energy Research and Development Roadmap* is achievement of sustainable fuel cycle options, defined as those that improve uranium resource utilization, maximize energy generation, minimize waste generation, improve safety, and limit proliferation risk. Through a long-term science-based approach, the FCR&D program will develop a suite of technology options that will enable informed decisions about the management of nuclear waste and used reactor fuel. The program supports Roadmap objectives regarding current reactors, new reactors, and minimized nuclear proliferation and terrorism risks.

Today's nuclear power plants run on a once-through fuel cycle, which utilizes only about five percent of the fuel's energy potential before the used fuel is placed in intermediate-term storage or discarded as waste. Advanced fuel cycles, fuels and processing techniques may allow more energy to be drawn from the same amount of nuclear material, while reducing the quantity of long-lived radiotoxic elements in the used fuel. Fuels R&D aims to increase the efficient use of uranium resources, reduce the amount of used fuel requiring direct disposal, and evaluate the inclusion of non-uranium materials to reduce the long-lived radiotoxic elements in used fuel. The FCR&D program ultimately seeks to develop a cost-effective sustainable closed fuel cycle that eliminates much of the high-level waste, reclaiming the energy from used fuel by recycling the long-lived actinide elements. In a full recycle system, only waste products require disposal, not used fuel. The program is applying a methodical systems engineering analysis approach to identify suitable technologies.

FCR&D has five campaigns addressing different program elements that support the overall objectives of sustainable fuel cycle options.

- **Fuel Cycle Options.** This campaign is developing and managing the processes to guide selection of one or more sustainable alternative fuel cycle options and prioritizing associated R&D. Researchers perform integrated fuel cycle analyses and technical assessments and provide information that can be used to inform NE's fuel cycle R&D activities and strategies. The campaign is studying options for once-through, modified recycle and full recycle systems, looking at all stages from mining to disposal. Research under this initiative also supports the sodium-cooled fast reactor (SFR), whose design is geared toward improved management of high-level wastes, specifically actinides.
- **Advanced Fuels.** NE is supporting R&D for various fuel forms, including cladding, needed to implement those fuel cycle options. For any given fuel type, fuel qualification requires engineering-scale demonstration of the fabrication processes and irradiation of lead-test assemblies to demonstrate in-pile performance. NE is working toward developing a state-of-the art R&D infrastructure to support a goal-oriented science-based approach. The campaign is investigating both transmutation fuels, which have potential for enhanced resource utilization and proliferation resistance, and next-generation LWR fuels that exhibit enhanced performance and safety and reduced waste generation.
- **Separations, Waste Forms, and Fuel Resources.** Features of a sustainable fuel cycle include reduced processing, waste generation, and proliferation risk. NE is working toward next-generation fuel cycle separation and waste management technologies that enable these improvements. Research scope includes developing and demonstrating technologies that separate transuranic elements and fission products from used nuclear fuel and developing advanced waste forms, as well as investigating cutting-edge alternatives that could widen fuel cycle options.
- **Used Fuel Disposition.** This program aims to provide a sound technical basis for a new national policy to manage the back end of the nuclear fuel cycle, including identification and evaluation of safe and secure options for storage, transportation, and permanent disposal of radioactive wastes resulting from existing and future fuel cycles. Objectives range from identifying and addressing gaps in existing data and methodologies to using advanced modeling tools to study potential disposal system concepts and environments; research scope ranges from interim storage to final disposal. International activities are a cornerstone of these efforts and include participation in international working groups addressing relevant challenges, support for bilateral interactions between the United States and the Republic of Korea and the United States and Japan, and planning for U.S. involvement in disposal R&D in European underground research laboratories (URLs).
- **Material Protection, Accounting, and Control Technologies.** As nuclear systems grow more complex and their use becomes more widespread, NE aims to enhance safety and security while minimizing proliferation risk. This program supports efforts to develop innovative technologies and analysis tools to enable next-generation nuclear materials management for future U.S. nuclear fuel cycles, significantly advancing the state of the art in accounting and control. NE is also supporting the necessary research to integrate safeguards and security into the earliest stages of the design cycle.

Accomplishments

Past I-NERI project teams have contributed to the knowledge base that has formed the scope of both programs. In support of reactor concepts, completed I-NERI projects have investigated such topics as next-generation materials (e.g., nano-composited and oxide dispersion-strengthened steels, silicon carbide composites, and zirconium alloys); energy conversion through the Brayton cycle; advanced sensors, instrumentation, and controls; hydrogen production through thermochemical reactions and high-temperature electrolysis; production viability and efficiency; safety issues and proliferation risk reduction; and analysis of distribution and storage methods. In addition, some of the first I-NERI project teams utilized modeling and simulation tools; and roughly half the current projects explicitly state within their objectives the use, qualification, and/or improvement of such tools. Sample research topics investigating fuels and fuel cycles include advanced transmutation fuels, inert matrix fuels, waste forms, separation of fission products from nuclear waste, and advanced head-end processes that condition used fuel.

2.3 International Agreements

In order to initiate an international collaboration, a government-to-government agreement must first be in place. I-NERI bilateral agreements serve as the vehicles to conduct joint R&D under the various DOE programs, enabling U.S. researchers to establish collaborative projects with their international colleagues that support development of next-generation nuclear energy systems and fuel cycle technologies.

To date, DOE has implemented agreements with six countries and two international organizations. Brief descriptions of and links to these agreements can be found on the I-NERI website.³ The agreements were signed by DOE and the international partners noted in the table below. The table also presents the number of projects undertaken to date with each partner.

The United States also collaborates with the international community via the Generation IV International Forum (GIF), the International Atomic Energy Agency (IAEA), and the International Framework for Nuclear Energy Cooperation (IFNEC). Please visit their websites for more information.⁴

Table 1. I-NERI international partners and number of projects awarded.

Collaborator	Organization	Total
Brazil	Ministério da Ciência e Tecnologia (MST)	2
Canada	Department of Natural Resources Canada (NRCan) and Atomic Energy of Canada Limited (AECL)	12
The European Union	European Atomic Energy Community (Euratom)	22
France	Commissariat à l'énergie atomique (CEA)	21
Japan	Agency of Natural Resources and Energy (ANRE) and the Ministry of Education, Culture, Sports, Science, and Technology (MEXT)	2
The Republic of Korea	Ministry of Education, Science and Technology (MEST) ⁵	46
The Organization for Economic Cooperation and Development (OECD)	The Nuclear Energy Agency (NEA) of OECD	1
The Republic of South Africa	The Government of the Republic of South Africa	
Total		106

3 http://www.nuclear.gov/I-NERI/neINERI_bilateralcollaborations.html

4 <http://www.gen-4.org>, <http://www.iaea.org/>, and <http://www.ifnec.org/>

5 Signatory agency was the Ministry of Science and Technology (MOST), superseded by MEST in March 2008.

2.4 Funding

I-NERI is an important vehicle for enabling international R&D in nuclear technology on a leveraged, cost-shared basis. Each country in an I-NERI collaboration provides funding for its respective project participants; funding provided by the United States may be spent only by U.S. organizations. The United States funds I-NERI projects through its national laboratories, with the annual contribution based upon current-year budgets for DOE-NE R&D programs. I-NERI projects typically last three years, although budgeting protocols require the U.S. portion to be funded annually. While actual cost-share amounts are determined jointly for each selected project, the program's goal is to achieve approximately 50–50 matching contributions from each partnering country. This section provides approximate domestic and international funding numbers for FY 2011 and the I-NERI program to date.

In FY 2011, the United States provided \$5.89 million to support I-NERI projects: \$4.47 million toward ongoing projects and \$1.42 million to launch new projects. International funding for FY 2011 was \$3.34 million toward ongoing projects and \$1.81 million for Year 1 of FY 2011 projects, for a total of \$5.15 million.

The total pledge for FY 2011 projects (i.e., the three-year sum) is \$9.79 million. The United States has committed just over \$4.25 million. The Republic of Korea will provide \$.5.46 million to fund five new U.S.-ROK projects, and Euratom's commitment is \$80 thousand for a single new U.S.–Euratom collaboration.

To date, I-NERI sponsors have committed a total R&D investment of \$250.1 million: \$133.8 million contributed by the United States and \$116.3 million by international collaborators (see Figure 3).

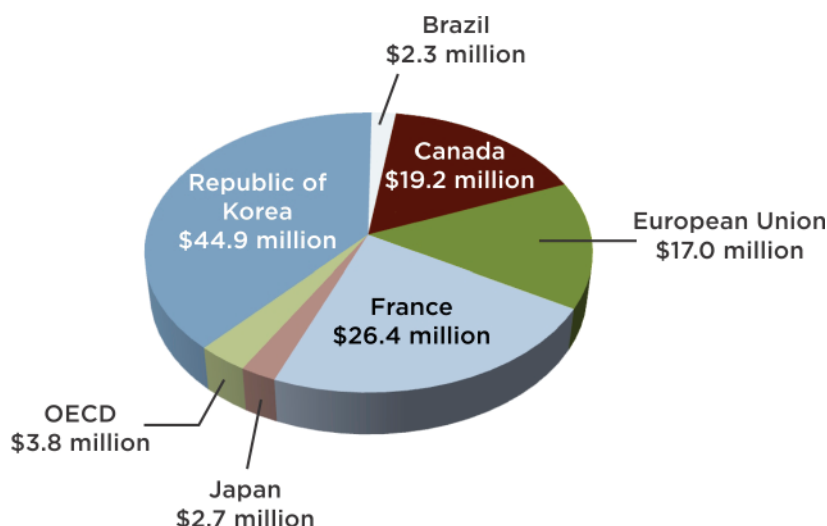
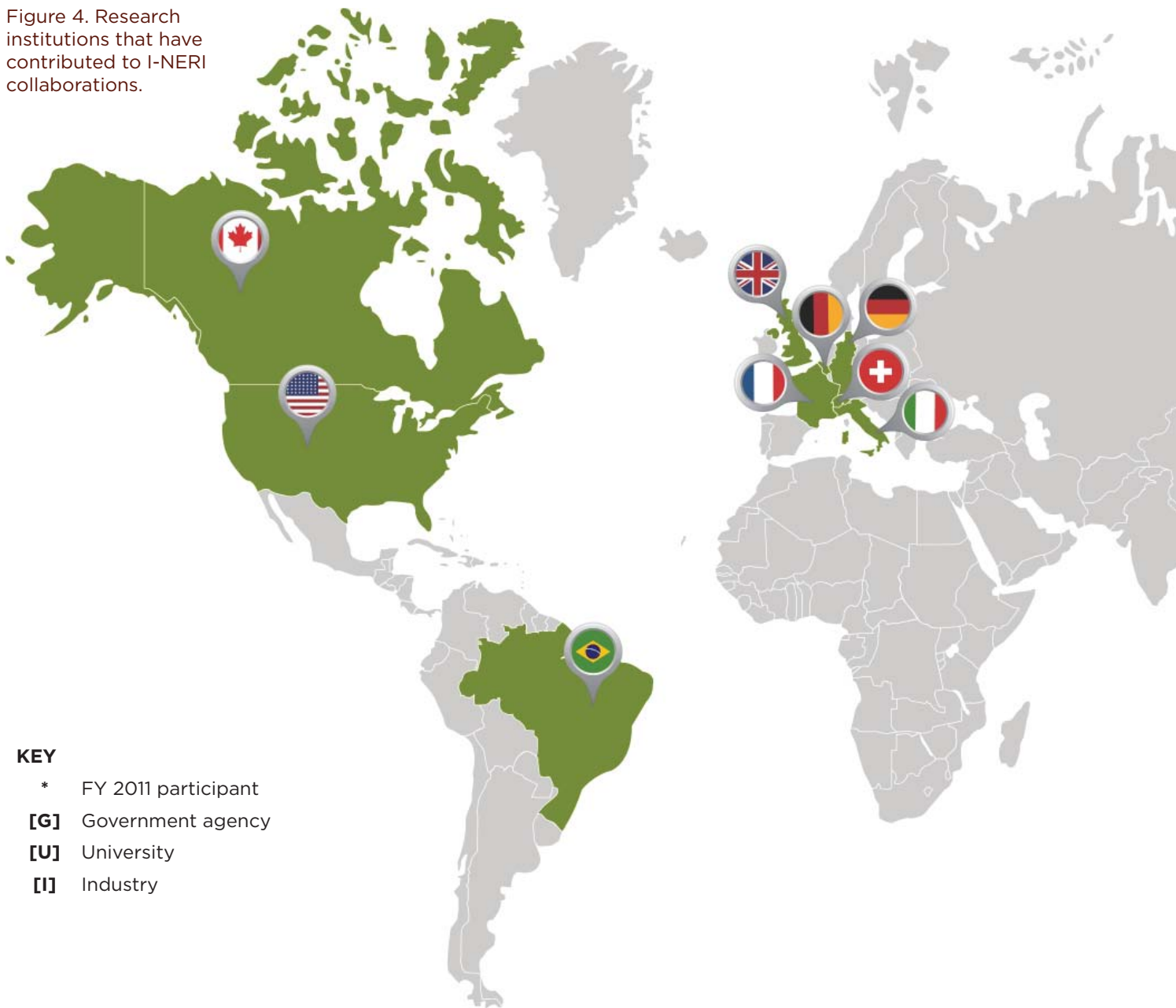


Figure 3. Breakdown of funding since I-NERI's inception by international collaborator (numbers are approximate).

2.5 Program Participants

I-NERI encourages global sharing of resources. The program crosses both institutional and geographical boundaries, soliciting projects from international proposal teams that comprise participants from universities, industry, and government organizations, including federal laboratories. Collaborative efforts between the public and private sectors in both the United States and partnering international entities have resulted in significant scientific and technological enhancements in the global nuclear power arena. I-NERI collaborative projects produce findings that would take the United States alone far more time and money to accomplish. The international infrastructure also brings multiple perspectives and priorities together to address shared obstacles. Figure 4 (on the next page) shows the broad spectrum of participants in the I-NERI program since its inception; asterisks indicate participants in ongoing projects.

Figure 4. Research institutions that have contributed to I-NERI collaborations.



National Laboratories and Government Organizations

Argonne National Laboratory (ANL) *
Brookhaven National Laboratory (BNL)
Idaho National Laboratory (INL) *
Lawrence Livermore National Laboratory (LLNL)
Los Alamos National Laboratory (LANL) *
National Institute of Standards and Technology (NIST) *
Oak Ridge National Laboratory (ORNL) *
Pacific Northwest National Laboratory (PNNL) *
Sandia National Laboratories (SNL) *

Industry

Gas Technology Institute
General Atomics
Ultra Safe Nuclear Corporation, Inc. *
Westinghouse Electric

Universities

Colorado School of Mines *
Idaho State University *
Iowa State University
Massachusetts Institute of Technology
Ohio University *
The Ohio State University
Pennsylvania State University
Purdue University

Rensselaer Polytechnic Institute
Texas A&M University *
University of California–Berkeley *
University of California–Santa Barbara
University of Florida
University of Idaho *
University of Illinois–Chicago
University of Maryland
University of Michigan *
University of Nevada–Las Vegas
University of Notre Dame
University of North Texas *
University of Tennessee *
University of Wisconsin *
Utah State University



Brazil

Eletronuclear [I]
Instituto de Pesquisas Energéticas e Nucleares (IPEN) [G]
Ministério da Ciência e Tecnologia (MST) [G]



Canada

Atomic Energy of Canada Limited (AECL) *[I]
Chalk River Laboratories (CRL) *[G]
CanmetENERGY [G]
Ecole Polytechnique de Montréal [U]
Gamma Engineering [I]
Université Bordeaux [U]
Université de Sherbrooke [U]
University of Manchester [U]
University of Manitoba [U]



Republic of Korea

Cheju National University [U]
Chosun University [U]
Chungnam National University *[U]
Hanyang University [U]
Korea Advanced Institute of Science and Technology (KAIST) *[G]
Korea Atomic Energy Research Institute (KAERI) *[G]
Korea Electric Power Research Institute (KEPRI) [G]
Korea Hydro and Nuclear Power Company (KHNP) [I]
Korea Maritime University [U]
Kyung-Hee University *[U]
Pusan National University [U]
Seoul National University *[U]
Ulsan National Institute of Science and Technology *[U]



Italy

Ente per le Nuove Tecnologie, l'Energia e l'Ambiente (ENEA) [G]
Società Informazioni ed Esperienze Termoidrauliche (SIET) [I]



Belgium

Joint Research Centre–Institute for Energy (JRC-IE) *[G]
Joint Research Centre–Institute for Reference Materials and Measurements (JRC-IRMM) *[G]

Joint Research Centre–Institute for Transuranium Elements (JRC-ITU) *[G]

SCK•CEN (Belgian Nuclear Research Centre) *[G]



France

Commissariat à l'énergie atomique (CEA) *[G]
Électricité de France (EDF) [G]
Framatome ANP [I]

Laboratoire des Composites Thermostructuraux (LCTS) [G]

Organisation for Economic Co-operation and Development–Nuclear Energy Agency (OECD/NEA) [G]



Japan

Hitachi, LTD [I]
Hitachi Works [I]
Japan Atomic Energy Agency (JAEA) [G]

Japan Atomic Energy Research Institute (JAERI) [G]

Tohoku University [U]

Toshiba Corporation [I]

University of Tokyo [U]



UK

University of Ontario Institute of Technology [U]



Germany

Karlsruhe Institute of Technology *[U]



Switzerland

Paul Scherrer Institute (PSI) *[G]

Student Participation

One benefit of the I-NERI program is development of nuclear-related educational research opportunities. Encouraging young academics to participate in nuclear R&D promotes the nuclear science and engineering infrastructure, both in the United States and abroad. Support from the I-NERI program helps educational institutions remain at the forefront of science education and research, advance the important work of existing nuclear R&D programs, and create training for the next generation of nuclear scientists and engineers—those who will resolve future technical challenges. In FY 2011, ten U.S. and five foreign academic institutions participated in I-NERI research projects.

As shown in Figure 5, approximately 27 U.S. students and 34 students from partner countries worked on active I-NERI research projects.

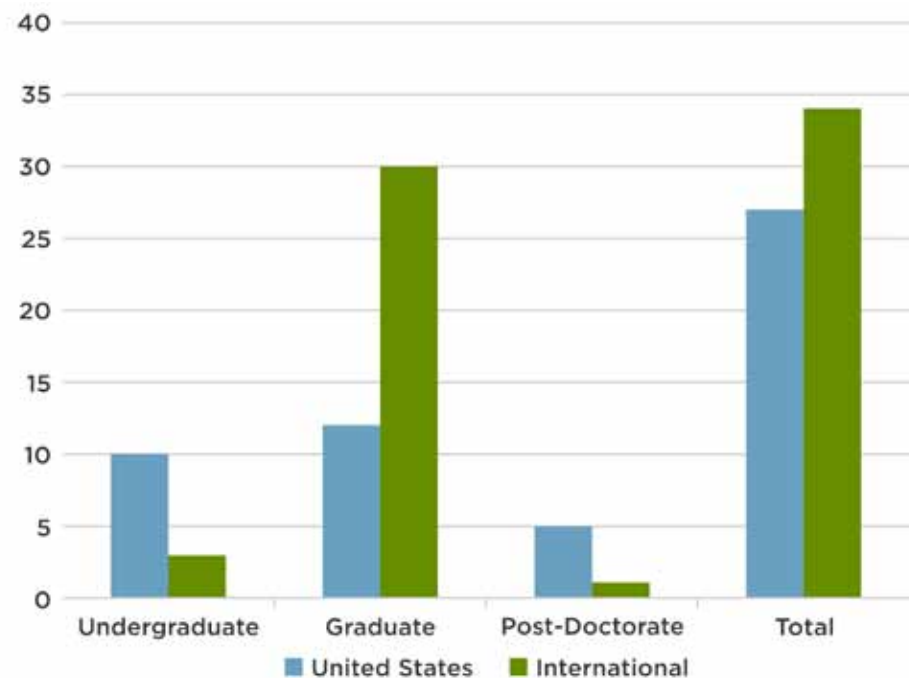


Figure 5. I-NERI student participation broken down by degree level (numbers are approximate).

UNIV



**3. Summary
of FY 2011
Accomplishments**

3.1 Research Activities

Since the program's inception, 106 projects have been awarded, 73 of which have been completed to date. Both the number of awards and the consistency of project achievement demonstrate I-NERI's success in fostering international collaboration. The following sections provide an overview of ongoing and recently completed research in each of the two program areas. This year marked the completion of five I-NERI research projects, four from ROK and the other from Canada:

- Upgrading of the Athabasca Oil Sands for the Production of Diesel and Gasoline (Reactor Concepts RD&D, 2008-001-C)
- Advanced Multi-Physics Simulation Capability for Very High-Temperature Gas-Cooled Reactors (Reactor Concepts RD&D, 2008-001-K)
- Experimental and Analytic Study on the Core Bypass Flow in a Very High-Temperature Reactor (Reactor Concepts RD&D, 2008-002-K)
- Development and Characterization of New High-Level Waste Forms for Achieving Waste Minimization from Pyroprocessing (FCR&D, 2007-004-K)
- Nuclear Data Uncertainty Analyses to Support Advanced Fuel Cycle Development (FCR&D, 2008-003-K)

Reactor Concepts RD&D

Three of these completed projects fell under the Reactor Concepts RD&D work scope. The U.S.-Canada collaboration is part of a longer-term effort to examine the feasibility of an integrated complex consisting of a nuclear reactor and electrolytic hydrogen plant providing process steam for a bitumen upgrader, along with electricity. This work expands on research at Idaho National Laboratory to develop solid oxide electrolysis cells suitable for long-term commercial operation, as well as on work on splitting water and carbon dioxide to produce synthesis gas (syngas). Two of the completed U.S.–ROK projects worked with advanced modeling tools to study thermofluid behavior of prismatic very high-temperature gas-cooled reactors (VHTRs). One project developed a suite of advanced multi-physics simulation methods and codes to analyze VHTR coupled neutronics and thermofluid behavior; the other collaboration successfully identified and tested measures to reduce core bypass flow.

A continuing Reactor Concepts RD&D project is contributing to future modeling efforts by archiving, analyzing and exchanging data, and using the data to generate models that will better validate advanced computational methods and design analysis methods. This team also plans to develop models to study the physics of a transuranic (TRU) burner reactor. To date, the U.S. team has compiled and analyzed the Zero Power Plutonium Reactor (ZPPR)-15A physics experiment database and has generated detailed as-built Monte Carlo models for six of the twelve planned configurations of ZPPR-15B experiments. The ROK team is conducting similar work on data from the BFS-75-1 critical experiment that was conducted at the Institute of Physics and Power Engineering (IPPE) in Russia. Another project aims to produce new and essential experimental data on fission fragment mass distributions and prompt neutron emission as a function of incident neutron energy for major and minor actinides. In FY 2011, the project team measured prompt fission neutron spectra from uranium-235 and plutonium-239 for a range of incident neutron energies and measured fission fragment mass yields from uranium-238 as a function of incident neutron energy.

Advanced materials are being investigated by two other ongoing Reactor Concepts RD&D project teams: one is increasing radiation tolerance in candidate alloys through optimization of grain size and grain boundary characteristics, and the other is investigating the effects of aging on the microstructure and stress–corrosion cracking behavior of dissimilar-metal welds. In addition, one project team is addressing interoperability of materials test databases—which currently differ in format and associated semantics—to facilitate data exchange between research partners. This U.S.–Euratom project is reviewing databases from the respective countries, and the review thus far suggests that the databases share many commonalities—a promising result for next steps.

FCR&D

Two projects completed in FY 2011 were supported through the FCR&D program. One provided improved neutron cross-section data for isotopes important for advanced fuel cycle and nuclear safeguards applications, such as neptunium-237 and plutonium-240, as

well as assessing uncertainties that slight errors in cross-section data would create in the nuclear integral parameters. These efforts will contribute to system design optimization that could improve safety validation and reduce capital costs. The other project developed and characterized three high-level waste forms, increasing the available options for waste management associated with the electrochemical and pyro-metallurgical processing of used nuclear fuel.

Two ongoing FCR&D projects are also contributing to improved waste management. One project seeks to optimize electrochemical technology methods for recovery of zirconium from used nuclear fuel. The project team has performed a literature review of the properties of zirconium and its chloride salts, designed and set up an experiment to determine parameters important to the electrochemical recovery of zirconium in a molten eutectic salt, and has begun developing an electrorefining model. The other project team is improving both prompt fission neutron multiplicity and neutron spectral data and, in FY 2011, identified the neutron detectors that will be used to verify the (n,p) angular distribution and to measure the neutron spectra.

Two other projects are investigating fuel fabrication processes: one is advancing fabrication and performance of particle fuel and targets, and the other is enhancing the metallic fuel fabrication process for sodium-cooled fast reactors to minimize fuel losses and reduce waste streams. A third project is focused on gaining a more fundamental understanding of fuel–cladding chemical interaction phenomena for metallic fuels using new tools that can extend existing scientific and technological knowledge.

Materials for advanced fuel cycles and reactor systems are being studied by two FCR&D projects. One team is investigating irradiation and corrosion effects in materials used for innovative reactor systems. In FY 2011, the team produced a heat of an advanced oxide dispersion-strengthened alloy that shows excellent mechanical properties in initial testing. Another has designed, processed and begun to characterize two alloys in an effort to develop a nanoparticle-strengthened dual-phase composite material with high fracture toughness for application to high-performance reactor core structures. In addition, this project aims to produce a material characterization database, which will support future high-temperature applications and materials development.

Section 4 provides detailed summaries of each of these projects.

3.2 Program Activities

I-NERI accomplishments in FY 2011 include the initiation of six new projects: five with the Republic of Korea and one with Euratom. These projects were identified for final selection during annual project performance reviews and bilateral program planning meetings.

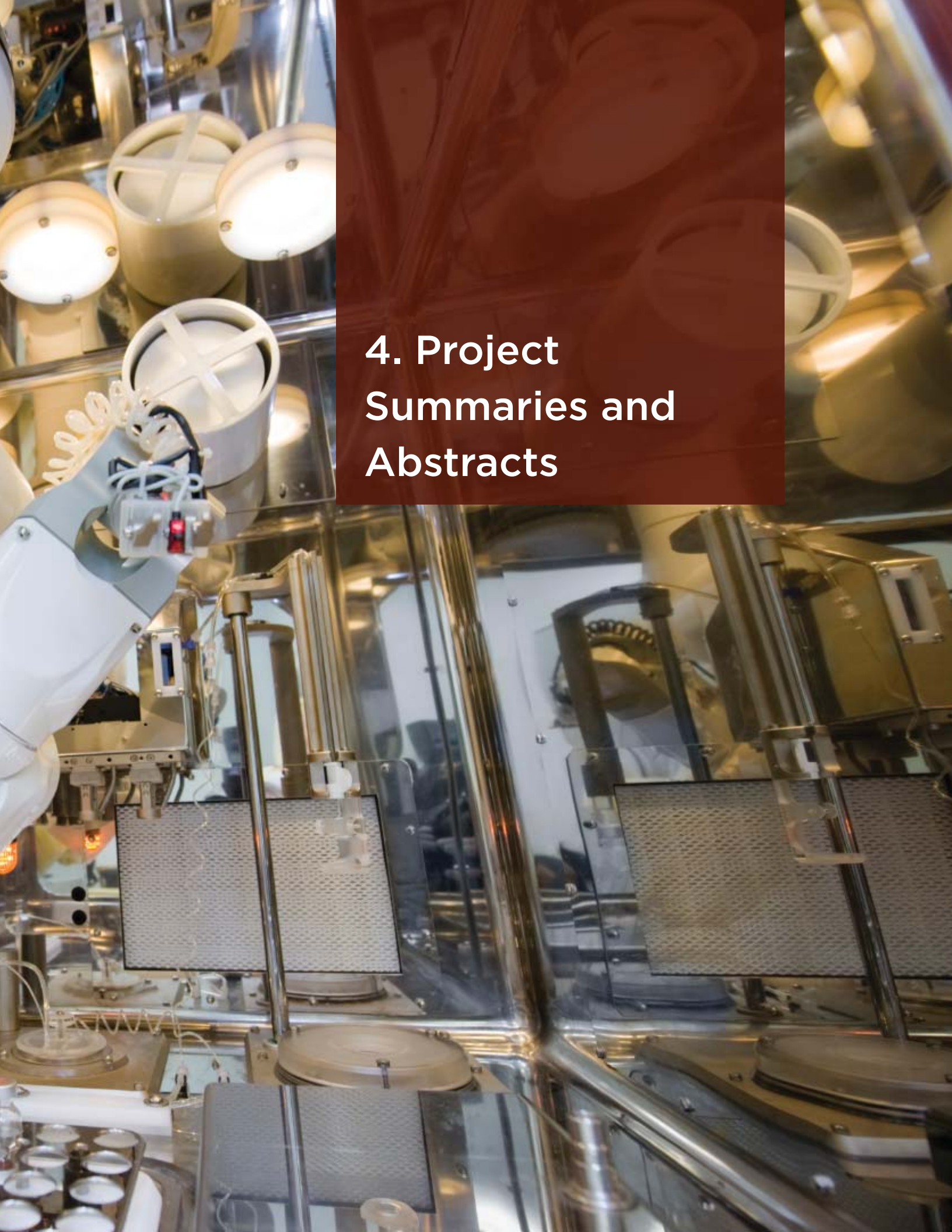
These annual meetings facilitate information exchange and provide opportunities for the parties to review ongoing projects, investigate new opportunities for collaboration, and update research scopes to support current R&D priorities. In FY 2011, DOE held a formal meeting with their colleagues at Euratom and two meetings with the Republic of Korea; all events were hosted by DOE in the United States. DOE has also held recent discussions with Canada to identify priority areas for collaboration and plans to issue a solicitation for new U.S.–Canada projects in FY 2012.

In light of the recent events at the Fukushima nuclear power plant, all planning meeting participants agreed that reactor safety should hold a renewed focus in terms of research scope. The U.S.–Euratom discussions confirmed existing program emphases; reactor safety is a new area for collaboration between the United States and the Republic of Korea. The United States and Euratom also identified a strong mutual interest in advanced modeling and simulation techniques.

In FY 2012, Euratom will host the annual U.S.–Euratom project review and bilateral meeting. Two U.S.–ROK meetings will take place, one hosted in the Republic of Korea and the other in the United States. As appropriate, DOE will also pursue new cooperative agreements with prospective partner countries.

These international collaborations have forged lasting ties that will continue promoting the strong infrastructure necessary to overcome future challenges to the expanded use of nuclear energy. The resulting technological and scientific advances are responding to the need for economical and environmentally conscious sources of energy. I-NERI’s goals and objectives continue to be satisfied.





4. Project Summaries and Abstracts

4.1

U.S.-Canada Collaboration



Director William D. Magwood IV of DOE-NE signed a bilateral agreement

on June 17, 2003, with the Assistant Deputy Minister of the Department of Natural Resources Canada, Ric Cameron, and the Senior Vice President Technology of Atomic Energy of Canada Limited, David F. Torgerson. The first U.S.-Canada collaborative research projects were awarded in FY 2004.

As noted in Section 3, the United States and Canada are in the process of revisiting and refining research scope for future collaborative efforts, which are likely to focus on one or more of the following: enhanced accident-tolerant fuels, advanced fuel cycle options, fast reactors, reactor life sustainability, modeling and simulation, and physics modeling of advanced fuels.

During FY 2011, work was completed on one U.S.-Canada collaborative project, noted below. This project contributed to development of an integrated complex consisting of a nuclear reactor, electrolytic hydrogen plant, and bitumen upgrader. The complex aims to produce hydrogen and, ultimately, synthetic crude oil, gasoline, and diesel fuel. Following is a summary of FY 2011 accomplishments for this project.

2008-001-C Upgrading of the Athabasca Oil Sands for the Production of Diesel and Gasoline

Upgrading of the Athabasca Oil Sands for the Production of Diesel and Gasoline

PI (U.S.): J. Stephen Herring, Idaho National Laboratory

PI (Canada): Sam Suppiah, Atomic Energy of Canada Limited

Collaborators: Canadian Light Source, Saskatchewan Research Council, University of Saskatchewan

Program Area: Reactor Concepts
RD&D

Project Start Date: June 2008

Project End Date: May 2011

Research Objectives

This collaboration between Idaho National Laboratory (INL) and Atomic Energy of Canada Limited (AECL) examined the feasibility of an integrated complex consisting of a nuclear reactor and electrolytic hydrogen plant providing process steam for a bitumen upgrader, along with electricity. The hydrogen produced would be sent to the bitumen upgrader to produce synthetic crude oil, gasoline and diesel fuel. The integrated plant should be optimized to maximize thermal efficiency and minimize water usage.

This project built on a previous I-NERI project that developed a preliminary design to integrate a nuclear reactor with a high-temperature electrolysis system to provide hydrogen for the bitumen upgrading of the oil sands in northern Alberta. In that project, a process model was developed that coupled nuclear reactors with high-temperature electrolysis plants. Several nuclear reactor designs were considered, including very high-temperature reactors (VHTRs) and low-temperature reactors such as the ACR-1000. The study showed that the coupling of low-temperature nuclear reactors and high-temperature electrolysis plants is technically feasible.



Figure 1. INL High-Temperature Electrolysis Experiment Laboratory – small-scale test area.

While much of the bitumen produced from the Athabasca Oil Sands to date has been recovered through surface mining operations, most of the remaining reserves are found in deeper deposits that must be recovered by *in situ* techniques instead of surface mining. Most *in situ* techniques are based on thermal recovery methods that use high temperatures to reduce the viscosity of the tar-like bitumen to increase recovery rates.

One technique chosen for large-scale *in situ* recovery is the Steam Assisted Gravity

Drainage (SAGD) process. In the SAGD process, steam is injected via a horizontal drill pipe to heat the reservoir to reduce the viscosity of the bitumen, allowing its extraction. At present, large quantities of natural gas are used to generate the

steam, a process which produces large volumes of greenhouse gases and leaves operators exposed to volatile natural gas prices. In addition, between 2.0 and 4.5 barrels of water are needed to extract each barrel of crude oil. As Alberta has a limited supply of fresh water, this level of usage poses a potential barrier to growth in the oil sands.

An integrated facility containing a nuclear reactor, hydrogen plant and bitumen upgrader is capable of utilizing the available heat and water resources most efficiently. For example, heat from the reactor, upgrader and high-temperature electrolysis plant may be used to produce steam for SAGD. Water may be used for cooling before it is fed to boilers or electrolysis cells.

Research Progress

Idaho National Laboratory. Since 2003, INL researchers have been pursuing detailed work to develop cells suitable for long-term commercial operation, with a focus on the primary challenge of cell degradation. INL work on high-temperature electrolysis utilizes their role as a nuclear lab to use nuclear heat and electricity to produce raw materials without producing greenhouse gases. This work has also led to work on splitting water and carbon dioxide to produce synthesis gas. High-temperature electrolysis has been identified as the most promising technology for greenhouse gas-free hydrogen production.

INL's scope included bench scale-testing, computational fluid dynamics simulations, system modeling and scale-up. The largest experimental system, the Integrated Laboratory-Scale (ILS) experiment, consisted of 720 cells (15 kW) that ran for 1080 hours.

Solid oxide electrolysis cells (SOECs) are very similar in composition to solid oxide fuel cells (SOFCs), as both consist of an oxygen ion conductive electrolyte and porous electrical conductivity electrodes. The industry standard electrolyte is yttria-stabilized zirconia, but scandia-stabilized zirconia is also under consideration. Also, while electrolyte-supported designs are used, electrode-supported designs are more common.

However, some significant differences between SOFCs and SOECs include the direction of the mass fluxes and the heat requirements. The result of these differences is that SOEC performance degrades faster than SOFC—8.15% per 1000 hours—whereas in the latest 2500-hour test of an SOFC cell stack, the typical degradation seen in SOFCs was 1% per 1000 hours.

INL has also studied co-electrolysis of water and carbon dioxide as a route to produce methane or synthetic liquid fuel products. When combined with methanation, the product stream contained 40% methane. Other products can be methanol and dimethyl ether.

Atomic Energy of Canada, Limited. AECL's work with INL on high-temperature electrolysis includes modeling and economic analysis. During the last year of this I-NERI project and continuing after its conclusion, AECL has been developing capabilities to test high-temperature SOECs. Working with both U.S. and Canadian solid oxide cell producers and building on the experience of the INL in testing such cells, AECL is now a leader in SOEC development. In addition, AECL has expanded on a study conducted as part of the INL High-Temperature Steam Electrolysis program in FY 2008. Program scope included systems analyses of high-temperature steam electrolysis using VHTRs, liquid metal reactors and light water reactors. In FY 2011, AECL expanded the study to CANDU-based supercritical water reactors.

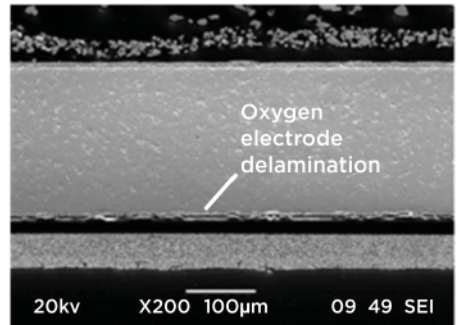


Figure 2. Post-test examination of ILS module showing oxygen electrode delamination.



Figure 3. Wide-angle view of the Canadian Light Source.

Collaborators. Project team members conducted a series of conference calls and reciprocal visits to investigate various areas of collaboration in support of the upgrading of oil sands, leading to a better understanding of the possible use of the Canadian Light Source (CLS) synchrotron light beams to examine SOECs before and after use at high temperatures. The CLS has the tools to detect the oxidation state of materials in various sections of the electrolysis cell.

This collaboration has grown out of INL work on high-temperature electrolysis and AECL efforts in the establishment of a Saskatchewan Centre of Nuclear Excellence for nuclear research and development. The Saskatchewan Research Council is home to a facility, normally used to prepare geological samples for analysis, that will be suitable for preparing samples from button cells and cell stacks with minimal damage. In addition, the Saskatchewan Research Council operates an ion probe that is suitable for analysis of electrolytic cells. These facilities could be used to study various cell degradation phenomena. Team members continue investigating the use of CLS and Saskatchewan Research Council facilities for collaboration on degradation phenomena in electrolytic cells.

Planned Activities

This I-NERI project ended in May 2011.

4.2 U.S.-European Union Collaboration



DOE and Euratom, an international organization composed of the members of the European Union (EU), signed a bilateral agreement on March 6, 2003. Secretary of Energy Spencer Abraham signed the agreement for DOE, and Commissioner for Research Phillippe Busquin signed on behalf of Euratom. In 2004, the United States and Euratom selected the first ten projects for collaboration.

Active Projects

Research areas of interest to both the United States and Euratom include advanced reactor concepts and associated fundamental nuclear science; existing plant life extension, integrity of components, and performance optimization; waste transmutation and management; severe accident management; advanced fuels; nuclear medicine and radioprotection; and uranium programs. As noted in Section 3, both countries have expressed interest in renewing and expanding focuses on reactor safety and on modeling and simulation.

In FY 2011, efforts continued on six ongoing projects, and a new project was initiated. Two projects are producing data on prompt fission neutron multiplicity and spectra, which will help address reactor safety and waste management issues. Two are investigating advanced nuclear fuels; in one case, the project team is characterizing minor actinide-bearing transmutation fuels, and in the other, the team is investigating fabrication and performance of particle fuel and targets. Two project teams are contributing to materials studies. One collaboration is researching irradiation and corrosion effects in materials used for innovative reactor systems. The second is investigating the viability of using standards-compliant schemas and ontologies to address interoperability of materials test databases, as materials test data currently differ in format and associated semantics, impeding information exchange between partners.

Below is a listing of current I-NERI U.S.–Euratom projects, followed by summaries of their FY 2011 accomplishments and an abstract of the new project.

- 2010-001-E** Measurements of Fission Fragment Mass Distributions and Prompt Neutron Emission as a Function of Incident Neutron Energy for Major and Minor Actinides
- 2010-002-E** Spherical Particle Technology Research for Advanced Nuclear Fuel/Target Applications
- 2010-003-E** Irradiation and Testing of Advanced Oxide Dispersion-Strengthened and Ferritic–Martensitic Steels
- 2010-004-E** Development of a Standard Neutron Detector for the Energy Range up to 20 MeV and its Application
- 2010-005-E** Interoperability of Material Databases
- 2010-006-E** State-of-the-Art Post-Irradiation Examination of Advanced Nuclear Fuels
- 2011-001-E** Development of a 2E-2V Instrument for Fission Fragment Research

Measurements of Fission Fragment Mass Distributions and Prompt Neutron Emission as a Function of Incident Neutron Energy for Major and Minor Actinides

PI (U.S.): Robert Haight, Los Alamos National Laboratory

PI (Euratom): Franz-Josef Hambisch, Joint Research Centre-Institute for Reference Materials and Measurements

Collaborators: Commissariat a l'Energie Atomique, Centre DAM Bruyeres-le-Chatel

Program Area: FCR&D

Project Start Date: November 2009

Project End Date: October 2012

Research Objectives

This project aims to produce new and essential experimental data on fission fragment mass distributions and prompt neutron emission as a function of incident neutron energy for major and minor actinides. Improved fission fragment mass distributions, prompt fission neutron multiplicity, and spectral data are needed to optimize the design and safety assessment of fast reactors, accelerator-driven systems, and waste management scenarios. Researchers will measure fission fragment mass distributions and produce accurate data files for the relevant isotopes as a function of incident neutron energy. Results will contribute to the ENDF and JEFF libraries. The work will be performed by personnel at the Los Alamos National Laboratory (LANL), the Institute for Reference Materials and Measurements (IRMM), and Commissariat a l'Energie Atomique Bruyères-le-Châtel (CEA) using neutron facilities at LANL and IRMM together with advanced detectors being developed in these laboratories and at the CEA/DAM laboratory.

Research Progress

Fission neutron emission. The project team measured prompt fission neutron spectra from ^{235}U and ^{239}Pu for incident neutron energies from 1 to 200 MeV at the Weapons Neutron Research (WNR) facility at the Los Alamos Neutron Science Center (LANSCE). The experimental data were analyzed with the Los Alamos model for incident neutron energies of 1 to 8 MeV using CEA's multiple-foil fission chamber containing deposits of 100 mg ^{235}U and 90 mg ^{239}Pu to detect fission events. Outgoing neutrons were detected by the FIGARO array of 20 liquid organic scintillators. A double time-of-flight technique was used to deduce the neutron incident energies from the spallation target and the outgoing energies from the fission chamber. The team used these data to test the Los Alamos model and optimized the total kinetic energy (TKE) parameters to obtain a best fit to the data. The researchers also compared prompt fission neutron spectra with the evaluated data in ENDF/B-VII.0, as well as calculating average energies from both. Figure 1 provides sample data from this effort. The results were published in FY 2011.¹

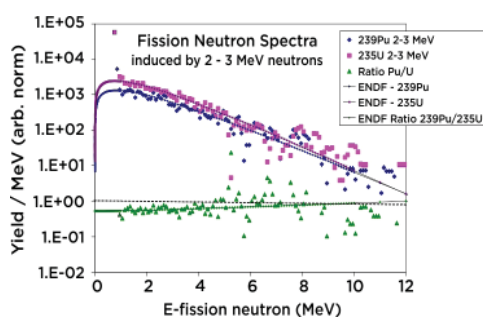


Figure 1. Prompt fission neutron spectra for fission induced by neutrons of 2–3 MeV on ^{235}U (pink squares) and ^{239}Pu (blue diamonds), both arbitrarily normalized. The ratio is also shown (green triangles) and the data are compared with the ENDF/B-VII.0 evaluated data.

1 S. Noda, R. C. Haight, R. O. Nelson, M. Devlin, J. M. O'Donnell, A. Chatillon, T. Granier, G. Belier, J. Taieb, T. Kawano and P. Talou. "Measurement and analysis of prompt fission neutron spectra from 1 to 8 MeV in neutron-induced fission of ^{235}U and ^{239}Pu using the double time-of-flight technique," Phys. Rev. C 83, 034604 (2011).

Fission fragment mass yields. The research team carried out experiments at LANSCE-WNR to measure fission fragment mass yields from ^{238}U as a function of incident neutron energy. The IRMM team developed a double Frisch-gridded ion chamber for this purpose. The cathode of the ionization chamber is a thin, metalized polyimide film onto which the actinide has been uniformly deposited with a low areal density ($<200 \mu\text{g}/\text{cm}^2$). The ionization chamber is used to measure in coincidence the kinetic energies and angles of emergence of both fission fragments. Researchers obtain fragment mass distribution through rough mass and momentum conservation while correcting for prompt neutron emission, energy loss in sample/substrate and pulse height defect.

The team performed a preliminary analysis of the fragment characteristics for incident energy below 12 MeV. Figure 2 shows the fragment anisotropy, defined as the ratio of the fragment emission at 0° to that at 90° with respect to incident neutron ($R = W(0^\circ)/W(90^\circ)$). Preliminary results are in good agreement with previous measurements and models proposed by Shpak and Ryzhov. The team also investigated the mean TKE and the fragment mass distribution. The first study, however, did not account for the information from the neutron counter, and the correction from neutron emission was performed on the base of a parameterization of nu-bar. The results are thus necessarily a first approximation. The data on fragment yields were analyzed by a graduate student at IRMM, but more statistics will be needed for definitive results.

Planned Activities

The project team plans further measurements of prompt neutron emission from neutron-induced fission at WNR with a new flight path, parallel-plate avalanche fission counters at Lawrence Livermore National Laboratory, new detector arrays for high-energy neutrons ($>0.6 \text{ MeV}$) and lower-energy neutrons (50 keV to 1 MeV). The team is also working on a new data acquisition system based on waveform digitizers, which will be commissioned by the end of FY 2012; production measurements will begin shortly thereafter.

Analysis of the $^{238}\text{U}(n,f)$ experiments is ongoing, and the neutron multiplicity measurement that was carried out in the same experiment will be coupled to the fission fragments observables. Using these data, the researchers will investigate neutron multiplicity as a function of fragment mass asymmetry. The project team also foresees new measurements with different actinides, such as ^{235}U or ^{239}Pu , in the second half of 2012.

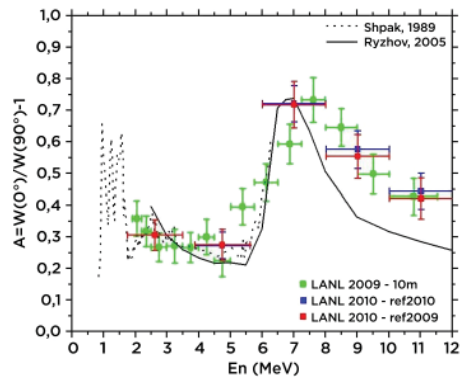


Figure 2: Anisotropy of the fragments from neutron-induced fission of ^{238}U as a function of incident neutron energy up to 12 MeV for different data samples. The preliminary results are compared to Shpak and Ryzhov models.

Spherical Particle Technology Research for Advanced Nuclear Fuel/Target Applications

PI (U.S.): Stewart Voit, Oak Ridge National Laboratory

PI (Euratom): Mariano Menna, Joint Research Center Institute for Transuranium Elements

Collaborators: Los Alamos National Laboratory, Sandia National Laboratory

Program Area: FCR&D

Project Start Date: February 2010

Project End Date: January 2013

Research Objectives

This project will advance the state of understanding of particle fuel technology by addressing technical questions related to fabrication and performance of particle fuel and targets. Work on this project will fall under three primary task areas, as described below.

- **Sol-gel technology.** The work in this project task area will investigate the fabrication of microspheres with controlled open and interconnected porosity to allow infiltration of a second oxide phase into the pore network. The desired outcome of this task area is a fundamental understanding of the sol-gel microsphere calcination and infiltration process and an assessment of the range of second-phase loading.
- **Resin-loading technology.** Work on this task area will investigate the decomposition behavior of strong acid resin particles. The desired outcome of this task area is a fundamental understanding of resin-loading technology process-to-product relationships and an assessment of the suitability of this technology for nuclear fuel/target applications.
- **Mesoscale modeling of fuel/target fabrication and performance.** This task area will leverage the collaboration between Oak Ridge National Laboratory (ORNL) and Los Alamos National Laboratory (LANL) with the development of a sintering/microstructural evolution model that is applicable to particle fuel technology. The desired outcome of this task is a first-generation model for sintering/microstructural evolution, which can begin to answer outstanding questions related to fuel performance.

Research Progress

Sol-gel technology. Researchers have been investigating solution-based routes for the production of spherical particle fuels since the 1960s and have demonstrated the ability to form oxide microspheres of controlled size and shape.^{1,2} Thus this task will not focus on sol-gel technology but instead will concentrate on the controlled reduction of the UO_3 particles to UO_2 in such a way that they remain porous with an open and interconnected pore network.

1 Lackey, W., et al., Assessment of Gel-Sphere-Pac Fuels for Fast Breeder Reactors, ORNL-TM-5468 (1978).

2 Haas, P., et al., Engineering Development of Sol-Gel Process at the Oak Ridge National Laboratory, ORNL-TM-1978 (1968).

Urania sol-gel particles were synthesized using the internal gelation process, then air-dried. The project team then characterized the UO_3 spheres optically for size, shape, and phase purity. An example of the results is shown in Figure 1.

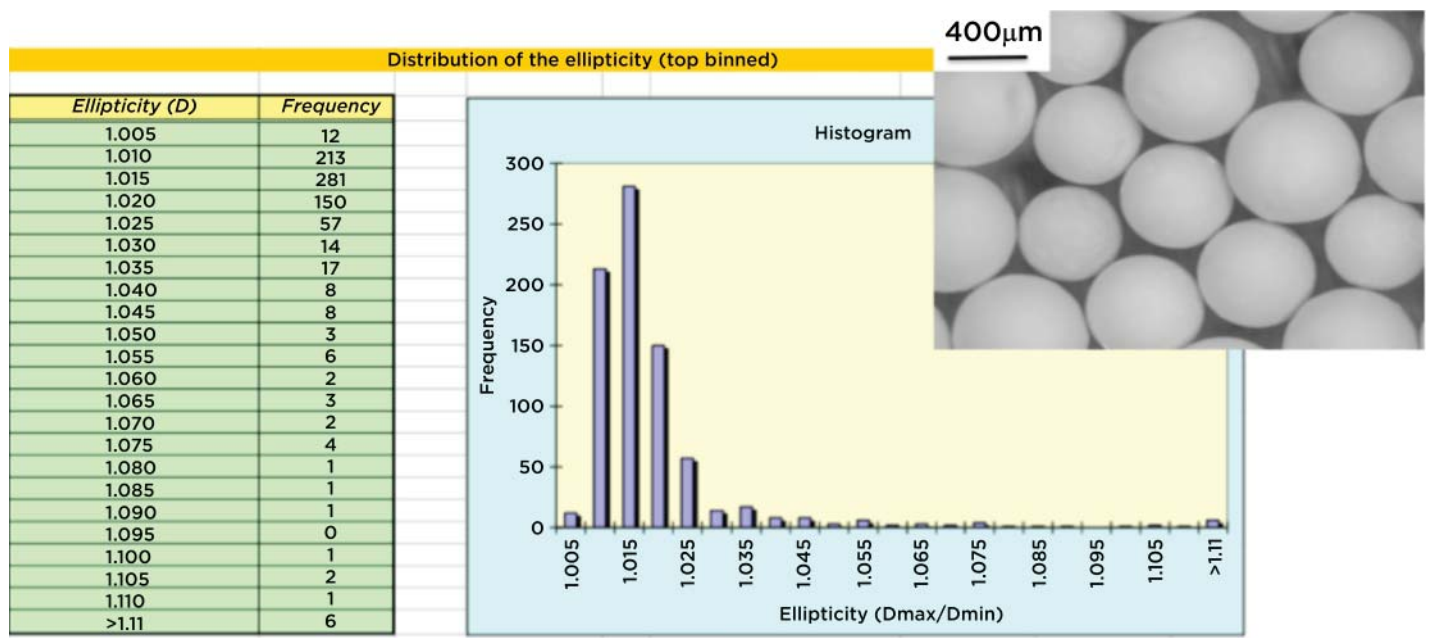


Figure 1. Aspect ratio of air-dried UO_3 sol-gel particles.

The particles were found to be uniform in shape with a mean particle size of 426 μm . X-ray diffraction revealed amorphous UO_3 , likely the β -phase and stable in air up to $\sim 550^\circ\text{C}$. The parent batch of particles was split into sub-batches, each of which will undergo thermal reduction to UO_2 under varied conditions. The reduction process was divided into two categories: (1) conversion of UO_3 to U_3O_8 in air followed by reduction to UO_2 under 4% hydrogen, and (2) direct reduction to UO_2 in 4% hydrogen. The project team carried out a total of six reduction runs.

The UO_3 to U_3O_8 to UO_2 conversion was performed parametrically using a two-by-two temperature matrix. The conversion to U_3O_8 in air was done with low and high temperatures of 550°C and 700°C , respectively, and the subsequent reduction to UO_2 under 4% hydrogen was performed at 475°C and 700°C . The direct reduction of UO_3 to UO_2 took place at temperatures of 475°C and 700°C . The team characterized samples from each of the six batches for particle size, aspect ratio, surface area, density, and open porosity; the researchers used mercury porosimetry to determine particle density and open porosity. The results are displayed in Figure 2.

Property	Measured Data					
Particle diameter (μm)	531.7	526.3	540.8	521.0	612.1	539.4
Particle aspect ratio	1.019	1.018	1.017	1.019	1.017	1.017
Specific surface area (m^2/g)	3.816E+01	3.538E+01	3.912E+01	3.415E+01	8.297E+01	3.571E+01
Average particle weight (g)	2.389E-04	2.487E-04	2.391E-04	2.576E-04	2.763E-04	2.608E-04
Average particle envelope volume (cm^3)	8.19E-05	7.77E-05	8.49E-05	7.77E-05	1.23E-04	8.46E-05
Average particle envelope density (g/cm^3)	2.92E+00	3.20E+00	2.82E+00	3.32E+00	2.25E+00	3.08E+00
Open porosity (ml/m^2)	8.98E+01	6.27E+01	3.26E-01	4.84E-01	6.53E+01	6.39E+01
Reduction Conditions	Air @ 550°C Ar-H ₂ @ 475°C	Air @ 550°C Ar-H ₂ @ 700°C	Air @ 700°C Ar-H ₂ @ 475°C	Air @ 700°C Ar-H ₂ @ 700°C	Ar-H ₂ @ 475°C	Ar-H ₂ @ 700°C
	UO_3 to U_3O_8 to UO_2					UO_3 to UO_2

Figure 2. Characterization results for UO_2 particles as a function of reduction conditions.

The particles that were converted first to U_3O_8 at 550°C and the ones directly reduced under 4% hydrogen retained a large amount of open porosity. Particles from the two batches converted in air at 550°C were more friable than particles from the other batches, probably as a result of the hexagonal-to-fluorite phase conversion at low temperatures. The microstructure of the particles that were converted to U_3O_8 at 700°C tended to close at the particle surface. Figure 3 shows scanning electron microscope (SEM) images of a particle reduced in air at 550°C followed by 4% hydrogen at 475°C. The images confirm an open porous network, which should be ideal for the next phase of this work task.

Mesoscale modeling of fuel/target fabrication and performance.

Researchers selected a mesoscale model of microstructural evolution that had been co-developed with colleagues at Sandia National Laboratory, as it includes the physical mechanisms necessary to model sintering and has been extensively validated.³ The model simulates the complex solid-state sintering behavior using a Potts Kinetic Monte Carlo (KMC) framework and captures curvature-driven grain growth, pore migration, mass transport, and vacancy migration and annihilation. A comparison of the results from a simulation with experimental data for the sintering of copper metal is

shown in Figure 4. The colored circles in Figure 4 are digital representations of the microstructure associated with a real sintered copper disc (upper image) and a simulated sintered body (lower image) measured at an equivalent point in time. The different colors within each image reflect grain orientation, i.e., grains with the same crystallographic orientation are represented with the same color. Under this I-NERI project task, the macroscopic model of porous body sintering will be extended to include swelling and thermal gradients. Swelling will be driven by temperature and the stochastic conversion and accumulation of unit cells with lower density. The project team will impose a thermal gradient in the model and assess the effects on microstructural evolution.

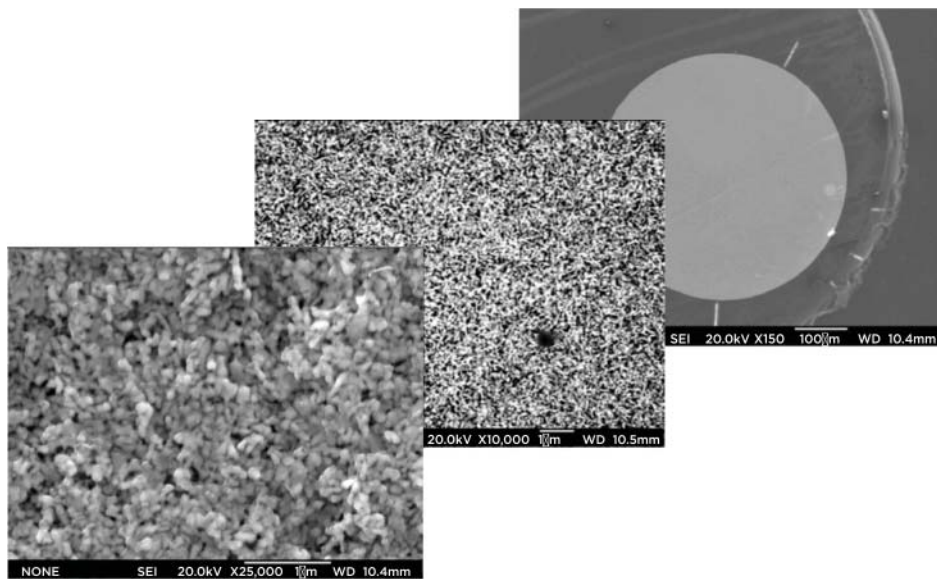


Figure 3. SEM micrographs of a reduced UO_2 porous particle.

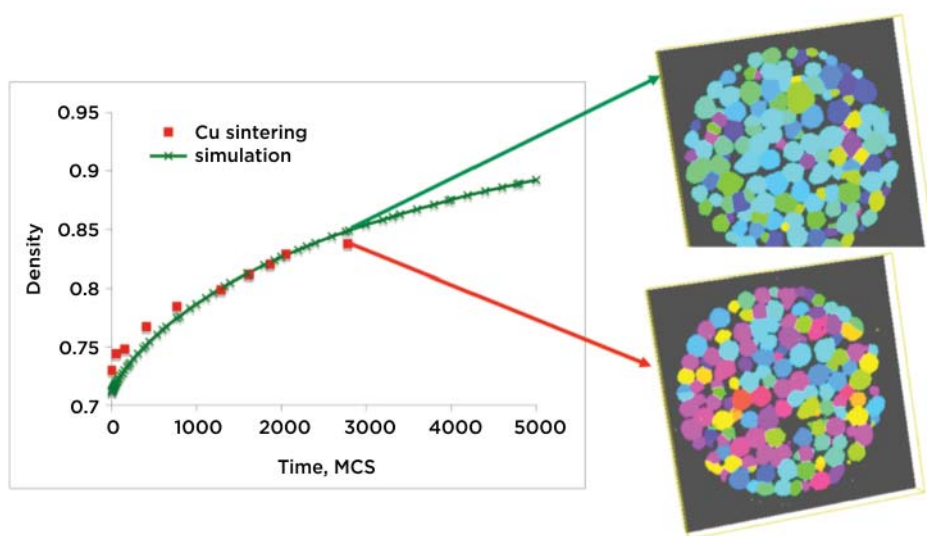


Figure 4. Comparison of copper sintering curves from experiment and simulation.

³ Olevsky, E., "Multi-Scale Study of Sintering: A Review," *Journal of the American Ceramic Society*, 89 [6] 1914-1922 (2006).

Planned Activities

Sol-gel-derived UO₃ particles were reduced to UO₂ under varied conditions. Results showed that it is possible to fabricate low-density spherical particles with open and interconnected porosity. The next step is to evaluate the crushability of these particles and assess the degree to which representative pellet microstructure is achieved. The particles may also be used for infiltration studies to gain a fundamental understanding of the sol-gel microsphere calcination and infiltration process and to assess the range of second-phase loading.

Work on the resin-loading technology task as pertains to this I-NERI project was completed in FY 2010. The results are being employed for further study under a different DOE program.

Although the project team had identified a mesoscale model for use in the third task, a shift in FCR&D priorities has partially redirected project scope. An attempt is being made to identify other mesoscale modeling activities that may be leveraged to support this work task.

Irradiation and Testing of Advanced Oxide Dispersion-Strengthened and Ferritic-Martensitic Steels

PI (U.S.): Stuart Maloy, Los Alamos National Laboratory

PI (Germany): Concetta Fazio, Karlsruhe Institut für Technologie (formerly Forschungszentrum Karlsruhe)

Collaborators: Idaho National Laboratory, Lawrence Livermore National Laboratory, Oak Ridge National Laboratory, Pacific Northwest National Laboratory, Paul Scherrer Institute, SCK•CEN

Program Area: FCR&D

Project Start Date: December 2009

Project End Date: December 2013



Figure 1. A 2.4-kilogram extruded bar of 14YWT advanced ODS alloy.

Research Objectives

This collaboration is investigating irradiation and corrosion effects in materials used for innovative reactor systems, including fast reactors cooled with sodium, heavy liquid metal (HLM), and gas. The project team will develop and characterize advanced oxide dispersion-strengthened (ODS) and ferritic-martensitic (F-M) steels, investigate corrosion effects of these steels in sodium, and examine the ODS steels' irradiation behavior. They will perform materials modeling and post-irradiation analysis on several irradiation programs, such as those conducted at MEGAPIE and the Fast Flux Test Facility (FFTF).

The primary purpose is to share collaborative research results between scientists at U.S. national laboratories, the U.S. Department of Energy, and Euratom's GETMAT (Generation IV and Transmutation Materials). Results will improve understanding of these innovative systems' potential viability and competitiveness, support development of improved safety features, and provide information about transmutation systems using HLM coolant and a fast-spectrum spallation neutron flux.

Research Progress

Significant progress has been made through collaborative meetings and data sharing.

Development of advanced ODS steels (including welds). The U.S. team produced a 50-kilogram heat of 14YWT, and initial testing of this advanced ODS alloy shows excellent mechanical properties. Figure 1 shows an extruded bar of 14YWT after consolidation. In addition, researchers produced a small heat of 9Cr ODS, and initial testing is under way. The U.S. team shared these data with GETMAT research scientists. The GETMAT team is making similar progress on development of 12Cr and 9Cr ODS alloys.

Advanced materials coolant compatibility. Los Alamos National Laboratory (LANL) is restarting its DELTA lead-bismuth loop test facility. Simultaneously, GETMAT researchers are conducting long-term (up to 10,000 hours) corrosion testing on ODS alloys in lead and lead-bismuth.

Irradiation behavior of advanced ODS steels. U.S. researchers are conducting initial testing to measure the tensile properties of ODS steel alloy MA-957 after irradiation to 100 dpa in the FFTF. Euratom researchers will obtain high-dose irradiation data from materials irradiated in the MATRIX program, which reproduces the fast spectrum conditions for core components. However, this activity is presently delayed because of hot cell repairs.

Multiscale modeling of F-M iron–chromium alloys and experimental validation. U.S. researchers are developing models to study creep in F-M steels. In addition, data are being obtained through detailed microscopy on the defects formed in HT-9 after irradiation to 155 dpa, which will aid in development of iron–chromium models.

Planned Activities

Team members will continue attending technical meetings to share results, and the U.S. and Euratom research teams will exchange specimens of ODS alloys. Both teams will conduct tests on the alloys and share results. There will be increased collaboration in modeling and simulation activities.

Development of a Standard Neutron Detector for the Energy Range up to 20 MeV and its Application

PI (U.S.): Nikolay Kornilov, Ohio University

PI (Euratom): Franz-Josef Hamsch, Joint Research Centre-Institute for Reference Materials and Measurements

Collaborators: Idaho State University, Los Alamos National Laboratory, National Institute of Standards and Technology

Program Area: FCR&D

Project Start Date: November 2010

Project End Date: October 2013

Research Objectives

The objective of this project is to improve the knowledge for both prompt fission neutron spectra and (n,p) angular distribution in the neutron energy range up to 20 million electron volts (MeV). Project findings will ultimately address issues with high-level waste management and waste transmutation and increase the accuracy of (n,p) and californium (Cf) standards. To begin this effort, the project team is conducting detailed investigation of the properties of two different neutron detectors that will be used to verify the (n,p) angular distribution and to measure prompt fission neutron spectra. The team will use two scintillators—an NE213 and a p-terphenyl—that have high accuracy in the neutron energy range up to 20 MeV.

The team initially planned to develop a standard neutron detector (SND) with an accurately measured response function confirmed by Monte Carlo (MC) modeling. However, detailed investigation of five p-terphenyl detectors has revealed variation in energy dependences of the light output, a critical scintillator characteristic. Therefore, the SND portion of this project has been modified. During FY 2011, the Euratom research team members identified the best of the five p-terphenyl detectors for use in the remainder of the project.

Research Progress

Researchers at the Joint Research Centre (JRC) investigated the properties of five p-terphenyl scintillation detectors, all with 8-cm diameter and 5-cm height. Using the time-of-flight method with a ^{252}Cf neutron source, the team investigated and compared response functions and dependences of light output in a wide energy range for proton and electron energy. One scintillator had twice the light output of an NE213 detector, so will be used for the remainder of this project, while light output of the other four detectors ranged from 0% to 20% higher than NE213 (see Figures 1a and 1b at the top of the next page).

The Ohio University project team focused on the following activities utilizing an NE213 detector with 12.5-cm diameter and a 5-cm height:

- Increase the detector's stability.
- Test a method to calibrate the energy scale with gamma-ray sources.

- Develop a method to measure detector efficiency in the 2–20 MeV energy range using a ${}^6\text{Li}({}^6\text{Li},\text{n})$ reaction.
- Measure the ${}^{252}\text{Cf}$ neutron spectrum during a long run to collect statistics in the energy range nearing ~20 MeV.

Detector stability and energy scale calibration.

The high voltage of the detector was checked during a two-month run. The stability was $<5 \cdot 10^{-2}\%$. Pulse-

height spectra of a ${}^{207}\text{Bi}$ source were measured regularly and, together with gamma rays from ${}^{252}\text{Cf}$ and background, were used to estimate a gain correction of $<1.5\%$ during offline analysis. Gamma rays applied for calibration of the energy scale in the range 0–5 MeV are collected in Table 1.

This investigation revealed a non-linearity effect of $<10\%$ below 5 MeV, which the research team took into account during the offline data evaluation.

Table 1. Gamma rays used to calibrate the NE213 neutron detector in the 0.5–5 MeV energy range.

Source	E_γ , MeV	E_e , MeV	Position in spectrum*
${}^{22}\text{Na}$	0.511	0.340	1
${}^{207}\text{Bi}$	0.570	0.393	1
${}^{137}\text{Cs}$	0.662	0.477	1
${}^{207}\text{Bi}$	1.064	0.857	1
${}^{22}\text{Na}$	1.275	1.061	1
${}^{207}\text{Bi}$	1.770	1.547	1
np-capture	2.225	1.995	1
${}^{208}\text{Tl}$ (thorium chain)	2.615	2.381	1
${}^{12}\text{C}$	4.438	3.416	2
${}^{12}\text{C}$	4.438	4.200	3

*N – position in spectrum. 1. Compton effect: $N = (N_{\max} + N_{1/2})/2$. 2. Pair production: $E_e = E_\gamma - 2mc^2$, $N = N_{\max}$ in the first peak. 3. Pair production: $E_e = 4.2\text{MeV}$. Result of MC simulation. $N = N_{0.75}$ where N_{\max} – channel number of maximum, $N_{1/2}$ – channel number for half of maximum, $N_{0.75}$ – channel number for 75% of maximum.

Measuring the ${}^{252}\text{Cf}$ neutron spectrum. During a 915.6-hour run, researchers took real-time measurements of the prompt fission neutron spectrum from a ${}^{252}\text{Cf}$ neutron source. Figure 2 shows the estimated efficiency of the neutron detector relative to the ${}^{252}\text{Cf}$ standard versus the efficiency calculated using the Monte Carlo method. Significant differences between experimental and calculated curves are visible in the energy range >12 MeV. They may be caused by either $\text{C}(n,\alpha)$ reactions, which occur in the scintillator and cannot be calculated precisely, or differences in the californium spectrum shape (which would demonstrate the importance of this activity).

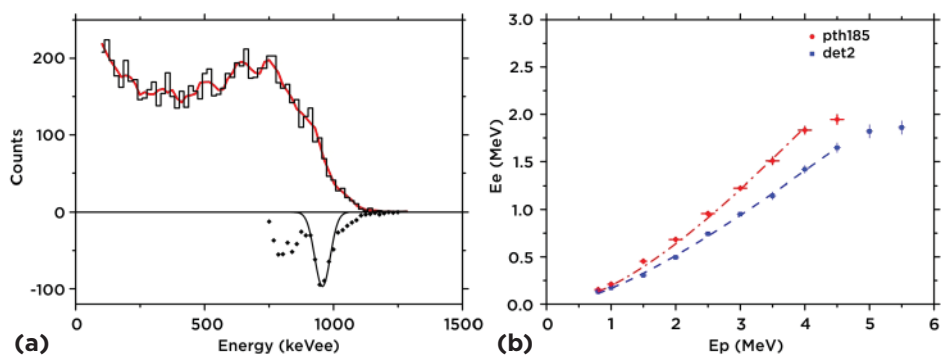


Figure 1a. The p-terphenyl detector response function for 2-MeV neutron energy. Figure 1b. Light output as a function of electron energy for NE213 (det2) and p-terphenyl (pth185) detectors.

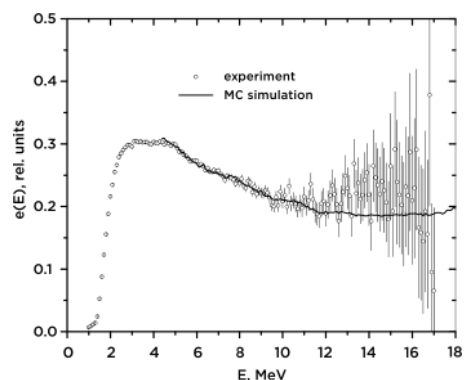


Figure 2. Experimental and calculated efficiencies of the NE213 detector.

Measuring detector efficiency. Because of the symmetry of the ${}^6\text{Li}({}^6\text{Li},\text{n})$ reaction, the center-of-mass system gives the same neutron yield for forward and backward angles. The laboratory system gives different neutron energies, allowing researchers to estimate the detector's efficiency at high energy if the low-energy efficiency is known. The primary challenge is proper preparation of the lithium target, which must be protected from oxygen and other atoms that may induce neutrons from the target. The project team has investigated many metal combinations for the target, including lithium metal evaporated onto gold and nickel with a gold or nickel input window. Lithium atoms diffuse outside the window and produce Li_2O or LiOH . LiCl cannot be used because this chemical is very hydroscopic. Additional nickel or gold did not provide protection from water.

Planned Activities

The project team will continue investigating the ${}^6\text{Li}({}^6\text{Li},\text{n})$ reaction to measure the neutron detectors' efficiency and will investigate an ${}^6\text{LiF}$ target on gold backing to determine the neutron background from ${}^{19}\text{F}$ and whether it affects the ${}^6\text{Li}$ results. Researchers will continue the ${}^{252}\text{Cf}$ run, gather more data, and utilize these to determine the NE213 detector's stability. They will also begin research utilizing the selected p-terphenyl detector, which will be shipped from JRC to Ohio University.

Interoperability of Material Databases

Research Objectives

This project will investigate the viability of using standards-compliant schemas and ontologies to address interoperability of materials test databases, facilitating data exchange between research partners. Extended materials qualification testing of Generation IV (Gen IV) system components that are exposed to high temperatures, neutron fluences, and corrosive environments is necessary to ensure safe and economic system operations. However, materials test data currently differ in format and associated semantics. The data are stored in both heterogeneous and distributed database repositories with different working environments, and a variety of software tools are used to access the data, all of which are in a constant state of change.

Although there have been efforts to develop an ontology that will organize the knowledge base, systems interoperability of materials databases has remained largely unaddressed until very recently. The main goal of this project is the implementation of web-based software for data import and export into/from an agreed standardized schema at the Joint Research Centre (JRC) and Oak Ridge National Laboratory (ORNL). The project will build on the MatML schema for materials properties using as a starting point results of a recently completed CEN (European Committee for Standardization) workshop in which participants examined the economics and logistics of standards-compliant schemas and ontologies for interoperability of engineering materials data. Areas of workshop focus included a tensile test schema in correlation with current technology standards and a guide for using and developing data formats for engineering materials test data. The introduction and adoption of standards-compliant data formats—i.e., schemas and ontologies that faithfully represent procedural standards for mechanical testing—will allow researchers to leverage established and emerging web-based technologies for data storage and retrieval.

Research Progress

Major tasks during the first year of the project included establishing agreements on standardized schemas for interoperability of the individual materials databases for uniaxial creep, tensile, fatigue and creep-fatigue interaction tests. The project has identified two databases for interoperability development: the MatDB managed

PI (U.S.): Weiju Ren, Oak Ridge National Laboratory

PI (EU): Peter Hähner, Hans-Helmut Over, Joint Research Centre – Institute for Energy and Transport

Collaborators: None

Program Area: Reactor Concepts RD&D

Project Start Date: January 2011

Project End Date: December 2013

by the JRC and the Gen IV Materials Handbook managed by ORNL. The MatDB has several decades of development history with well-established structures and data contents, while the Gen IV Materials Handbook, which provides support to international nuclear collaboration under the Generation IV International Forum, is relatively new and still under development. Initial project efforts included a review of both database structures. The review suggested that although the two databases were developed separately, they share many commonalities as relational, web-enabled materials information management systems, particularly in metadata traceability, which is highly desirable for modern materials databases. The high-level schemas of the two databases are presented in Figure 1.

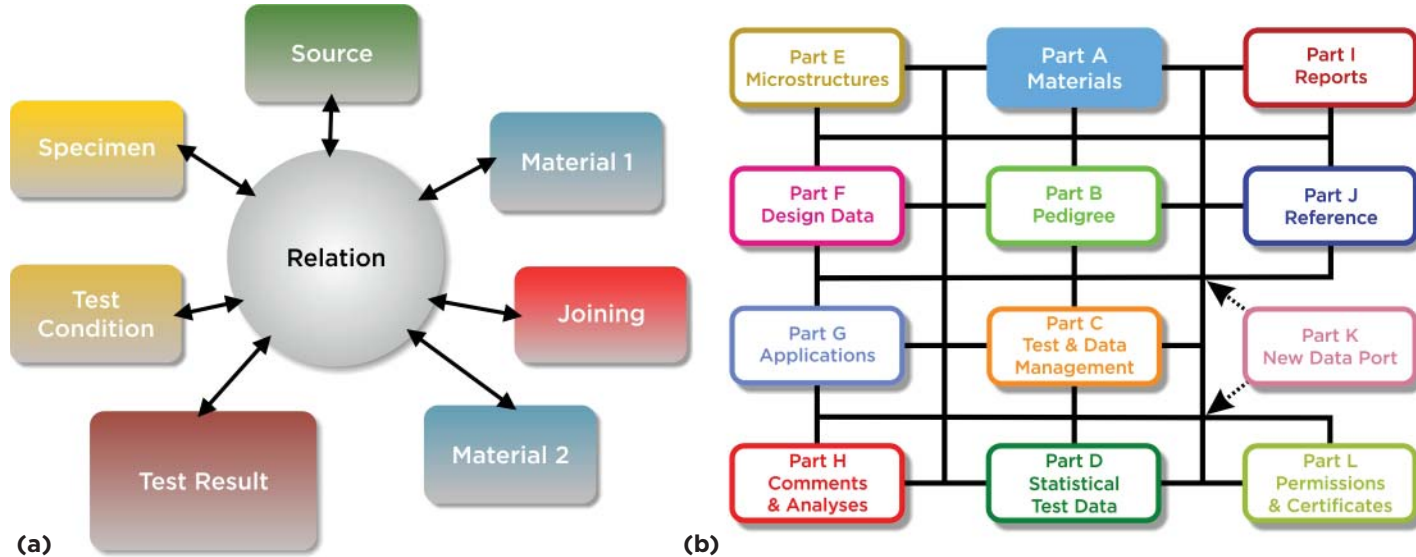


Figure 1: High-level schemas of (a) the MatDB and (b) the Gen IV Materials Handbook.

Analysis of the review results further indicated that counterparts of major data management components exist in both databases, which provides the crucial foundation for interoperability development.

Having established some promise in the structural overview, the U.S. and Euratom teams exchanged more detailed information. The JRC provided XML schema proposals of the MatDB for tensile, creep, and fatigue test data, while ORNL provided proposals of the Gen IV Materials Handbook tensile test data in return. As the Gen IV Materials Handbook is still undergoing frequent structural upgrades, only the tensile test data schema was provided to facilitate comparisons and to further verify viability of the interoperability development approach. The comparison revealed that each schema has its own specific—and complicated—detailed structures for data storage and relationship tracking. For example, chemical composition does not exist in the ORNL tensile test data schema; such information is managed separately in the pedigree data schema with hypertext links to the related tensile test data records. This structure was designed to reduce redundancy in tensile test data records that share the same chemical composition. The single data source also facilitates any needed composition record revisions in a signal pedigree record. The comparison suggests that, although the intended interoperability development approach is viable, it will entail significant efforts because of the complexity of the two database systems.

To gain more detailed knowledge of each other's database structures, the principal investigators exchanged login protocols to allow direct access to both systems for exploration.

Planned Activities

Based on the knowledge gained about both database structures through the comparison of tensile test data schemas, the project team will carry out exchanges for more data types. The remaining schemas are creep and fatigue test data. However, the researchers will extend the exchanges beyond these to deal with differences in specific structures and complicated details for data storage and relationship tracking. As needed, team members will provide data schemas of the pedigree, test specimen, test method, and other related information in the Gen IV Materials Handbook. To accelerate progress, ORNL plans to add a post-doctoral student to the Gen IV Materials Handbook development effort.

Following the evaluation of exchanged schemas, team members will initiate discussions to reach agreements on a set of unified or standardized schemas that facilitate data exchangeability, thus establishing the foundation for further development of database interoperability.

Once the agreements are reached, web-service software will be implemented for data import and export into/from JRC and ORNL standardized schemas. As a test study, researchers will exchange tensile data files in reference to the ISO 6892 Part 1 XML schema. Finally, the project will demonstrate database interoperability by exchanging materials datasets between the MatDB and the Gen IV Materials Handbook.

State-of-the-Art Post-Irradiation Examination of Advanced Nuclear Fuels

PI (U.S.): J.R. Kennedy, Idaho National Laboratory

PI (Euratom): V.V. Rondinella, Joint Research Centre, Institute for Transuranium Elements

Collaborators: Colorado School of Mines, Los Alamos National Laboratory, Massachusetts Institute of Technology, University of Central Florida

Program Area: FCR&D

Start Date: January 2011

End Date: December 2014

Research Objectives

Many new nuclear fuel cycle concepts support the adoption of a closed nuclear fuel cycle employing fast reactors. The fuel behavior characteristics of the various proposed advanced fuel forms must be investigated using state-of-the-art experimental techniques before implementation, augmented by effective synergy with advanced multiscale modeling efforts.

The objectives of this project are three-fold:

- To extend the available knowledge of properties and irradiation behavior of high burnup and minor actinide-bearing advanced fuel systems.
- To establish a synergy with multiscale and code development efforts in which experimental data and expertise on nuclear fuel irradiation behavior is properly conveyed for the upgrade/development of advanced modeling tools.
- To promote the effective use of international resources to the characterization of irradiated fuel through exchange of expertise and information among leading experimental facilities.

Fuel systems under consideration include minor actinide (MA) transmutation fuel types such as advanced mixed oxide (MOX) fuels, advanced metal alloy fuels, inert matrix fuels (IMFs), and nitride or carbide ceramic fuels for fast neutronic spectrum conditions. Most advanced fuel compounds have already been the object of past examination programs, which usually involved irradiation in research reactors. The knowledge derived from previous experience constitutes a significant, albeit incomplete, body of data. New or upgraded experimental tools are available today that can extend the scientific and technological knowledge towards achieving the objectives associated with the new generation of nuclear reactors and fuels.

Research Progress

Experimental work by U.S. team members during the 2011 timeframe was primarily directed towards gaining a more fundamental understanding of fuel-cladding chemical interaction phenomena for metallic fuels, developing a focused ion beam (FIB) system for application to radioactive and highly radioactive materials, and taking first steps towards implementation of a joint characterization effort in the study of irradiated silicon carbide (SiC).

Investigation of properties and behavior of advanced fuels. In this area, the project places particular emphasis on high burnup, fast reactor irradiation behavior, and effects of minor actinides.

Uranium (U) versus iron (Fe) diffusion couples were annealed in the α -U temperature range (580°C, 615°C, and 650°C) and the β -U temperature range (680°C and 700°C). Figure 1 shows the backscattered electron (BSE) images and averaged concentration profiles of diffusion couples at 650°C. The four phases presented are pure uranium, U_6Fe , UFe_2 , and pure iron, which correspond well to the equilibrium phase diagram.

The interfaces between phases are uniform and planar, although the U_6Fe phase grew faster than UFe_2 . There is negligible solubility in both the U_6Fe and UFe_2 phases, so the interdiffusion coefficient cannot be calculated. Instead, researchers calculated integrated interdiffusion coefficients, \tilde{D}_{Int} (Table 1), first kind growth constant (“extrinsic”) K_p and second kind growth constant (“intrinsic”) K_{tr} . Based on these data, the team concludes that diffusion in U_6Fe is faster than in UFe_2 , and U_6Fe grew faster than UFe_2 . The difference of activation energy for each phase between the α -U temperature range and the β -U temperature range is small, which means allotrophic transformation of uranium played only a small role in the growth of U_6Fe and UFe_2 .

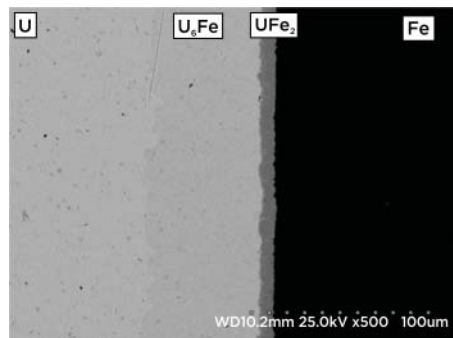


Figure 1. Backscatter electron micrograph and concentration profile of uranium versus iron diffusion couple annealed at 650°C for four days.

Table 1. Integrated interdiffusion coefficients of U_6Fe and UFe_2 in α -U and β -U terminal ends.

U Phase	T (K)	\tilde{D}^{Int, U_6Fe} ($\times 10^{-16}$ at. frac. m^2/s)	Q^{Int, U_6Fe} (kJ/mol)	\tilde{D}^{Int, UFe_2} ($\times 10^{-16}$ at. frac. m^2/s)	Q^{Int, UFe_2} (kJ/mol)
α -U (orthorhombic)	853	1.56	148.46	0.040	243.37
	888	3.60		0.162	
	923	7.63		0.534	
β -U (tetragonal)	953	11.35	112.73	0.680	225.97
	973	15.21		1.22	

Advanced instrumentation. The project team used a FIB to mill lamellae from two diffusion couples, U,Pu-Mo and U,Pu-Zr, a technique for directly preparing samples for transmission electron microscopy (TEM). This is the application of this technique for FC RD diffusion couples used to study fuel cladding chemical interactions. Figure 2 shows the two diffusion couples and locations from which lamellae were obtained; Figure 3 shows representative lamellae from each diffusion couple; and Figure 4 shows TEM images and representative spectra from the U,Pu-Zr diffusion couple.

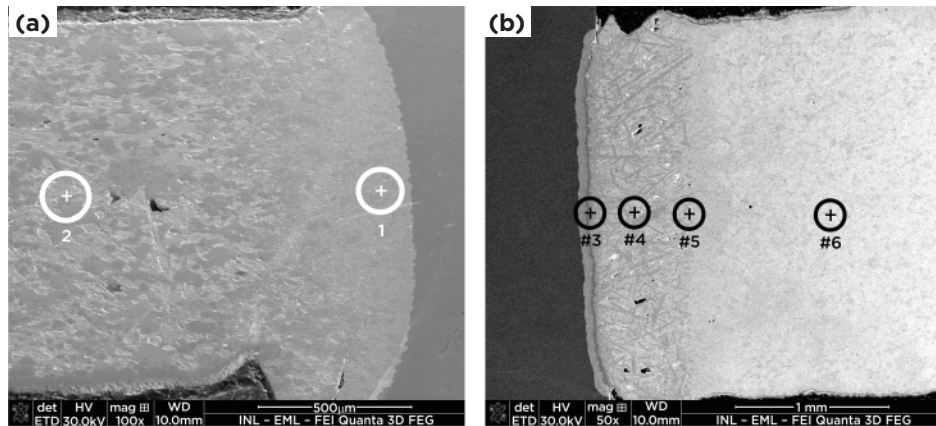


Figure 2. Secondary electron images showing locations (indicated by circles) from which lamellae were obtained: (a) the U,Pu-Mo diffusion couple with the uranium-plutonium shown as the lighter region to the left and molybdenum as the uniform gray region to the right; (b) the U,Pu-Zr diffusion couple with the uranium-plutonium shown as the lighter region to the right and zirconium as the uniform dark region to the left.

Combined characterization studies. A key project task—and perhaps one of the more logically difficult to institute—will be a combined characterization effort of irradiated fuel samples. Team members have discussed several irradiated and non-irradiated fuel materials and are addressing with several other Euratom institutions the viability of sharing METAPHIX irradiation test samples with U.S. researchers. The transport of samples between Idaho National Laboratory (INL) and the Institute for Transuranium Elements (ITU) remains a difficult issue, but the project has identified several transport containers and begun to analyze costs. However, there is no current budget to support highly radioactive material transport.

The project has initiated a cooperative study of irradiated SiC. Four samples of β -SiC have been investigated, three of which were irradiated in the Massachusetts Institute of Technology reactor as part of the Advanced Test Reactor National Scientific User Facility. Colorado School of Mines has performed Hall coefficient measurements to determine electrical carrier densities and impedance measurements. INL is employing FIB techniques to prepare atom probe tomography, TEM, and nano- and micro-indentation measurements, as well as samples for shipment to ITU for their research team to conduct micro-indentation and TEM measurements.

The team prepared three sets of irradiated β -SiC samples, each of which represents a different level of irradiation. The first is a control, which has not been irradiated, and the subsequent samples have been subjected to 9.63×10^{17} , 9.26×10^{18} , and 2.82×10^{19} neutrons/cm 2 fluence. A typical nuclear reactor requires refurbishment or retirement after undergoing a fluence of 1×10^{21} neutrons/cm 2 .

The preliminary data suggest a linear relationship between fluence levels experienced and electronic properties (impedance). There is concern that at high levels of irradiation, the β -SiC electronic property correlation will not maintain this linear relationship. Fast neutrons may affect the sensor differently by increasing the electronic scattering on the resulting damaged lattice. It has been proposed that the SiC sample be half-covered with cadmium to prevent the slow-moving neutrons from reaching the coated portion of the sample, which would then be exposed only to fast neutrons. This specimen design would allow a comparative assessment of nuclear transmutation relative to lattice damage.

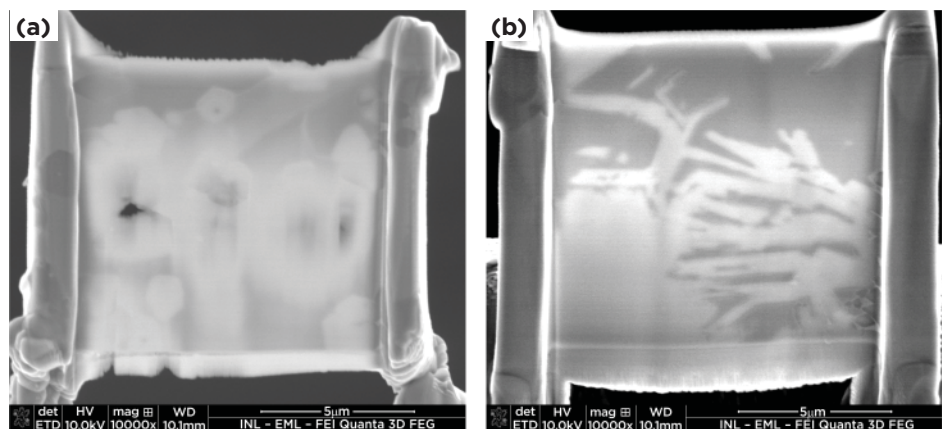


Figure 3. Secondary electron images showing lamellae from (a) Position 2 in the U,Pu-Mo diffusion couple, and (b) Position 4 in the U,Pu-Zr diffusion couple.

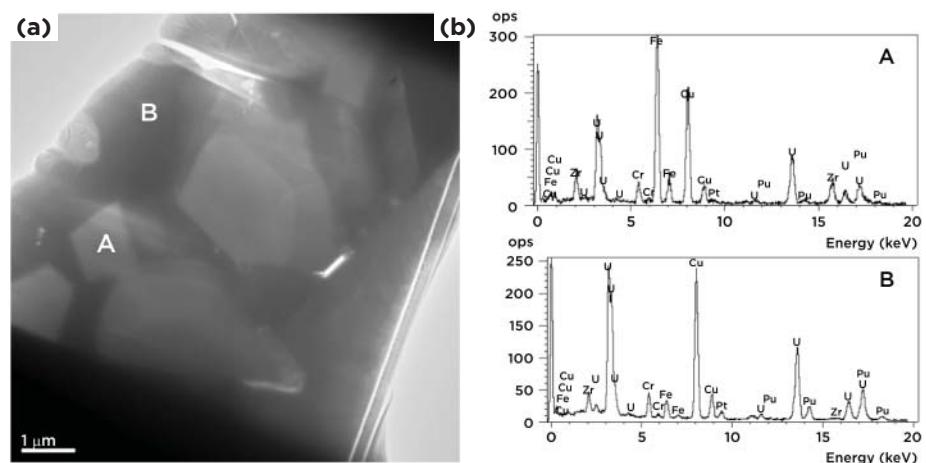


Figure 4. (a) TEM image from the lamellae from the U,Pu-Zr diffusion couple; (b) energy dispersive X-ray spectroscopy (EDS) spectra from the designated positions.

Impedance analysis. In impedance analysis, current is generated in the test material by mutual induction. Since eddy currents are affected by electrical conductivity, impedance is dependent on both carrier content and scattering sites. The back response signal of the induced material carriers relays information about radiation damage in the material.

The high-frequency impedance testing has shown a strong direct relationship between the electronic impedance and fluence in all of the SiC samples. Four samples were tested after irradiation at the three different fluence levels. Figure 5 shows the results, including those from the unirradiated control. The impedance of each sample measured at higher frequencies increases with fluence, indicating the frequency influence on penetration and the need to maintain sufficient induced current in the thin specimens.

The increase in impedance with fluence is most likely due to increased structural disorder within the β -SiC crystal lattice, as increasing the charge carrier concentration would decrease impedance. As fast neutrons bombard the material, there is a greater tendency for structural radiation damage to occur within the samples. Increasing disorder in the lattice contributes to greater scattering of any electrical carriers within the material. The tests performed at the two lowest frequencies, however, do not show a strong increase in impedance of the irradiated samples and, in fact, the lowest frequency shows a slight decrease in impedance at the mid-range fluence levels. The decrease could be due to increased phosphorus doping, as silicon is transmuted to phosphorus by interaction with thermal neutrons. If these electronic defects dominate over structural changes in the lattice, then the impedance would decrease as the number of phosphorus dopants (and therefore electrical carriers) increased. Also, since lower frequencies probe at depths beyond the samples, there is less interaction with the β -SiC and thus lower impedance.

Hall coefficient. The irradiation of SiC samples results in the transmutation of silicon into phosphorus in the crystal lattice producing electrons, thus increasing the material's electron density. Increasing the electron concentration would be expected to decrease the impedance measurement values. The carrier concentration was taken before and after irradiation to calculate the carrier concentration increase. Carrier concentration increased with increasing fluence as can be seen in Figure 6. The fraction of carriers created per fluence was also calculated and is shown in Figure 7.

The general increase of impedance with fluence, as seen in Figure 5, and the observed changes in ultrasonic wave speed and resonance modes suggest that structural damage is occurring and that the impedance is controlled by scattering phenomena and not carrier content. SiC can take on a variety of polytype structures. There are only minor differences in the energy levels of the different sites in the cubic and the hexagonal structures. One would expect that the cubic β -SiC could be converted to 6H-SiC (33% hexagonal: 67% cubic) through radiation damage and possibly to either 4H-SiC (50% hexagonal: 50% cubic) or 2H-SiC (100% hexagonal).

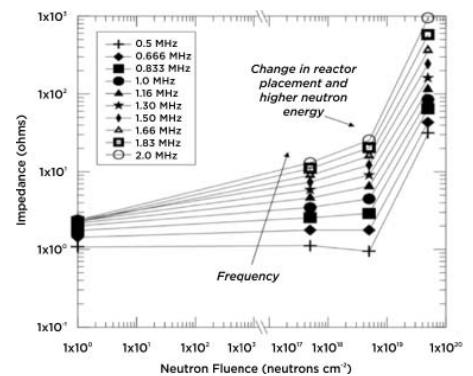


Figure 5. The graph above shows the increasing impedance levels determined from increasing irradiation experienced by the samples, indicating greater structural damage at higher fluence levels.

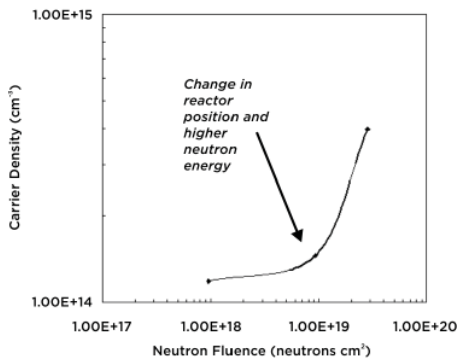


Figure 6. The increased carrier density gives a 1:1 ratio relating doping and new charge carriers. For every new charge carrier created, it is surmised that one silicon-to-phosphorus transmutation took place.

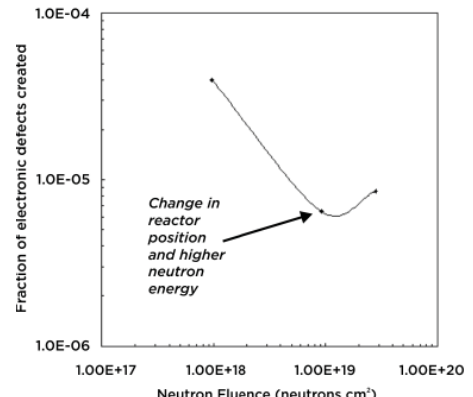


Figure 7. The fraction of electronic defects over the fluence is related above. The third data point may increase due to increased flux levels compared with other samples, or it could be noise within the data set as the points all fall within a small range.

Planned Activities

The INL team will transport FIB-prepared samples of irradiated SiC to ITU while continuing efforts to resolve the issues associated with transport of higher-level radioactive material samples, including fuels. The identification of a viable transport solution to enable sample exchanges between INL and ITU is essential for deployment of the full scope of the present collaboration program. Researchers will continue interactions related to post-irradiation examinations with emphasis on electron probe microanalysis and advanced technique development, such as micro X-ray diffraction, FIB, and thermal diffusivity measurements.

Development of a 2E-2V Instrument for Fission Fragment Research

The objective of the project is to produce accurate data files of fission measurements and evaluations for several key isotopes over the incident neutron energy range relevant to present and future nuclear applications. Design, optimization, and safety assessment of future fast reactor systems require improved fission fragment nuclear data for major and minor actinides. The project will contribute to the ENDF/B-VII and JEFF 3.1 nuclear data libraries.

The research team will develop instrumentation for high-resolution fission fragment velocity, energy, and nuclear charge measurements. The resulting data provide fission fragment mass and the corresponding yield curves. This work supports ongoing developments at two spectrometer facilities: the VERDI (VElocity foR Direct particle Identification) spectrometer at the Institute for Reference Materials and Measurements, and a similar dual-arm spectrometer at Los Alamos National Laboratory (LANL). The current VERDI spectrometer measures energy and velocity from only one of the two fission fragments emitted in binary fission (hence, *1E-1V*), while the advanced instruments will simultaneously measure *both* fission fragments (*2E-2V*). In addition, the LANL dual-arm instrument will also use Bragg curve spectroscopy to measure nuclear charge.

The collaboration will consist of exchange of expertise and technologies, joint experimental efforts, sharing of detector designs, and communication of technical and scientific information. The two instruments will be developed in parallel, and the teams will share technologies that benefit the joint program. Experimental activities will be carried out at both laboratories' facilities, including the Geel Linear Accelerator (GELINA), the 7 MV Van de Graaff neutron source (MONNET), and the Los Alamos Neutron Science Center (LANSCE). Key project milestones are as follows:

- Design study (Year 1)
- Prototype design/technical report (Year 2)
- Initial measurements (Year 3)

PI (U.S.): Fredrik Tovesson, Los Alamos National Laboratory

PI (Euratom): Stephan Oberstedt, Joint Research Center – Institute for Reference Materials and Measurements

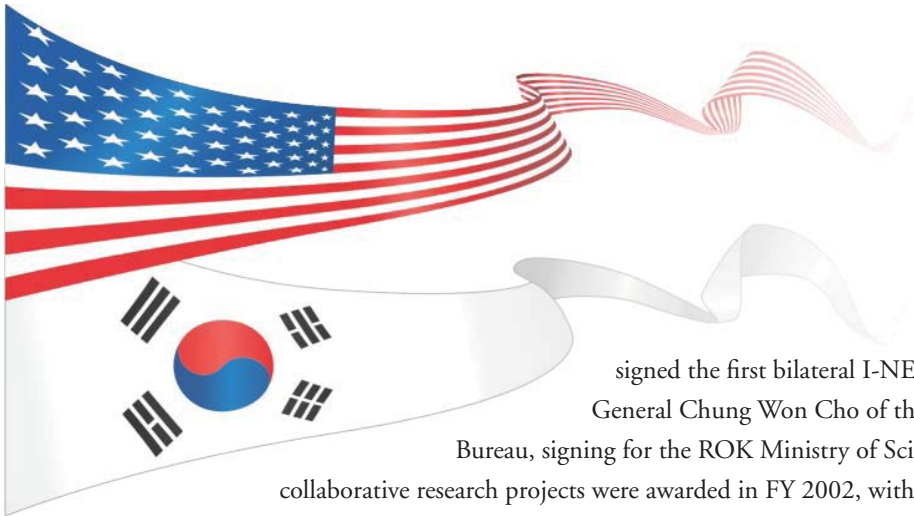
Collaborators: Idaho National Laboratory

Program Area: Reactor Concepts RD&D

Project Start Date: October 2011

Project End Date: September 2014

U.S.–Republic of Korea Collaboration



Director William D. Magwood IV of DOE-NE

signed the first bilateral I-NERI agreement on May 16, 2001, with Director General Chung Won Cho of the Republic of Korea (ROK) Atomic Energy

Bureau, signing for the ROK Ministry of Science and Technology. The first U.S.–ROK

collaborative research projects were awarded in FY 2002, with a total of 46 projects awarded to date.

Active Projects

Areas of mutual interest between the two countries cover next-generation reactor and fuel cycle technology concepts that increase efficiency, safety and proliferation resistance; innovative nuclear plant design, manufacturing, construction, operation, maintenance and decommissioning activities; advanced nuclear fuels; and fundamental nuclear sciences. As noted in Section 3, the two parties have recently established reactor safety as its own topic area.

Four U.S.–ROK projects—two supporting FCR&D and two supporting Reactor Concepts RD&D—were completed during the past fiscal year. Research continued on six other collaborative projects awarded to ROK partners in FY 2009 and FY 2010. In addition, five new projects were awarded during the past year.

During FY 2011, ongoing and completed research project scope ranged from conducting fundamental science studies to enhancing and utilizing cutting-edge modeling and simulation tools. Two U.S.–ROK projects worked with advanced modeling tools to study thermofluid behavior of prismatic very high-temperature gas-cooled reactors (VHTRs), and another is contributing to future modeling efforts by archiving an existing database and using the data to generate Monte Carlo models. Three more project teams are investigating advances in nuclear system materials. In support of an advanced fuel cycle, one project team provided improved neutron cross-section data for isotopes. Two projects investigated waste management, one through new waste forms and the other through used fuel processing. Another project is working toward an improved method of fabricating metallic fuel pins.

This section provides a listing of current I-NERI U.S.–ROK projects—those that are currently under way, those completed last year, and those newly awarded—along with summaries of FY 2011 accomplishments and abstracts of the new projects.

- 2007-004-K *** Development and Characterization of New High-Level Waste Forms for Achieving Waste Minimization from Pyroprocessing
- 2008-001-K *** Advanced Multi-Physics Simulation Capability for Very High-Temperature Gas-Cooled Reactors
- 2008-002-K *** Experimental and Analytic Study on the Core Bypass Flow in a Very High-Temperature Reactor
- 2008-003-K *** Nuclear Data Uncertainty Analysis to Support Advanced Fuel Cycle Development
- 2009-001-K** ZPPR-15 and BFS Critical Experiments Analysis for Generation of Physics Validation Database of Metallic-Fueled Fast Reactor Systems
- 2009-002-K** Enhanced Radiation Resistance through Interface Modification of Nanostructured Steels for Gen IV In-Core Applications

2010-001-K	Investigation of Electrochemical Recovery of Zirconium from Spent Nuclear Fuels
2010-002-K	Advanced Instrumental Science-Based Approach to Nickel Alloy Aging and its Effect on Cracking in Pressurized Water Reactors
2010-003-K	Low-Loss Advanced Metallic Fuel Casting Evaluation
2010-004-K	Development and Characterization of Nanoparticle-Strengthened Dual-Phase Alloys for High-Temperature Nuclear Reactor Applications
2011-001-K	Atomic Ordering in Alloy 690 and its Effect on Long-Term Structural Stability and Stress–Corrosion Cracking Susceptibility
2011-002-K	Development of Microcharacterization Techniques for Nuclear Materials
2011-003-K	Verification and Validation of High-Fidelity Multi-Physics Simulation Codes for Advanced Nuclear Reactors
2011-004-K	Development of Diagnostics and Prognostics Methods for Sustainability of Nuclear Power Plant Safety Critical Functions
2011-005-K	Fully Ceramic Microencapsulated Replacement Fuel for Light Water Reactor Sustainability

* Completed in FY 2011

Development and Characterization of New High-Level Waste Forms for Achieving Waste Minimization from Pyroprocessing

Research Objectives

The purpose of this project was to develop new high-level waste (HLW) forms and fabrication processes to dispose of active metal fission products recovered from electrorefiner (ER) salts during the electrochemical/pyrometallurgical processing of used nuclear fuel. The current technology for disposing of fission products accumulated during electrochemical processing involves converting the entire volume of fission product-loaded salt into a glass-bonded sodalite ceramic waste form (CWF). By selectively removing fission products from the ER salt, the quantity of HLW generated from electrochemical operations can be greatly reduced, while allowing the cleaned ER salt to be reused. This project investigated a number of separations methods to selectively remove fission products from ER salt and, based on this research, developed three novel waste forms to immobilize the separated fission products. In addition, the research team optimized processes for fabrication of the new waste forms and characterized and tested the resultant products. In the project's final year, the team fabricated and characterized the three selected waste forms using ER salt containing fission products and actinide elements.

Research Progress

In the first year of this project, the research team investigated potential waste forms compatible with various separation processes used to clean and recycle ER salt. An extensive literature review of immobilization technologies indicated that the best overall option for waste minimization is dechlorination of the separated fission products, followed by immobilization with a reactive agent. The research team at Korea Atomic Energy Research Institute (KAERI) performed a series of experiments to find effective materials for fission product immobilization, which involved assembling processing equipment that integrated the dechlorination and solidification methods. Other methods were investigated to increase the fission product loading of the CWF in an effort to minimize the quantity of waste generated. Figure 1 (on the opposite page) illustrates the selected separation options and novel waste forms resulting from each option. These options were chosen based on the maturity of the process and on the potential benefit of waste minimization.

PI (U.S.): Steven Frank, Idaho National Laboratory

PI (Korea): Yung-Zun Cho, Korea Atomic Energy Research Institute

Collaborators: None

Program Area: FCR&D

Project Start Date: January 2008

Project End Date: September 2011

Option A is a modification of the Experimental Breeder Reactor-II (EBR-II) used fuel treatment process—that is, instead of adding ER salt to zeolite and processing a low-loaded CWF, the zeolite is submerged in the molten salt, which causes the cationic fission products to ion exchange (or occlude) into the zeolite at high concentrations. This high-loaded zeolite is then fabricated into an advanced CWF material. In options B and C, oxygen sparging of the molten ER salt causes the lanthanide fission products to chemically react, producing oxychloride and oxide precipitates. In option B, the fission product-concentrated salt is distilled, separating the salt containing Group I, Group II, and halide fission products from the lanthanide fission product precipitates. The precipitated fission products are then immobilized in a zinc/titanium (ZIT) oxide matrix. In option C, the salt distillate is immobilized in a silicon-aluminum-phosphate (SAP) host matrix.

Researchers at Idaho National Laboratory (INL) then conducted radioactive testing of the advanced waste forms in the Hot Fuels Examination Facility (HFFEF) hot cell using high fission product-loaded ER salt to process the three small-scale waste forms. The ER salt was a concentrate containing lanthanide fission product precipitates; Group I, Group II, and halide fission products that remain in the salt; and residual actinide elements. After fabricating the waste form sample, the research team conducted characterization measurements and testing in the hot cell, consisting of density measurement, elemental analysis, X-ray diffraction, scanning electron microscopy and a product consistency test (PCT).

Results of the characterization and testing indicated that the team had successfully fabricated three durable waste forms. Density values of the high-loaded CWF, SAP, and ZIT waste forms were comparable to the non-radioactive baseline materials. Microscopy and X-ray diffraction of the waste forms confirmed the formation of expected phase compositions, and the PCT results showed that the waste forms had low elemental release, confirming the durability.

The ZIT waste form produced from the isolated lanthanide precipitate showed very low release of both lanthanide elements (lanthanum, cerium, neodymium, and praseodymium) and actinide elements (uranium and plutonium). Three of the lanthanide precipitate components had normalized mass releases below 0.0003 g/m², while the fourth (praseodymium) was not found in the PCT leachate solution above the measurement detection limit. For the actinides, residual uranium had a release of 0.004 g/m²; plutonium was not detected in the leachate solution. The matrix elements also had low elemental release, with boron and silicon being the highest at 0.34 g/m² and 0.03 g/m², respectively. The matrix elements phosphorus and titanium were not detected in the leachate solutions, while zinc was detected in a moderate amount. Residual salt material in the lanthanide precipitate product is not readily retained in the ZIT waste form and had high release during the PCT. The quantity of salt material detected in the lanthanide precipitate after distillation ranged from 0.04 wt% and 0.3 wt% for cesium and lithium to 1.1 wt% and 1.2 wt% for strontium and potassium, respectively. Residual chlorine salts were also detected.

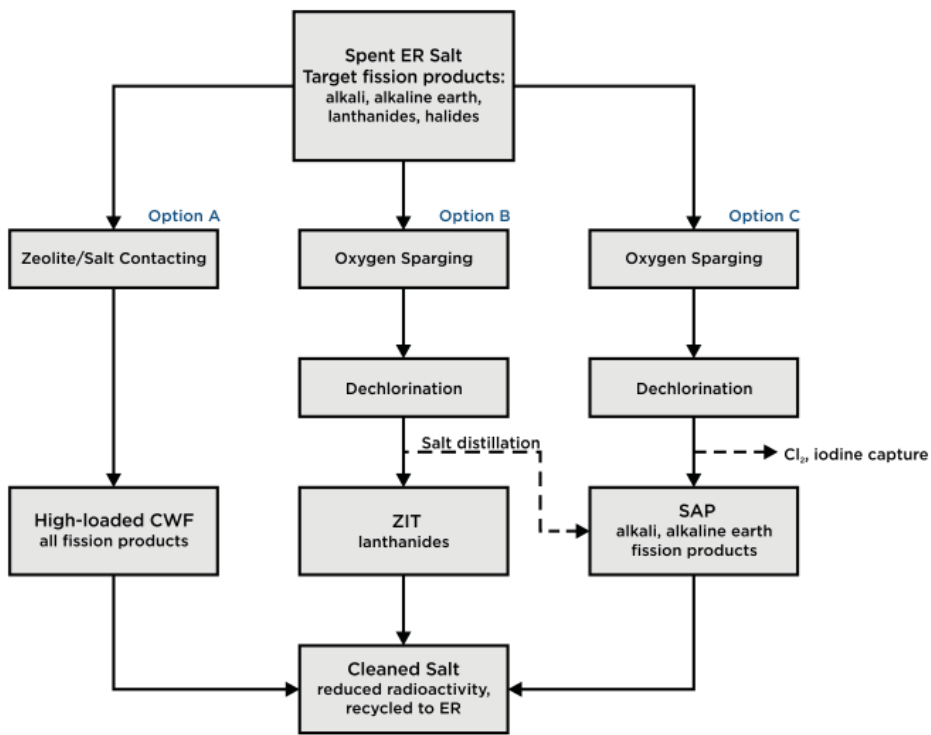


Figure 1. Separation options for removing fission products from ER salt and subsequent waste forms.

The SAP waste form produced from a mixture of the lanthanide/actinide precipitate-loaded salt contained the full complement of salt, fission products and actinide elements. All components measured in the PCT had releases of less than 1 g/m², indicating good performance of the SAP waste form. Cesium and strontium had release concentrations of approximately 0.01 g/m², whereas the typical lanthanide and actinide element release was somewhat less. The matrix elements of boron, aluminum, silicon, and phosphorus had release values an order of magnitude higher, approximately 0.1 g/m².

As determined from the PCT, the elemental release from the high-loaded CWF was greater than the elemental release from the full-scale CWF produced during EBR-II used fuel treatment. This discrepancy was due to different processing methods that affected incorporation of the salt/precipitate mixture into the zeolite: the high-loaded CWF was prepared with sequential salt-zeolite heating and mixing, causing incomplete incorporation, while the simultaneous heating and mixing performed during full-scale CWF operations resulted in full incorporation. The salt components from the high-loaded CWF had release values of approximately 1 g/m². Matrix elements ranged from 0.56 g/m² for boron to 0.032 g/m² for silicon. The lanthanide and actinide elements had release rates of approximately 0.01 g/m².

Project Summary

This project is complete. Researchers successfully implemented small-scale fabrication methods for producing three novel and durable waste forms in a hot-cell environment. In addition to fabricating and characterizing these products, the project team demonstrated the de-chlorination processes required to fabricate the SAP and ZIT waste forms. The favorable results from this demonstration project have increased the available options for fission product immobilization and waste management associated with the electrochemical/pyrometallurgical processing of used nuclear fuel.

Advanced Multi-Physics Simulation Capability for Very High-Temperature Gas-Cooled Reactors

PI (U.S.): Changho Lee, Argonne National Laboratory

PI (ROK): Hyun Chul Lee, Korea Atomic Energy Research Institute

Collaborators: Seoul National University

Program Area: Reactor Concepts RD&D

Project Start Date: October 2008

Project End Date: September 2011

Research Objectives

The project objective was to develop a suite of advanced multi-physics simulation methods and codes that are applicable to high-fidelity, spatially detailed analyses of the coupled neutronics and thermo-fluid behavior of prismatic very high-temperature gas-cooled reactors (VHTRs).

The research scope for the final year of this project included improvement of the 190-group DeCART cross-section library generated in FY 2010, implementation of transient analysis capability in DeCART, development of a methodology for plane-wise decoupled whole core transport calculation with thermal feedback, benchmark analysis of the coupled multi-physics analysis code system DeCART/CORONA, and validation of DeCART against the high-temperature reactor critical experiments.

Research Progress

High-performance 3-D whole core transport calculation. During the project's previous years, the team implemented most of the functions required for actual design calculations into the DeCART code. The new features incorporated this year were additional output edits such as summary file, fluence, and optional 3-D pin-wise output.

The project team previously generated the initial version of the 190-group library for DeCART using the Korea Atomic Energy Research Institute (KAERI) library processing system. Some fission product nuclides such as Ag-109, Nd-145, Pm-147, Sm-147, Sm-152, and Eu-153 had formerly been treated as non-resonant nuclides in both the DeCART and HELIOS libraries. The project team found that these nuclides had large errors in reactivity at 150 GWD/T. By treating those fission product nuclides as resonant nuclides, the researchers were able to regenerate resonance integral tables and subgroup data and produce a new library. Figure 1 compares the reactivity errors during depletion calculation of a

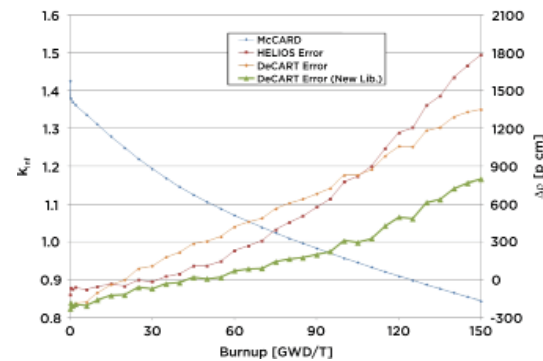


Figure 1. Depletion calculation for the typical VHTR fuel element.

typical VHTR fuel element using this new DeCART library against the k_{∞} obtained with three earlier calculation models: the Monte Carlo depletion code McCARD, HELIOS with the 190-group HELIOS library, and DeCART with last year's 190-group library. Note that the errors of both HELIOS and DeCART increase with burnup, opposite the Monte Carlo solution. However, as the green line in Figure 1 shows, the reactivity error of DeCART with the new library was reduced to about 800 pcm at 150 GWD/T, greatly improved from the 1800 pcm and 1400 pcm at 150 GWD/T errors of HELIOS and the older DeCART, respectively.

Researchers also incorporated three additional features into the DeCART code: a control rod model, the cusping effect treatment, and transient analysis capability based on the 3-D coarse-mesh finite-difference (CMFD) formulation. A simple test calculation was performed with a single-fuel-column model for the purpose of verifying the new capabilities. In the test simulation, the control rod moves from 300 steps to 500 steps in 0.1 seconds and then back to 300 steps in the next 0.1 seconds. As a result, the core power initially increased with rod withdrawal, and then decreased with rod insertion before returning to the initial core power level. These results show that the transient capability is correctly implemented in the DeCART code.

For better computational efficiency, the team developed a new strategy for the decoupled planar method of characteristics (MOC) with thermal feedback. The strategy eliminates additional planar MOC calculations arising from thermal feedback. Numerical tests showed that the error introduced by adopting the new strategy was only a few pcm for eigenvalue and less than one percent for pin power, while the computation time was reduced significantly.

Development of the coupling strategy. The team conducted sensitivity studies to optimize coupled analysis with DeCART/STAR-CD, and demonstrated a coupled analysis of a VHTR core derived from the Next Generation Nuclear Plant (NGNP). Since no reference solutions are available for such a coupled calculation, Argonne verified the coupled system by providing KAERI with the detailed data from the VHTR benchmark problem, allowing for comparison of various solutions between DeCART/STAR-CD (Argonne) and DeCART/CORONA (KAERI). However, a significant amount of work would be required to complete comparisons and conduct a follow-on analysis—more than the time remaining in this project schedule allowed. This actual-size 3-D VHTR problem would be quite helpful in benchmarking the coupled code system, which the researchers are targeting for continued future collaboration.

Verification and validation. The project team built on an earlier DeCART analysis of the 2-D core depletion problem combined with the 47-group HELIOS cross-section library by analyzing the problem again with the new 190-group DeCART cross-section library.

Figure 2 compares the effective multiplication factors (k_{eff}) of DeCART with those of McCARD, a Monte Carlo code with depletion capability. Compared to the Monte Carlo solutions, DeCART underestimates k_{eff} by a maximum of 160 pcm over all burnup steps. The block power errors are a maximum of 2.5% for all burnup steps. Compared to the depletion calculation results with the 47-group HELIOS library, the accuracy of the DeCART solutions, especially k_{eff} , was significantly improved.

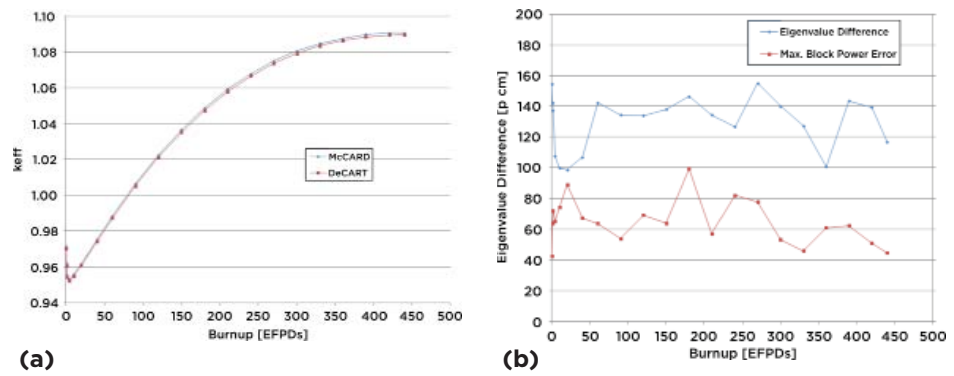


Figure 2. Depletion calculation for the 2-D core problem: (a) effective multiplication factor (k_{eff}) and (b) eigenvalue error and maximum power error.

Using the coupled code system DeCART/CORONA, the team analyzed two seven-column benchmark problems developed last year for coupled analysis. Figure 3 shows the axial power and fuel temperature distributions for one of the problems. Figure 4 shows the relative power distribution at the top plane of the control column and the fuel temperature distribution at the bottom plane of the control column in the other problem. The six data exchanges between CORONA and DeCART were conducted until solutions were converged. The result of the coupled calculation shows the highest power peak at the top due to the temperature feedback and the presence of the top reflector. A small peak at the bottom is due to the presence of the bottom reflector. At the high power peak regions, high temperature peaks are also observed.

The project team validated the DeCART code against the High-Temperature Test Reactor (HTTR) criticality experiments and the Very High-Temperature Reactor Critical Assembly (VHTRC) experiments. The validation results of the MCNP5 and DeCART codes against HTTR and VHTRC experiments overestimated k_{eff} by 2%-3% and about 1%, respectively, compared to the experimental measurements. However, recent nuclear data in JENDL 4.0 (2010) and ENDF/B-VII.1 β 3 (2011) have shown increased capture cross sections of carbon by up to 13.5%. In order to examine the impact of this increase on k_{eff} , the researchers performed Monte Carlo calculations for the two high-temperature reactor experiments using both the previous data (ENDF/B-VII.0) and the 2011 data (ENDF/B-VII.1 b3). For clear comparison, the calculations were conducted twice, once with all ENDF/B-VII.0 data and once using the carbon cross sections from ENDF/B-VII.1 β 3 (while leaving unchanged all other cross sections from ENDF/B-VII.0). Comparison results with MCNP5 calculations using the new carbon cross sections showed significantly reduced k_{eff} —by about 0.9%-1.6% for HTTR and 1.2% for VHTRC. With the new carbon cross-section data, the k_{eff} from DeCART would be in much better agreement with measurements for both experiments.

Planned Activities

This project is complete.

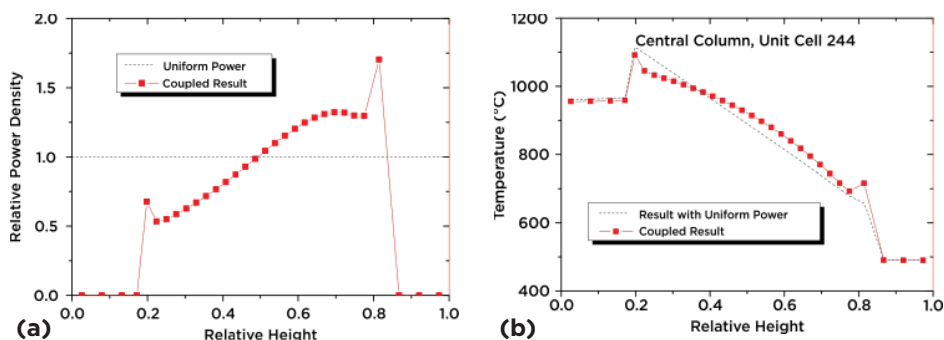


Figure 3. Axial solutions of the coupled calculation for a seven-fuel-column benchmark problem showing (a) axial power distributions and (b) axial fuel temperature distribution.

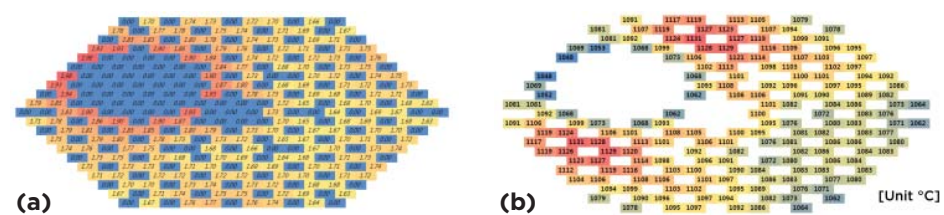


Figure 4. Radial solutions of the coupled calculation for a seven-fuel-column benchmark problem showing (a) relative power density and (b) fuel temperature.

Experimental and Analytic Study on the Core Bypass Flow in a Very High-Temperature Reactor

Research Objectives

This project had three primary objectives: 1) generate experimental data for validating the software for calculating bypass flow in a prismatic very high-temperature reactor (VHTR) core, 2) validate thermofluid analysis tools and improve the model used for analysis, and 3) identify and assess measures to reduce bypass flow. To achieve these objectives, five tasks have been defined:

- Design and construct experiments to generate validation data for software analysis tools.
- Determine the experimental conditions and define the measurement requirements and techniques.
- Generate and analyze the experimental data.
- Validate and improve the thermofluid analysis tools.
- Identify measures to control the bypass flow and assess their performance in experiments.

The specific objectives for the past fiscal year were to:

- Generate experimental data from both air and matched-index-of-refraction (MIR) testing.
- Perform benchmark calculations to validate the analysis model adopted in the thermofluid analysis codes and to improve the model.
- Design test models for bypass flow reduction measures (identified earlier in the project) and verify their performance.

Research Progress

Air test experimental data. The project team generated data to validate core thermofluid analysis code in bypass flow prediction. For this they carried out air tests for both uniform and non-uniform bypass gaps. Testing uniform bypass gaps allowed researchers to evaluate the effect of bypass gap size, while testing non-uniform gaps allowed for investigations of the effect of axial gap distribution on the bypass flow. The uniform bypass gaps were 2 mm or 6 mm with no cross-flow gap.

PI (U.S.): Richard R. Schultz, Idaho National Laboratory

PI (ROK): Min-Hwan Kim, Korea Atomic Energy Research Institute

Collaborators: Argonne National Laboratory, Texas A&M University, Seoul National University

Program Area: Reactor Concepts RD&D

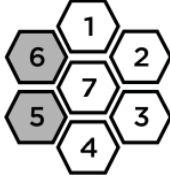
Project Start Date: November 2008

Project End Date: October 2011

The non-uniform gap was selected to mimic the bypass gap distribution estimated for a prismatic reactor, which varies from 6 mm, 2 mm, 4 mm and 2mm from top to bottom. The test section consisted of seven hexagonal block columns: two columns of reflector blocks and five of fuel blocks. Each column had four layers of blocks.

Table 1 shows the flow rate at each column and the total bypass flow ratio for the uniform gaps. The team compared results from computational fluid dynamics (CFD) analysis to check the experimental data's validity. When considering the deviation of bypass gap size, the experimental data show reasonable values equivalent to the CFD results. The team also measured pressure distribution at the coolant channel and the bypass gap and compared results with CFD predictions. Detailed flow distribution obtained from CFD analysis was helpful to explain pressure changes after every block layer. The difference between the two results was small, but it increased as the gap size increased. The project team thus concluded that, in selecting a turbulence model for CFD analysis, experimental data are essential for an accurate prediction of bypass flow.

Table 1. Bypass flow rate at each column and total bypass flow ratio.

Number of Block Column	2-mm Bypass Gap		6-mm Bypass Gap		Non-Uniform Bypass Gap				
	Experiment	CFD	Experiment	CFD	Inlet		Outlet		
					Experiment	CFD	Experiment	CFD	
 Column Bypass Flow (kg/s)	1	0.202	0.209	0.119	0.118	0.150	0.153	0.176	0.209
	2	0.208	0.209	0.122	0.118	0.148	0.153	0.195	0.209
	3	0.206	0.209	0.121	0.118	0.149	0.153	0.192	0.209
	4	0.206	0.209	0.120	0.118	0.151	0.153	0.1917	0.209
	7	0.205	0.209	0.122	0.118	0.144	0.153	0.192	0.209
Inlet Mass Flow (kg/s)		1.234	1.234	1.197	1.197	1.220	1.220	1.220	1.220
Bypass Flow Ratio (%)		16.82	15.01	49.61	50.67	39.08	22.44	37.18	22.44

Blind CFD benchmark for MIR test. Before collecting the MIR experimental data (below), the research teams made a blind benchmark comparison between their respective CFD analyses. INL used the commercial CFD code STAR-CCM+ and KAERI used ANSYS CFX13 to evaluate four gap-size combinations: 2 x 2 mm, 2 x 10 mm, 6 x 2 mm, and 6 x 10 mm. The analyses showed similar magnitudes of pressure differential between the channel and the gap but different pressure variations at the channel entrance with a view of vena contracta. Fully developed velocity profiles were compared with the universal law of the wall. Little difference was observed in the buffer region between the viscous sub-layer and log-layer regions. Comparison of contours for eddy viscosity ratio indicated that the differences are largely due to the prediction of turbulent flow behavior at the entrance.

MIR test experimental data. The project team collected a reference data set of stereo particle image velocimeter (PIV) images along the centerlines of three coolant channels, downstream, at a mid-level Reynolds number. No gap was involved when collecting the reference data. The bypass flow model and stereo PIV systems, which are performing as designed, have produced a reference data set for a Reynolds number of about 2800 based on coolant channel hydraulic diameter, such as shown in Figure 1. The data set will be used to refine the study parameters for collecting standard problem validation data sets.

Bypass experiments. Researchers at Texas A&M University set up an open-loop air flow experiment to measure volume flow rates through all flow passages in a prismatic core model. The team measured total flow rate, flow rate through each prismatic block, and flow rates through bypass gaps of three widths: 6.10 mm, 4.66 mm, and 3.21 mm. Two sets of air flow experiments were performed for each gap width; Figure 2 on the next page shows typical results. These data will be used for limited validation studies.

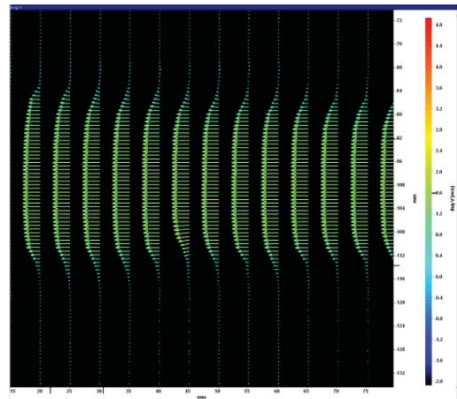


Figure 1. Bottom channel mean vector display.

Model improvement of GAMMA+ code. The project team modified a multichannel flow model that has been developed to represent the two-dimensional flow distribution found in the bypass gap to include convective and viscous terms. The normal junction momentum is used at the flow paths in the vertical direction, and the cross junction momentum is used at the flow paths in the lateral direction. The team tested the model for two-dimensional flow distribution and found that the new network model provided improved prediction of cross-flow velocity—similar to three-dimensional results.

In FY 2009, the project team found that a merging flow characteristic at the intersection of coolant channel and cross gap is an important factor in accurately predicting bypass flow. To model the flow, the team used a handbook calculation for form loss—a function of flow and area ratio—for diverging and converging wye. The team performed simple multiblock analysis to investigate the new model's performance and analyzed the air test with the improved GAMMA+ code. The comparison showed that pressure distribution and bypass flow prediction using the GAMMA+ code was reasonably good, although when axially variant, the bypass flow at the inlet was slightly under-predicted.

Model improvement and validation for GAS-NET code. Improvements were made to both the GAS-NET code's fluid flow and its heat transfer modeling capabilities. The channel loss correlation was extended from a single Blasius-type model for all channels to a model specific to each of the four channel types and at each block level. The channel types are block coolant hole, axial flow in inter-column gap, lateral flow in inter-column gap, and lateral leakage flow between two stacked blocks. For each of these channels and at each axial level, a user can select fit of the Darcy friction factor $f = C/Re^n$ to the Zigrang-Sylvester correlation at a given surface roughness. In addition, a capability has been added to model both fueled blocks, where the dominant heat transfer phenomena are internal heat generation and conduction to the block outer surface, and non-fueled blocks where the dominant phenomenon is radial heat conduction through the block.

Results of validation studies performed using data from an isothermal experiment in the Multi-Block Air Test Facility at Seoul National University showed that significant future effort will be needed to generate loss coefficient values if these codes are to reliably predict the pressure losses encountered in prismatic cores. Comparison of project data to RELAP5 calculations demonstrated that the RELAP5-type model better approximates a finite difference representation of the phenomena and, as a result, led to the development of a separate heat transfer model for unheated elements in the GAS-NET code.

Prismatic core and hot spot analysis. The research team investigated how replacing side reflectors affects the flow distribution and hot spot, assuming that reflector blocks are replaced every other refueling. Results of a recalculated gap size distribution for the PMR200 core indicated that the gap grew larger when the side reflector was not replaced, as irradiation over multiple cycles shrinks the reflector blocks more than the fuel blocks. If the reflectors are replaced every two cycles, the gap size in the side reflector region decreases.

The team conducted hot spot analysis for the new gap distribution. Researchers improved the GAMMA+ analysis model by 1) inserting flow channels between the permanent side reflectors and the core barrel for a conservative hot spot temperature prediction, 2) eliminating small flow nodes at the Y-shaped joint for numerical stability, 3) introducing a multi-channel model to represent a two-dimensional flow field, and 4) accounting for form loss at the converging and diverging wye. The new results showed little variation from the old results: the core restraint still reduces the maximum kernel temperature by 130°C and enhances the core thermal margin.

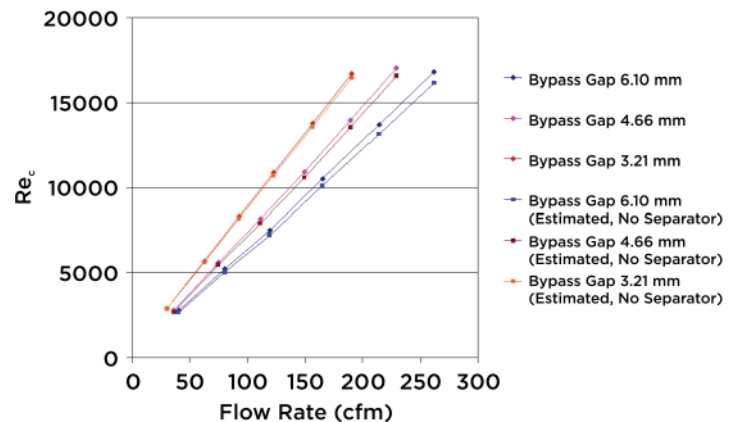


Figure 2. Reynolds number of flow through coolant channel.

Bypass flow reduction measures. In FY 2009, the project team identified measures for reducing bypass flow. The team conducted a design study to evaluate these measures in not only experiments but also an actual reactor core. Figure 3 shows modified blocks for the performance tests, which took place in the air test facility. The team used CFD analysis design optimization to determine the shape of the grooved reflector wall. Test results indicated that the staggered arrangement of transition blocks could block most of the bypass flow in the bottom region, and the grooved reflector reduced the bypass flow ratio at the exit from 22% to 14% for a non-uniform gap distribution. The team conducted CFD analysis to support the experimental data analysis. Pressure distribution and channel flow rate were also measured to provide additional data for the code validation.

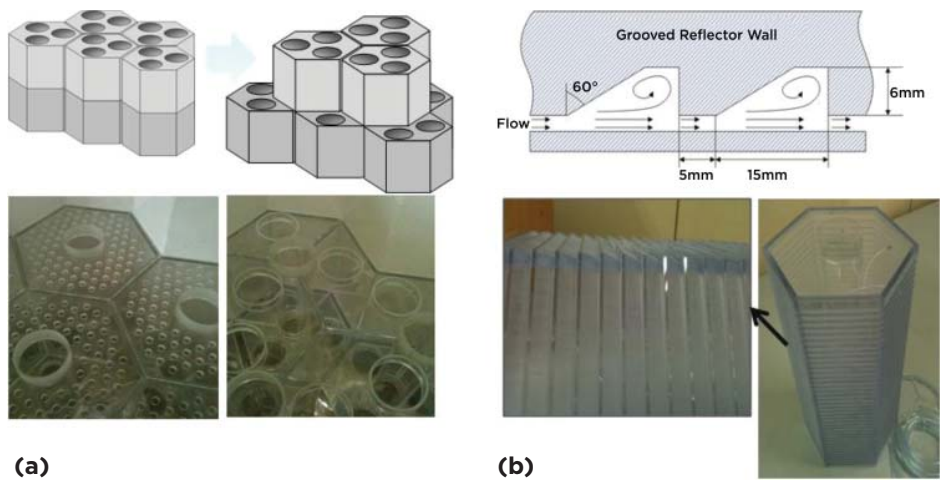


Figure 3. Modified blocks for the performance test of bypass flow reduction measures: (a) staggered transitional blocks and (b) a grooved side reflector wall.

Planned Activities

This project is complete.

Nuclear Data Uncertainty Analysis to Support Advanced Fuel Cycle Development

Research Objectives

The main objective of this collaboration was to provide improved neutron cross-section data with uncertainty or covariance data for isotopes important for advanced fuel cycle and nuclear safeguards applications. An additional objective was to assess uncertainties of the nuclear integral parameters due to the cross-section data. The goals are to improve safety validation and to reduce capital cost through system design optimization.

Research Progress

During the last three years, project teams from Oak Ridge National Laboratory (ORNL) and the Korea Atomic Energy Research Institute (KAERI) have worked to identify priority nuclides that need improved nuclear data with uncertainty information for advanced fuel cycle applications. Factors included importance for advanced fuel cycle and safeguards applications, discrepancies among the data libraries and experiments, and evaluation year. The project has completed comprehensive analyses and selected neptunium-237 (^{237}Np), plutonium-240 (^{240}Pu), and curium (Cm) isotopes for development of improved cross-section data, including covariance data.

ORNL has completed a resonance-region cross-section evaluation with covariance data for ^{237}Np and ^{240}Pu . Also, $^{242-248}\text{Cm}$ covariance data have been generated from the resonance parameters of JENDL-4.0. Likewise, KAERI has evaluated the cross-section data with covariance data above the resonance region for the noted isotopes.

Evaluations of ^{237}Np , ^{240}Pu and curium isotope data. The new ^{240}Pu evaluation was obtained by replacing the ENDF/B-VII.0 resonance parameters with the new resonance parameters and by adding the resonance parameter covariance matrices (RPCMs). In this evaluation, new experimental transmission data were added to the experimental database. These new data are the neutron transmission measurements that Harvey and Gwin obtained at the Oak Ridge Electron Linear Accelerator (ORELA) in 1988 and which were recently discovered in the ORELA archives. Calculated with the new resonance parameters, the total cross-section value at 0.0253 eV is 284.05 barns, which is in agreement with the Spencer experimental

PI (U.S.): Michael E. Dunn, Oak Ridge National Laboratory

PI (ROK): Choong-Sup Gil, Korea Atomic Energy Research Institute

Collaborators: None

Program Area: FCR&D

Project Start Date: November 2008

Project End Date: October 2011

data but is significantly smaller than the value of 289 barns recommended by the *Atlas of Neutron Resonances*. Consequently, the capture cross-section value at 0.0253 eV is also smaller than the recommended value provided by the *Atlas*. The capture resonance integrals calculated with the PUFF-IV covariance processing software in the energy range 0.5 eV to 7.7 keV are 8,479 barns, 8,480 barns, and 8,492 barns for the present evaluation, JEFF-3.1.1, and ENDF/B-VII.0, respectively.

KAERI has evaluated the ^{240}Pu cross sections above the resonance energy region with the EMPIRE code. The evaluation used experimental data for total, elastic, inelastic, capture and fission from EXFOR. The fission probability has been incorporated into the statistical model that describes particle emissions. With several fission models available, the researchers chose one that accounted for the transmission derived in the WKB (Wentzel-Kramers-Brillouin) approximation within an optical model through a double-humped fission barrier. The new resonance parameters and RPCMs generated by ORNL and the high-energy cross-section and covariance data evaluated by KAERI for ^{240}Pu were combined to create a complete ENDF-formatted file.

The new ^{237}Np evaluation represents an improvement over the existing evaluation because the energy limit of the resonance region has been extended up to 1 keV. As a result, the evaluation provides a set of resonance parameters that describe the experimental total, capture, and fission cross sections. To extend the new evaluation above 500 eV, total cross-section data derived from ORELA high-resolution transmission measurements by Auchampaugh were used. The transmission data were obtained by cross-section measurements on a ^{237}Np sample cooled to 77 K, thereby enabling better energy resolution. In addition to the Auchampaugh data, total cross-section measurements from Paya were also used. In addition to the total cross-section data, researchers used fission cross-section measurements performed by Paradela at the neutron time-of-flight (n_TOF) facility located at the European Organization for Nuclear Research (CERN) center. Two sets of capture cross-section data measured by Weston and Hoffman were used in the evaluation. The resonance parameters were obtained using the generalized least-squared approach of the SAMMY software to fit the experimental cross-section data. The ^{237}Np RPCM data generation was obtained with SAMMY as part of the evaluation process. The new ^{237}Np cross-section data above the resonance region have been generated with experimental data for total, elastic, inelastic, capture, fission, and (n,2n) and (n,p) cross sections. To generate the ^{237}Np covariance data, the team used sensitivity matrices generated with the EMPIRE code. To obtain the sensitivity matrices, about 15 of the most relevant model parameters (optical model, level densities, and the strengths of fission barriers) were varied independently $\pm 10\%$ around their optimal value to determine the effect on total, elastic, inelastic, capture, fission, (n,2n) cross sections in the full energy range of the evaluation. Consequently, sensitivity matrix elements were calculated as a change of a given reaction cross section in response to the change of the particular model parameter.

All curium isotope cross-section data for the resonance energy range were taken from JENDL-4.0, and the KAERI team has newly evaluated the cross-section data including covariance data above the resonance energy range with EMPIRE/KALMAN software. The ORNL team generated covariance data in the resonance region using the SAMMY code.

Comparisons of the new evaluated data with other data evaluations. The ^{237}Np capture cross section at 0.253 eV of ENDF/B-VII.0 is about 10% smaller than the new evaluation and JENDL-4.0 data. The elastic resonance integral of the new data is about 5% smaller than ENDF/B-VII.0 and JENDL-4.0. The capture cross sections around 1 MeV for the new data are smaller than ENDF/B-VII.0. The ^{237}Np fission cross-section data of the new evaluation are larger than ENDF/B-VII.0. The ^{240}Pu thermal elastic cross section of ENDF/B-VII.0 is 0.95 barns, while it is 2.67 barns in the new evaluation and JENDL-4.0. The ^{240}Pu elastic resonance integral of ENDF/B-VII.0 is over 5% smaller than the new data and JENDL-4.0. The ^{240}Pu capture cross sections above 100 keV show large discrepancies among the nuclear data libraries. The ^{244}Cm thermal cross sections of the new ENDF/B-VII.0 and JENDL-4.0 evaluations are almost the same because the new ^{244}Cm cross-section data in the resolved resonance region are taken from JENDL-4.0, and ENDF/B-VII.0 has been obtained from JENDL-3.3. The ^{244}Cm capture resonance integral of ENDF/B-VII.0 is about 5% larger than the new data and JENDL-4.0. The new ^{244}Cm capture data are smaller than ENDF/B-VII.0, especially above 100 keV. Figure 1 on the next page provides comparisons of the capture and fission cross sections among the data libraries.

Validation of the new data. In general, the small contribution of the nuclides to the estimation of k-effective (k_{eff}) makes it difficult to find appropriate benchmark problems for testing the cross-section and covariance data of minor actinides. Nonetheless, the new evaluated data have been tested using appropriate benchmarks. In order to test the new cross-section data, the project team selected two benchmarks each for ^{237}Np and ^{240}Pu , and one benchmark for ^{244}Cm from the “International Handbook of Evaluated Criticality Safety Benchmark Experiments” (IHECSBE). The benchmarks used for testing data performance for fast systems were FLATTOP-Np237-1, -3 for the new ^{237}Np data; Pu239-, Pu240-JEZEBEL for ^{240}Pu data; and CM244-JEZEBEL for ^{244}Cm data. Very small amounts of ^{237}Np (<0.5%) and ^{244}Cm (<0.05%) were contained in the FLATTOP-Np237-1, -3, and Cm244-JEZEBEL benchmarks, respectively. The Pu239-JEZEBEL (<5% ^{240}Pu) and Pu240-JEZEBEL (~20% ^{240}Pu) benchmarks contain relatively large amounts of ^{240}Pu . The uncertainties in k-effective values due to the cross-section data were also estimated using the available covariance data. To test the covariance data of the new evaluations, researchers estimated the uncertainties in k_{eff} due to the new covariance data of each isotope. The calculated k_{eff} in the benchmarks are shown in Table 1. Because the benchmarks have relatively small amounts of ^{237}Np , ^{240}Pu , and ^{244}Cm , except Pu240-JEZEBEL (20.1% ^{240}Pu), the effects of the new cross-section data are not distinguishable. The fast energy region fission cross sections of the new ^{240}Pu data are slightly larger than those in ENDF/B-VII.0. The k-effective in Pu240-JEZEBEL benchmark with the new ^{240}Pu data is about 0.3% larger than in ENDF/B-VII.0. The k-effectives with the new ^{240}Pu data in Pu240-, Pu239-JEZEBEL benchmarks show very good agreement with experiments relative to the other data libraries. The project team has performed additional testing with the new evaluations.

Table 1. The k-effective values in the benchmarks with the nuclear data libraries.

Isotopes	Benchmarks	JENDL 3.3	New Data (ORNL/KAERI)	ENDF/B-VII.0	JENDL-4.0
^{237}Np	FLATTOP-Np237-1	0.98883	0.98895	0.98883	0.98884
	FLATTOP-Np237-3	1.00365	1.00370	1.00363	1.00364
^{240}Pu	Pu239-JEZEBEL	0.99634	0.99647	0.99587	0.99571
	Pu240-JEZEBEL	0.99927	1.00002	0.99715	0.99613
^{244}Cm	Cm244-JEZEBEL	0.99921	0.99920	0.99921	0.99921

Planned Activities

The I-NERI project has concluded, and the evaluation work was completed in accordance with the project objectives.

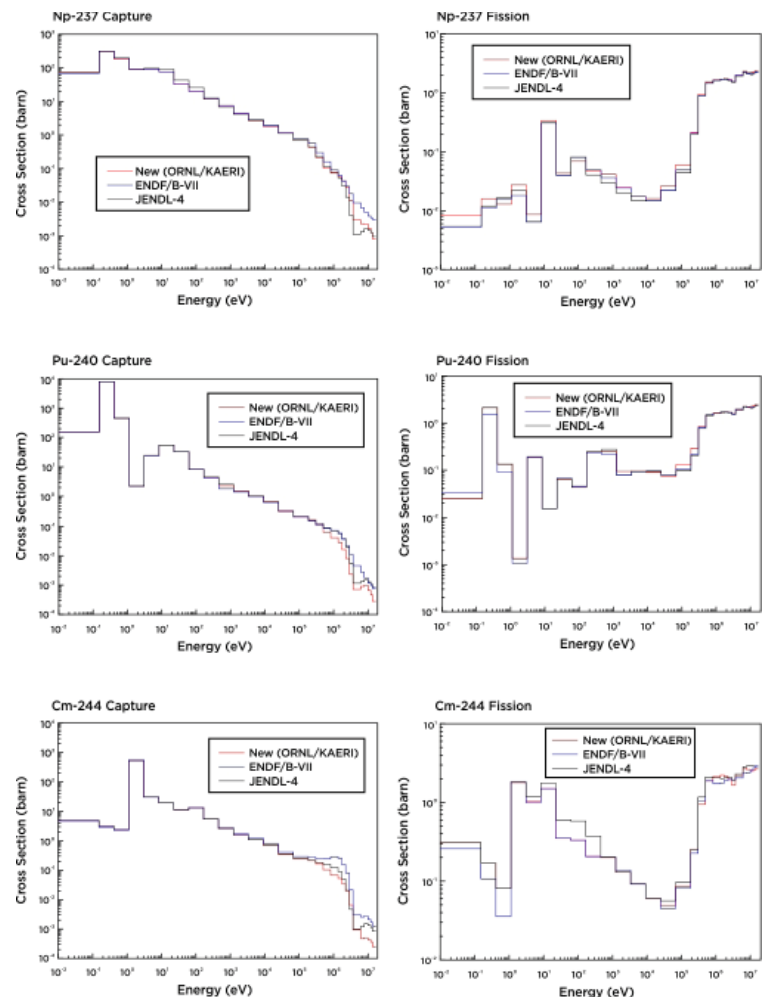


Figure 1. Comparisons of capture and fission cross sections of the ^{237}Np , ^{240}Pu and ^{244}Cm data.

ZPPR-15 and BFS Critical Experiments Analysis for Generation of Physics Validation Database of Metallic-Fueled Fast Reactor Systems

PI (U.S.): Richard McKnight, Argonne National Laboratory

PI (ROK): Sang Ji Kim, Korea Atomic Energy Research Institute

Collaborators: Korea Advanced Institute of Science and Technology

Program Area: Reactor Concepts RD&D

Project Start Date: November 2009

Project End Date: October 2012

Research Objectives

This collaborative research program comprises two related research areas designed to advance the physics and modeling of metallic fuel and transuranics for fast reactors. First, the project team will archive the Zero Power Plutonium Reactor (ZPPR)-15 physics experiment database, loading records for Phases A, B, C, and D. Researchers will use this data to generate high-fidelity as-built Monte Carlo models that allow these valuable metallic fuel measurements to contribute fully to reducing uncertainties in validating advanced computational methods and design analysis methods.

Second, the team will set up an experimental plan and develop models to study the physics of a transuranic (TRU) burner reactor. The last 20 years have seen a considerable evolution in the fast reactor core concept. Physics experiments will validate design features specific to a typical TRU burner core and produce valuable high-fidelity models. The experimental plan will cover the physics areas that the ZPPR-15 physics experiment did not, while considering licensing requirements for a commercial reactor.

Research Progress

Generation of the ZPPR-15B experimental database. In the project's first year, the project team at Argonne National Laboratory (ANL) compiled and analyzed the ZPPR-15A experimental database and provided the data to the team at the Korea Atomic Energy Research Institute (KAERI). In return, KAERI provided a detailed description of the BFS-73-1 experiments. ANL has now independently verified the accuracy of the as-built BFS-73-1 model, compiled all of the loading information for the ZPPR-15B experiments, and generated detailed as-built Monte Carlo models for 6 of the 12 planned ZPPR-15B experimental configurations. These experiments have been analyzed with continuous-energy Monte Carlo using VIM and MCNP5 with ENDF/B-VII.0 data. Results with ENDF/B-VII.0 are good, although slightly under-predicting k_{eff} values by approximately 200 percent millirho (pcm). Sodium void reactivity results with ENDF/B-VII.0 data are generally within about 5%–10%. The positive worths of voiding the central zones are slightly underpredicted. Furthermore, the performance of the ENDF/B-VII.0 data for ZPPR-15B was consistent with ZPPR-15A, indicating that the zirconium evaluation had good performance for these experiments.

Compilation of physics experiments at the Russian BFS facility. The KAERI team used archived information to develop a detailed as-built Monte Carlo model of the BFS-75-1 critical experiment that was conducted at the Institute of Physics and Power Engineering (IPPE) in Russia, and delivered the model to ANL. This model was evaluated using five nuclear data files: ENDF/B-VII.0, JEFF-3.1, JENDL3.3, JENDL-AC2008, and ENDF/B-VI.6. The resulting k_{eff} using the ENDF/B-VII.0 library was in a reasonable agreement—within 350 pcm Δk —with the measured value. Spectral indices using ENDF/B-VII.0 demonstrated significant improvement, especially in the fission reactions of U-238, Np-237 and Am-241.

KAERI is carrying out a related a TRU burner physics experiment in the BFS-2 facility at IPPE. Scheduled experimental work is completed, including the measurement of critical mass, spectral indices, control rod worth, and sodium void reactivity. A draft final report on the experimental results has been delivered to KAERI and is now under review. Among other relevant results, this experiment will make available a reference as-built Monte Carlo model.

Analysis of ZPPR-15 experiments.

The KAERI team analyzed seven ZPPR-15A configurations representing sodium void reactivity worth using various approximations of the drawer master. In addition to evaluating integral parameters, researchers analyzed the reaction balances of unit drawer models and compared results with as-built drawer models. The proposed one-dimensional drawer master model reproduced not only k_{eff} but also reaction rate by plate.

Researchers analyzed ZPPR-15A benchmark configurations for the one-dimensional drawer model and the homogeneous model with corresponding bias due to the change in drawer model. The analyses employed deterministic code system TRANSX/CRX-1D/THREEDANT. Neutron flux by plate was calculated using the CRX-1D solver developed in the first year of this project, and results were incorporated in the TRANSX code to handle heterogeneous self-shielding. Comparing the MCNP and THREEDANT calculations for the homogeneous model, the difference in calculated k_{eff} was about 390 pcm Δk for the configuration of control rod worth and around 120 pcm Δk for sodium void reactivity. When one-dimensional drawer models are used, the difference between MCNP and THREEDANT becomes larger, about 570–740 pcm Δk .

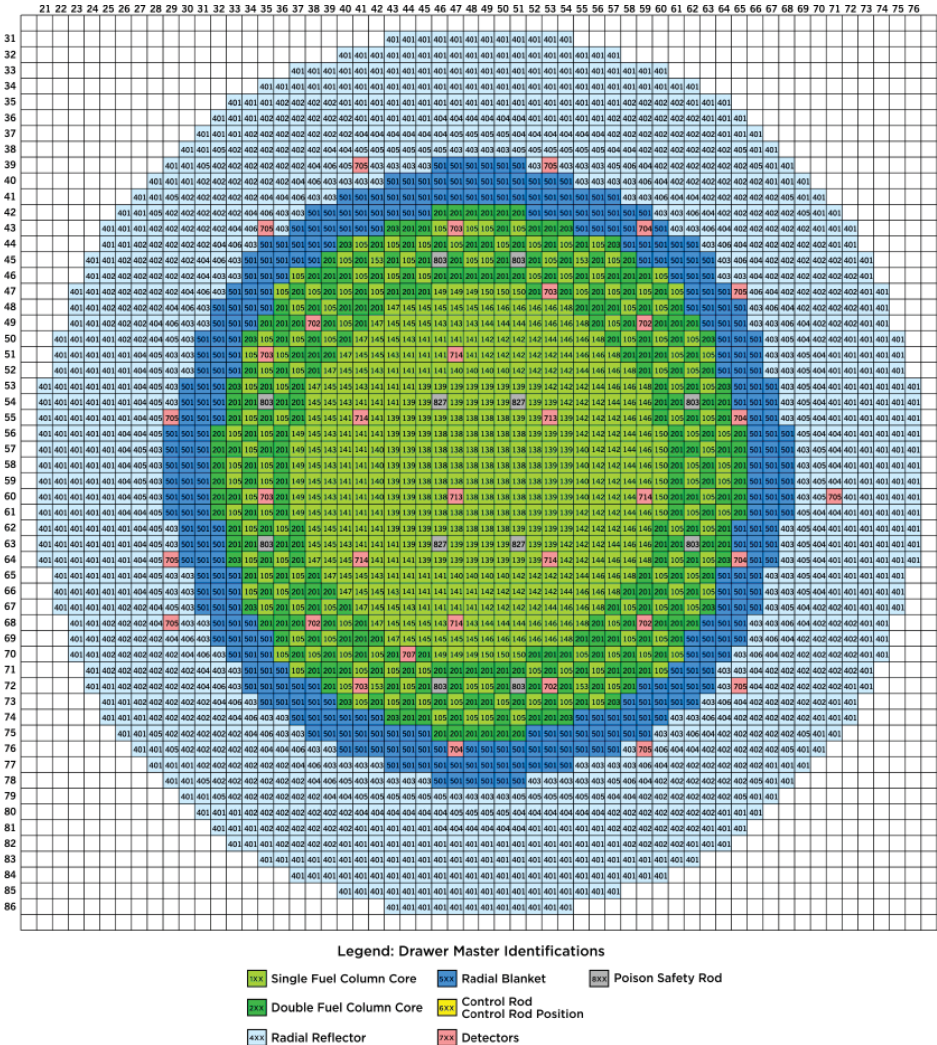


Figure 1. Core map of ZPPR-15A Loading 88.

The ANL team archived and transferred to KAERI as-built Monte-Carlo models and input decks for six loading configurations, representing the critical reference and sodium voided configurations, out of ZPPR-15 Phase B experiments. KAERI completed the analysis of models representing inner core and voided inner core drawer masters. This effort enabled the researchers to identify an appropriate one-dimensional model that accounts for the complex plate heterogeneity of ZPPR-15 drawer masters. Researchers then modeled the additional 25 drawer masters loaded into six configurations as one-dimensional plate geometries and compared the results with corresponding as-built configurations. The difference between the one-dimensional and as-built models was around 300 pcm Δk throughout the six configurations.

The team has also identified and addressed a weakness in that the design code did not sufficiently address cell heterogeneity. KAERI has now developed a transport theory-based two-dimensional neutron flux solver, equipped with a flux-volume homogenization routine, that will accurately account for the 2-D heterogeneity effect of the ZPPR-15 subassemblies.

Planned Activities

The team has generated detailed as-built Monte Carlo models for six of the twelve planned configurations of ZPPR-15B experiments and has analyzed five of these configurations. In FY 2012, the team plans to complete models for the remaining control worth configurations and analyze them. Additional effort on the ZPPR-15B database will also be required to identify the remaining experimental measurements and their uncertainties. The team will archive the remaining ZPPR-15C and -15D experimental data and will continue efforts to identify additional ZPPR-15 experimental measurements and their uncertainties.

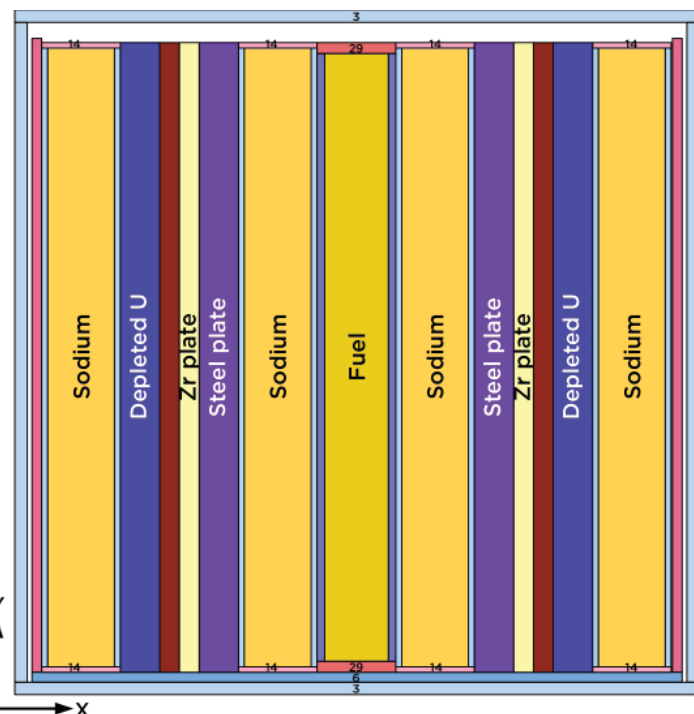


Figure 2. Plate loading of a ZPPR-15B inner core drawer.

Enhanced Radiation Resistance through Interface Modification of Nanostructured Steels for Gen IV In-Core Applications

Research Objectives

The objective of this project is to increase radiation tolerance in candidate alloys for Generation IV (Gen IV) fuel cladding through optimization of grain size and grain boundary characteristics. The focus is on nanocrystalline metal alloys with a face-centered cubic (fcc) crystal structure. The long-term goal is to design and develop bulk nanostructured austenitic steels with enhanced void swelling resistance, substantial ductility, and enhanced creep resistance at elevated temperatures through a combination of grain refinement and grain boundary engineering. This approach allows the project team to tailor the material strength, ductility, and resistance to swelling by 1) changing the sink strength for point defects, 2) increasing the nucleation barriers for bubble formation at grain boundaries, and 3) changing the precipitate distributions at boundaries.

Compared to ferritic–martensitic steels, austenitic steels possess good creep and fatigue properties at elevated temperatures and better toughness at low temperatures. However, a major disadvantage of austenitic steels is their vulnerability to significant void swelling in nuclear reactors, especially at the temperatures and doses anticipated in the Gen IV reactors. Because of the lack of resistance to void swelling in austenitic alloys, ferritic–martensitic steels became the preferred material for fast reactor cladding applications. However, Oak Ridge National Laboratory recently developed a high-temperature ultrafine precipitate-strengthened (HT-UPS) austenitic stainless steel that is expected to show enhanced void swelling resistance through the trapping of point defects at nanometer-sized carbides. Reducing the grain size and increasing the fraction of low-energy grain boundaries should reduce the available radiation-induced point defects because of the increased sink area of the grain boundaries, make bubble nucleation at the boundaries less likely by reducing the fraction of high-energy boundaries, and improve the strength and ductility under radiation by producing a higher density of nanometer-sized carbides on the boundaries. Although this project focuses on void swelling, advances in processing of austenitic steels are also likely to produce improved mechanical properties with better radiation response.

Research Progress

In the project's second year, the team made several major advances, briefly described on the following pages.

PI (U.S.): Todd R. Allen, University of Wisconsin-Madison

PI (ROK): Jinsung Jang, Korea Atomic Energy Research Institute

Collaborators: Seoul National University, Texas A&M University, University of Florida

Program Area: FCR&D

Project Start Date: October 2009

Project End Date: September 2012

Fe-14Cr-16Ni alloys. Researchers performed equal channel angular processing (ECAP) on Fe-14Cr-16Ni alloys and then examined the deformation mechanisms in the resulting samples. The process refined the average grain size from 700 microns (μm) down to approximately 400 nanometers (nm). The yield strength of ECAPed alloys is five to six times greater than coarse-grained (CG) alloys, while the ductility remains very high with about 15% uniform elongation. Furthermore, these ultrafine-grained (UFG) alloys retain strong work hardening capacity, a rare phenomenon for most ECAPed alloys. The strain rate sensitivity of the alloys is lower than that of bulk alloys.

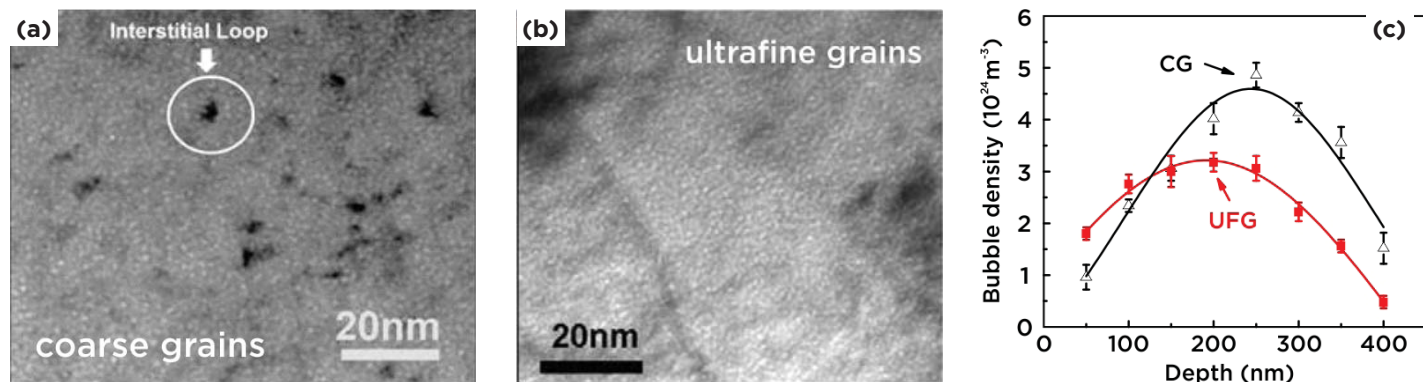


Figure 1. Cross-sectional TEM micrograph of Fe-Cr-Ni alloy irradiated with He ion at 150 keV and a fluence of $6 \times 10^{16} \text{ cm}^{-2}$: (a) CG alloys with grain sizes of 700 μm show high density of bubbles and interstitial loops (black dots); (b) UFG alloys with grain sizes of ~ 400 nm have lower density of He bubbles and no dislocation loops. (c) Helium bubble density is evidently lower in UFG alloys than in CG alloys.

The project team also examined helium ion irradiation resistance of the UFG Fe-14Cr-16Ni alloys. At a peak fluence level of 5.5 displacements per atom (dpa), helium bubbles of 0.5 nm to 2 nm in diameter were observed in both CG and UFG alloys. Compared to the CG alloy, the UFG alloy showed significantly reduced density of helium bubbles and dislocation loops, as well as radiation hardening. The results imply that radiation tolerance in bulk metals can be effectively enhanced by refinement of microstructures.¹

The team performed *in situ* krypton irradiation on the ECAPed Fe-14Cr-16Ni alloys. These studies show that the dislocation loop density in ECAPed alloys is much lower than in the as-received CG alloys (see Figure 2). Furthermore, no defect denuded zone was observed along grain boundaries in UFG specimens. This may be related to the fact that the 400 nm grain size exceeds TEM foil thickness of 100 nm, which results in the foil surfaces acting as defect sinks.

304L and 316L Stainless. Researchers performed ECAP on samples of 304L and 316L stainless steels and are now studying the microstructure and tensile behavior of these alloys. The final products have an average grain size of about 100 nm, and the grains are mostly equiaxed. Results of microstructure and tensile behavior studies thus far indicate that ECAP induces significant strengthening in these alloys. The team also performed torsion studies of 316L stainless steel.

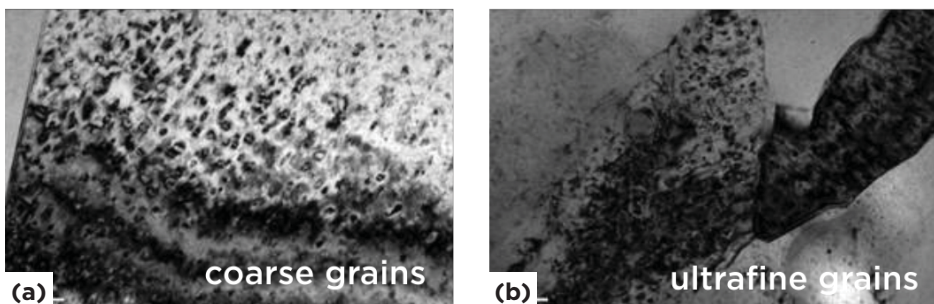


Figure 2. Microstructural evolutions in (a) CG and (b) ECAPed UFG alloys during *in situ* krypton radiation at 400°C up to 5 dpa (experiments performed at Argonne National Laboratory's IVEM facility). UFG alloys clearly had much lower dislocation loop density and smaller dislocation loop size.

¹ Yu, K.Y., Liu, Y., Sun, C., Wang, H., Shao, L., Fu, E.G., Zhang, X., "Radiation damage in helium ion irradiated nanocrystalline Fe," J. Nucl. Mater, In Press, 2011.

Oxide dispersion-strengthened alloys. Researchers prepared several oxide dispersion-strengthened (ODS) alloys via consolidation of mechanically alloyed powders, then performed ECAP on the consolidated bars. Preliminary microscopy studies show moderate grain refinement and uniform dispersion of nanometer-scale oxide particles. The results of microstructure and hardness investigations of ECAP-processed ODS alloy 2103/2B700, as shown in Figure 3, demonstrate that ECAP can refine the microstructure and introduce high-angle grain boundaries. The research team also initiated studies of PM2000 alloys. Alloy test results are still being analyzed.

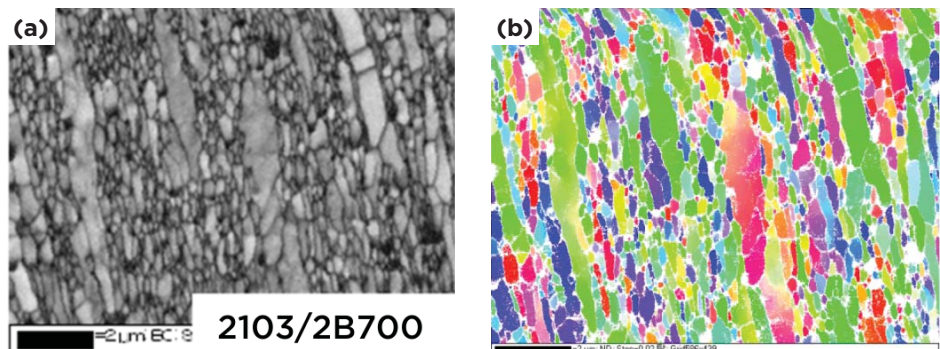


Figure 3. Microstructural ECAPed 2103 ODS alloys show (a) grain refinement and (b) the formation of predominantly high-angle grain boundaries.

Planned Activities

The project will continue to examine helium- and krypton-radiation-induced damage in austenitic steel and will perform mechanical testing of ECAPed ODS steels. In particular, researchers will:

- Determine and conduct proper heat treatment to engineer the grain boundaries of austenitic steels.
- Investigate the mechanical behavior of the ECAPed ODS alloys.
- Perform proton irradiation on the ECAPed alloys and investigate radiation damage.
- Perform *in situ* krypton radiation using TEM.

Investigation of Electrochemical Recovery of Zirconium from Spent Nuclear Fuels

PI (U.S.): Michael Simpson, Idaho

National Laboratory

PI (ROK): Il-Soon Hwang, Seoul

National University

Collaborators: Korea Atomic Energy Research Institute, University of Idaho

Program Area: FCR&D

Project Start Date: December 2010

Project End Date: November 2013

Research Objectives

This project uses both modeling and experimental studies to design optimal electrochemical technology methods for recovery of zirconium (Zr) from spent (used) nuclear fuel for waste management. The objectives are to provide a means of efficiently separating zirconium into metallic high-level waste forms and to support development of a process for decontamination of Zircaloy hulls to enable their disposal as low- and intermediate-level waste. Modeling work includes an extension of a three-dimensional model previously developed by Seoul National University for uranium electrorefining, adding the ability to predict zirconium behavior. Experimental validation activities include molten salt zirconium recovery tests and aqueous tests using surrogate materials.

Research Progress

The project team has performed a literature review of physical, chemical, and thermodynamic properties of zirconium and its chloride salts in the LiCl/KCl eutectic salt system. As zirconium tetrachloride ($ZrCl_4$) is the most stable and predominant salt species at 500°C, available data on $ZrCl_2$ is limited. Neither pure $ZrCl_2$ nor pure $ZrCl_4$ exists in a molten state at atmospheric pressure, with solid $ZrCl_2$ decomposing at 350°C and solid $ZrCl_4$ subliming at 331°C. The diffusion coefficient of Zr^{4+} , calculated via a correlation through a capillary method at 500°C, is $1.13 \times 10^{-9} \text{ m}^2/\text{s}$. There are no readily available published values for the divalent

$ZrCl_2$ molecule's diffusion coefficient in the LiCl/KCl eutectic salt, although zirconium's standard reduction potential and activity coefficient have been reported in the literature.

The project team designed and set up an experiment to determine parameters (e.g., diffusion coefficient, standard reduction potential, activity coefficient and exchange current density) important to the electrochemical recovery of zirconium in a molten LiCl/KCl eutectic salt (see Figure 1).

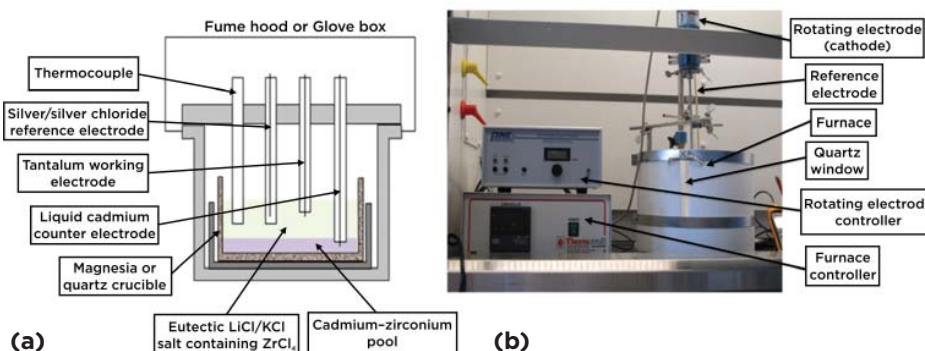


Figure 1. (a) The experimental design for the electrochemical recovery of zirconium; (b) the setup for zirconium recovery experiments.

Since Zircaloy-4 alloy cladding consists of various elements including zirconium, tin, chromium and nickel, numerous activation products are generated during irradiation. However, increasing the number of elements in a three-dimensional simulation requires substantially more expensive computational resources and modeling complexity, which can require a trade-off in computational accuracy. Therefore, to conduct three-dimensional simulation more efficiently, the researchers employed the computational codes ORIGEN-2 and REFIN to pre-select key elements for irradiated Zircaloy-4 cladding electrorefining. The team used ORIGEN-2 to investigate the amount and radioactivity of activation products in irradiated Zircaloy-4 cladding (see Figure 2). All activation products meet the criteria for low- and intermediate-level waste after three years' cooling. However, some nuclides—including ^{60}Co , ^{125}Sb and ^{93}Zr —have higher radioactivity than their clearance level. Also, Rudisill's research estimates that there could be about 1 g of uranium and 14 mg of plutonium in 1 kg of Zircaloy cladding.¹

The researchers then selected elements that could be codeposited with zirconium during Zircaloy-4 electrorefining. Using REFIN, the team conducted one-dimensional transient electrorefining simulations to examine major constituent elements, including activation products and actinides within irradiated Zircaloy-4. Along with major elements of Zircaloy-4, cobalt and uranium were utilized as composition elements of irradiated cladding to reflect activation products and actinides, respectively. Since tin (Sn),

chromium (Cr) and cobalt (Co) are more reductive than zirconium at the initial stage of electrorefining, Sn^{2+} , Cr^{2+} and Co^{2+} , which are contained in initial molten salt, are reduced on the cathode with zirconium deposition. Because of zirconium depletion in the molten salt and anode, other elements are deposited on the cathode during the last stage of electrorefining. However, since uranium and iron are much more oxidative than other elements, uranium is not deposited on the cathode in all simulation scenarios. Based on the ORIGEN-2 and REFIN simulations, the researchers determined that cobalt could be one of key elements in irradiated Zircaloy-4 electrorefining from the aspect of radioactivity and purity of recovered zirconium. Using the REFIN code, the research team also examined how the decontamination factor for cobalt was affected by diffusion boundary layer thickness and the initial concentration of Co^{2+} (see Figure 2).

The project team is developing an electrorefining model that can simultaneously handle both multispecies electrochemical reactions and fluid dynamics calculations. The team examined the model's capability to demonstrate the effects of electrochemical parameters, including exchange current density, transfer coefficient and equilibrium potential. Researchers conducted two-dimensional electrochemical reaction simulations on a rotating cylinder hull (RCH) cell geometry using two arbitrary ions, assuming tertiary distribution, and applying the concentration-modified Bolmer-Volmer equation to calculate overpotential distribution. The developed model shows good capability to handle not only electrochemical kinetic parameters, including exchange current density, but also equilibrium potential (see Figure 3). When two ions have different equilibrium potential, the model predicts local deposition according to the cathode's location.

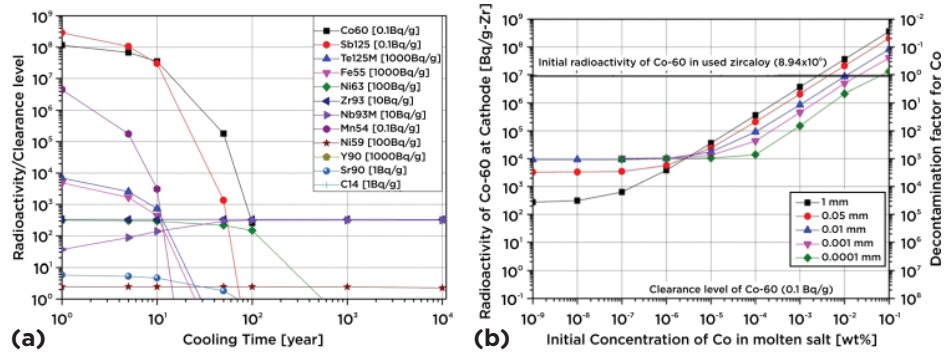


Figure 2. (a) Radioactivity of activation products within Zircaloy-4 cladding, and (b) the decontamination factor for cobalt according to diffusion boundary layer and initial concentration of Co^{2+} .

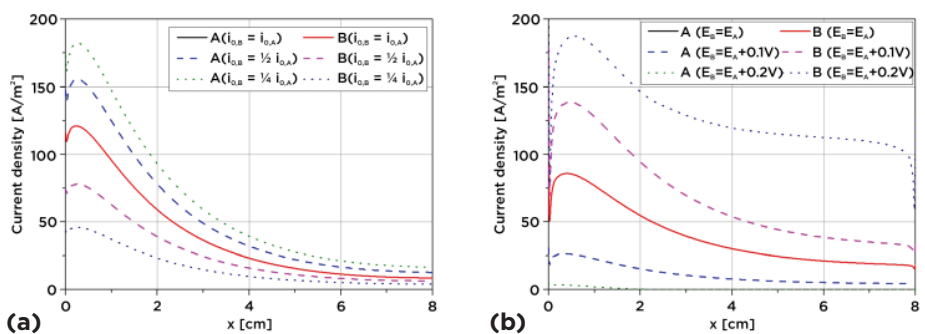


Figure 3. Current density distribution along the cathode in an RCH cell (a) for differing exchange current densities between A and B ions and (b) for differing equilibrium potentials.

¹ Tracy S. Rudisill, "Decontamination of Zircaloy cladding hulls from spent nuclear fuel," *Journal of Nuclear Materials*, 385, 193-195 (2009).

Planned Activities

Experiments using the zirconium recovery test system shown in Figure 1 will be performed in a fume hood with an argon gas constantly purging in the furnace to maintain an inert atmosphere. The anode will be a molten cadmium pool under the salt electrolyte containing zirconium metal. Current will be introduced to the anode using a tantalum lead. The cathode will also be an alumina sheathed tantalum wire. Most experiments will be run in magnesium oxide crucibles. Several runs using quartz crucibles will be selected, allowing researchers to digitally photograph the cathodic deposition process.

To validate the developed multispecies model, the project team will perform a codeposition experimental study using an RCH cell with CuSO_4 and NiSO_4 selected as surrogate materials. The RCH cell will be based on the RotaHull® set, and the cell geometry will be modified to measure overpotential distribution along the cathode. The team has also designed experiments to measure electrochemical properties of the surrogate materials, including exchange current density, transfer coefficient, and diffusion coefficient.

Advanced Instrumental Science-Based Approach to Nickel Alloy Aging and its Effect on Cracking in Pressurized Water Reactors

Research Objectives

This project is investigating the effects of aging on the microstructure and stress-corrosion cracking (SCC) behavior of dissimilar-metal welds. In particular, the project team is examining the chromium dilution effect at the interface of low-alloy steel (LAS) and Inconel Alloy 690 joined by Alloy 152 weld. To characterize the weld interface, the team is conducting advanced instrumental analysis, including energy dispersive X-ray spectroscopy (EDS), secondary ion mass spectroscopy, and three-dimensional atom probe tomography. *In situ* Raman spectroscopy is used to analyze the oxide film formed on weld interface samples exposed to simulated primary water conditions found in a pressurized water reactor (PWR). The team is also conducting fundamental studies of effects of lead on Alloy 600 steam generator tube corrosion/cracking. Synchrotron X-ray reflectivity reveals molecular-scale details of lead distribution and the chemical states at the metal oxide–liquid interface; results will be compared with those from typical *ex situ* oxide film analysis and *in situ* electrochemical spectroscopy. The team will use *in situ* impedance spectroscopy at high temperatures to characterize oxide film and determine how dissolved lead changes its properties. Researchers will then use energy dispersive X-ray spectroscopy to perform conventional *ex situ* surface oxide film analysis to profile the film's chemical composition.

Research Progress

The team fabricated a representative dissimilar metal weld mock-up comprising special well-characterized heats of Alloy 690 and Alloy 533 Grade B (Midland reactor lower head), with Alloy 152 filler. Crack-growth-rate testing on a non-aged Alloy 152 weld sample resulted in an SCC growth rate of 2E-11 m/s under moderate stress intensity, providing a baseline measurement for testing aged specimens. A one-inch-thick weld sample was cut and sent to a Korean project collaborator. The as-welded samples have been aged in furnaces under accelerated temperature conditions of 370°C and 400°C.

Several techniques were used to characterize as-welded dissimilar metal weld samples, including EDS in a scanning electron microscope (SEM) and transmission electron microscope (TEM), secondary ion mass spectrometry (SIMS), and three-dimensional atom probe tomography (3-D APT). Researchers found that the weld root area was divided into three distinct regions: an unmixed zone of nickel (Ni)

PI (U.S.): Chi Bum Bahn and Ken Natesan, Argonne National Laboratory

PI (Country): Ji Hyun Kim, Ulsan National Institute of Science and Technology

Collaborators: Korea Atomic Energy Research Institute, Seoul National University

Program Area: Reactor Concepts RD&D

Project Start Date: December 2010

Project End Date: September 2013

alloy, the fusion boundary, and a heat-affected LAS zone. Figure 1 represents the result of TEM EDS analysis showing the non-homogeneous elemental distribution; Alloy 533 Gr. B exhibited higher iron content but lower manganese, nickel and chromium than Alloy 152. The project team established an experimental facility for *in situ* oxide film analysis using Raman spectroscopy with dissimilar metal weld interface samples in a simulated PWR primary water environment. The facility is composed of three main parts: a test

loop for simulated PWR primary water conditions; an *in situ* Raman spectroscopy system utilizing a direct-immersion optical probe and spectrometer; and a hydrothermal optical cell made of a compression fitting with a sample stage.

Team members at Argonne National Laboratory (ANL) utilized the 33BM-C beam line at the Advanced Photon Source (APS) facility to measure film sample X-ray reflectivity at room temperature. First, high-resolution X-ray reflectivities were measured to determine the initial structure of a native oxide layer on single-crystal Ni(110). Figure 2a shows reflectivities of as-purchased and post-annealed Ni(110) surfaces, and Figure 2b shows a relative density profile near the surface. Researchers identified two initial layers. The inner and outer layers appeared to be composed of nickel oxide and nickel hydroxide, respectively, with estimated thicknesses of 18 Å and 11 Å. The reflectivity after annealing at 930°C indicates that the crystal size remained fairly constant, but only a nickel oxide layer was identified. The team developed a surface treatment consisting of argon sputtering and annealing in an ultra-high vacuum chamber to improve the surface crystallinity.

The project team also examined typical impedance spectra (Nyquist plots) of thermally treated Alloy 600 specimens immersed in leaded and unleaded solutions of 0.1 molar (M) sodium hydroxide (NaOH) at 315°C (see Figure 3). The impedance spectra of the unleaded solution imply that the equivalent circuit is composed of a series of solution resistance in parallel with oxide capacitance and oxide resistance, connected to Warburg impedance created by diffusion of the electrolyte or metallic cation. However, adding lead oxide to the solution generates

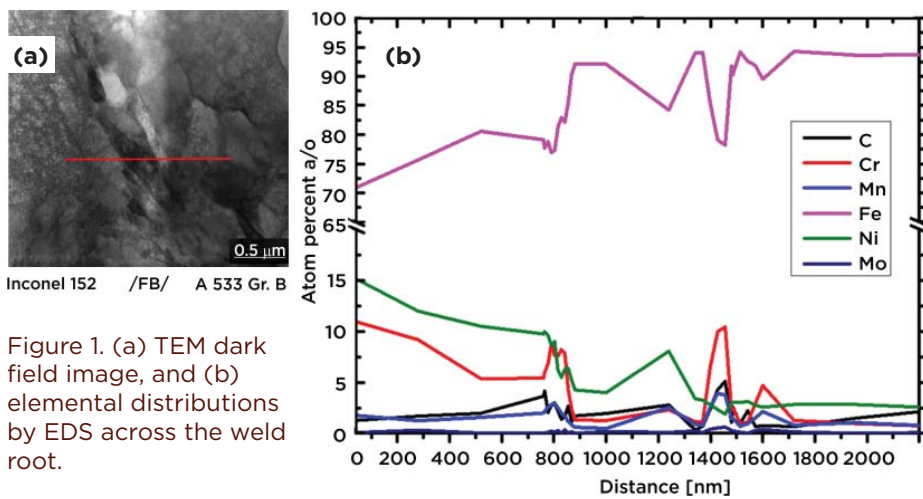


Figure 1. (a) TEM dark field image, and (b) elemental distributions by EDS across the weld root.

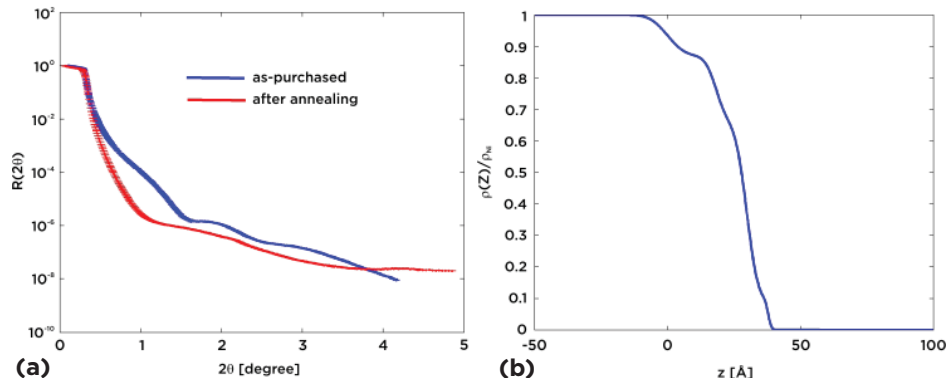


Figure 2. (a) X-ray reflectivities of as-purchased and annealed Ni(110) surfaces and (b) relative density profile near the Ni(110) surface.

reflectivity after annealing at 930°C indicates that the crystal size remained fairly constant, but only a nickel oxide layer was identified. The team developed a surface treatment consisting of argon sputtering and annealing in an ultra-high vacuum chamber to improve the surface crystallinity.

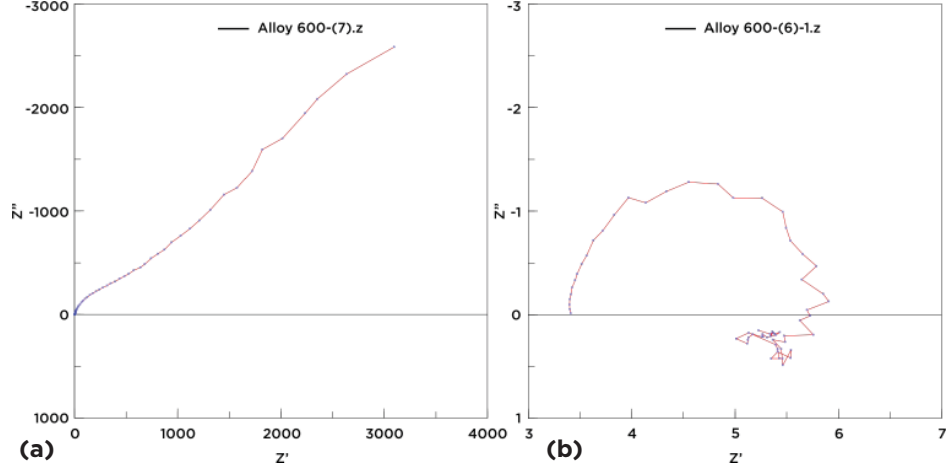


Figure 3. Typical Nyquist plots obtained from the electrochemical impedance measurements for thermally treated Alloy 600 immersed in 0.1 M NaOH solutions at 315°C: (a) unleaded and (b) leaded.

a double-layer capacitance in parallel with polarization resistance, rather than oxide capacitance and oxide resistance. This capacitive arc indicates that the oxide passivity was greatly decreased by electrodeposition of lead ions in the solution. The resulting decrease in oxide passivity could, in turn, increase SCC susceptibility.

Planned Activities

The research team will continue aging the dissimilar weld mock-up samples at temperatures of 370°C and 400°C for 5,000 and 20,000 hours. They will conduct microstructural characterization of the aged weld specimen interfaces utilizing microhardness testing, SEM, SIMS, TEM and 3-D APT, as well as Raman spectroscopy for *in situ* oxide analysis. Samples that have not been aged and those aged for 5000 hours will be tested in FY 2012. Researchers will utilize the Ni(110) surface treatment to improve the surface crystallinity and conduct synchrotron X-ray experiments to identify the surface interface between Ni(110) and the solution. The team will also carry out *in situ* impedance measurements to understand the effect of lead on the properties of oxides formed on steam generator tubing material. After conducting high-temperature experiments, the team will use TEM EDS to analyze the oxide's microstructure.

Low-Loss Advanced Metallic Fuel Casting Evaluation

PI (U.S.): Randall Fielding, Idaho National Laboratory

PI (ROK): Dr. Ki-Hwan Kim, Korea Atomic Energy Research Institute

Collaborators: None

Program Area: FCR&D

Project Start Date: December 2010

Project End Date: December 2013

Research Objectives

The objective of this project is to develop methods of minimizing fuel losses and reducing waste streams during fabrication of metallic fuel pins for sodium-cooled fast reactors (SFRs). This work will enhance the technical readiness level of the metallic fuel fabrication process. The fabrication process for metallic SFR fuel has three phases: (1) fuel pin casting, (2) loading and fabrication of the fuel rods, and (3) fabrication of the final fuel assemblies. Most fuel losses and waste/recycle streams occur during fuel pin casting. Recycle streams include fuel pin rework, returned scraps, and fuel casting heels, which are of special concern in the counter-gravity injection casting process because of the large masses involved. Large recycle and waste streams lower the productivity and economic efficiency of the fabrication process.

The project team will evaluate fuel losses that occur during casting of U-Zr/UTRU-Zr (uranium–transuranic–zirconium) fuel pins for an SFR. This will be accomplished by casting a considerable amount of fuel alloy in a furnace, and then quantitatively evaluating losses in the melting chamber, crucible, and mold. After identifying and quantifying materials at key process stages, the team will develop means of reducing losses, including permanent crucible coatings, permanent reusable molds, and advanced techniques such as continuous casting. The goal is to develop a coating technology for re-usable crucibles with good thermal cycling characteristics and excellent compatibility between fuel melt and coating layer. The scope of work consists of three major tasks:

- Casting development and mold loss comparison
- Coating development and characterization
- Continuous casting technology

Research Progress

Casting development and mold loss comparison. The research team at Korea Atomic Energy Research Institute (KAERI) cast a batch of U-10Zr-5Mn and one of U-10Zr-5Ce (weight basis) on approximately a one-kilogram scale. Chemical composition and mass balance of both batches were measured and used to determine fuel loss levels. Both batches cast well. For the U-10Zr-5Mn batch, mass balance determined that approximately 92.4% of the charge flowed into the mold

assembly, while 6.1% stayed in the crucible as residue and dross, and 1.5% was lost. A greater amount of cerium-containing material was retained in the crucible as residue and dross: 88.6% of the material flowed into the mold assembly and 11.3% remained in the crucible, leaving a fuel loss of only 0.1%. Both castings were done using an yttrium oxide (Y_2O_3)-coated crucible; however, the manganese crucible was slurry-coated, and the cerium crucible was plasma-spray-coated. The difference in coating deposition technique contributed to the differences in fuel losses seen in the two casting batches. The Y_2O_3 coating applied through slurry coating was porous and not as even throughout the crucible, thus easily penetrated by the melt, leading to higher losses. In contrast, the plasma-sprayed coating used in the cerium-containing melt was uniform and dense. The increased density precluded any melt infiltration, lessening losses.

As noted above, a higher percentage of the cerium-containing melt was retained in the crucible, due in large part to a greater amount of dross formation as compared to the manganese melt. Cerium is much more thermodynamically active and would more readily combine with any oxygen present, perhaps even in the coating, and form an oxide dross. Chemical analysis showed a composition of U-10.6Zr-4.9Mn, a loss of only 0.1%. Analysis of the cerium-containing melt resulted in a composition of U-10.4Zr-3.8Ce, a loss of 1.2%. Considering the higher vapor pressure of manganese, this result was somewhat surprising. However, because the cerium is more reactive, it is likely that cerium is preferentially oxidized in the melt, which would increase the losses seen in the final product and account for the increased amount of dross.

The Idaho National Laboratory (INL) team has taken the first steps in preparing fuel pins for analysis by designing a new furnace, which is currently in mock-up testing outside of the glovebox (see Figure 1). The furnace is sized for charges as large as 500 grams, although expected charges will be approximately 200 grams. The current mold is designed to cast three pins, each 4.3 mm in diameter and 250 mm in length. Both the mold and crucible are independently induction-heated with 10-kW power supplies and digital furnace controls. Heat-up rate, final temperature, or power supply output can be used to control the mold and crucible temperature, while the furnace vessel pressure can also be controlled. To make enough space in the glovebox for the furnace, the team must first remove an older counter-gravity injection casting system used to cast U-TRU-Zr pins along with the associated piping and control cabinet. Because these components are highly contaminated, the removal process has been somewhat slower than expected. However, all of the associated piping has been removed, and the old furnace is being dismantled.

Coating development and characterization. As noted above, the KAERI team confirmed that coating quality affects fuel losses during fabrication. Based on literature searches, team members have identified six potential coating candidates: HfC, TaC, TiC, ZrC, Y_2O_3 , and ZrO_2 . These materials were plasma sprayed onto graphite and niobium rods and discs. The team conducted thermal cycling testing on the disc coatings for one, five, and ten cycles, heating from room temperature to 1450°C. All the materials performed well in thermal cycling tests. However, some samples showed a small amount of non-interconnected cracking. Based on these results, the team exposed all samples to molten U-10Zr material heated to 1600°C for five and fifteen minutes. ZrO_2 , HfC, and ZrC showed significant interaction and coating failures after fifteen minutes. Y_2O_3 , TaC, and TiC had more promising results. However, the TiC coating did contain small non-connected cracks that were infiltrated by the melt and showed signs of separation from the niobium and graphite substrate. The TaC coating also showed signs of wetting by the melt.

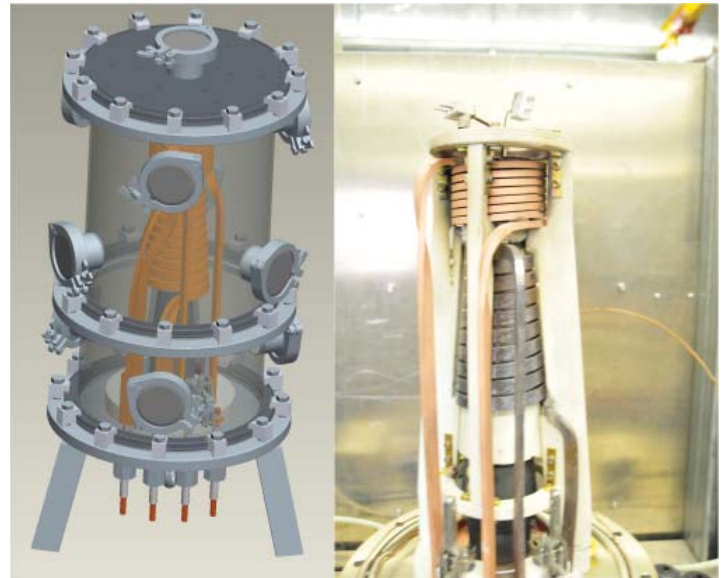


Figure 1. a) Schematic of newly designed casting development furnace; b) furnace in mock-up testing without outer chamber in place.

Continuous casting. The KAERI team repaired and reconstructed an existing engineering-scale continuous casting apparatus. An induction coil, a cooling jacket for the mold, and a withdrawal servo-motor for the driving roller were replaced, and a melting crucible and a casting mold were designed and machined. The team conducted successful initial testing under an inert atmosphere at approximately 760 torr with copper as a surrogate for uranium, based on similar melting temperatures. The researchers cast and characterized a 7-mm-diameter, 2300-mm-long fuel pin and found, by visual examination, the surface finish smooth and generally free of defects. They then used X-ray radiography to interrogate the integrity of the pin. A number of small defects were found on the tail end of the casting, but in general the pin was sound. Although a significant amount of dross was retained in the crucible, overall losses were on the order of 0.1%.

Planned Activities

Future activities will focus on continued casting development, including minor actinide-bearing alloys. INL plans to install the newly designed furnace into a minor actinide-capable glovebox, after which casting development will continue. Casting will include U-Zr, U-Pu-Zr, and U-Pu-Zr-MA. INL and KAERI researchers will identify and compare loss results, paying special attention to fuel losses and fuel loss paths in minor actinide-bearing batches. Both teams of researchers will conduct literature searches to identify potential coating candidates for testing in a U-Pu-Zr environment. Continued coating studies will include intermediate layers and optimized parameters, and KAERI-produced samples will be tested at INL. Research will also continue pursuing continuous casting techniques. Engineering-scale casting will be done with uranium and uranium-zirconium melts. Contingent on funding, the project team plans to complete the project with a final design and fabrication of a bench-scale continuous casting apparatus. When installed at INL, comparisons of INL and KAERI fuel loss results and efficiencies will be conducted.

Development and Characterization of Nanoparticle-Strengthened Dual-Phase Alloys for High-Temperature Nuclear Reactor Applications

Research Objectives

The main objective of the project is to develop a nanoparticle-strengthened dual-phase composite material with high fracture toughness for application to high-performance reactor core structures. To achieve this objective, the project will combine two modern material processing technologies used to produce nanostructured ferritic alloys (NFAs) and ferretic–martensitic (F-M) dual-phase steels. To optimize after-extrusion heat treatment conditions, researchers carry out both a computational simulation technique for phase equilibrium and basic microstructural and mechanical characterizations for base and treated materials.

This project also aims to produce a material characterization database for the optimized materials. This database is important for future high-temperature applications and for further materials development. At a minimum, the mechanical database will include tensile deformation data, fracture toughness data, and high-temperature deformation (including creep) data; while the microstructural characterization will include grain structure, phase transformation and stability data, and high-resolution structure analysis data for the distribution and thermal stability of nanoparticles.

Research Progress

Production of base materials. Project team members have designed two Fe-9Cr alloys, considering heat treatment capability and carbide formation behaviors, from two heats (about 17 kg each) of ferritic 9Cr pre-alloyed powder, produced by vacuum induction melting followed by argon gas atomization. The two heats had the same specified compositions with one exception: one heat contained a high carbon level (Fe-9Cr-2W-0.4Ti-0.2V-0.12C weight percent [wt%]) and the other a low carbon level (Fe-9Cr-2W-0.4Ti-0.2V-0.05C).

To produce the base materials—Fe-9Cr-based NFAs—the research team used multistep processing, including balling milling and consolidating. The ferritic 9Cr pre-alloyed powders were ball milled with 0.3% Y_2O_3 powder using a high-energy attritor mill, the Simolayer CM08. Three 1-kg batches of each powder heat were

PI (U.S.): Thak Sang Byun, David T. Hoelzer, Oak Ridge National Laboratory

PI (ROK): Ji-Hyun Yoon, Korea Atomic Energy Research Institute

Collaborators: None

Program Area: FCR&D

Project Start Date: December 2010

Project End Date: November 2011

ball milled for 40 hours in an argon gas atmosphere, making a total of 3 kg of milled powder for each ferritic 9Cr powder heat. The powder was sealed in 3-inch-diameter mild steel cans, degassed under vacuum at 400°C, and the degassed cans extruded at <850°C. The two oxide dispersion-strengthened (ODS) 9Cr alloys were designated as 9YWTV-PM1 for the high-carbon heat and 9YWTV-PM2 for the low-carbon heat. The extruded bars were cut into coupons about four inches long, as seen in Figure 1, and the base materials characterized.

Process development study. Researchers used CALPHAD, a computer-based phase equilibrium calculation method, to determine the heat treatment conditions that would evolve the as-extruded microstructure of Fe-9Cr NFA into the F-M dual-phase composite microstructure. As austenite and ferrite phases are expected to coexist in the temperature range of 850°C–975°C, heat treatment in this temperature range—called intercritical annealing—is targeted for obtaining a dual-phase microstructure.

Mechanical and microstructural characterization. Uniaxial tensile tests were performed for the as-extruded alloy in a temperature range of 25°C–700°C with a strain rate of $3.7 \times 10^{-4}/\text{s}$. The engineering stress-strain curves are presented in Figure 2. The alloy's strength was about twice that of conventional F-M steels over the test temperature range. The alloy retained relatively high strength up to 700°C, though there was a dramatic drop in strength above 500°C.

The team also carried out high-temperature fracture toughness tests for the first NFAs (9YWTV-PM1, high-carbon) in as-extruded condition. The higher-carbon alloy has low fracture toughness (<70 MPa $\sqrt{\text{m}}$) over the test temperature range of 22°C–700°C.

Using a scanning electron microscope (SEM), researchers applied electron backscattered diffraction (EBSD) automated acquisition and indexing to perform phase identification. They used SEM/EBSD to examine the extruded and annealed alloy and find the optimum heat treatment condition to generate dual phase in the 9Cr NFA.

Figure 3 displays EBSD phase maps that identify the ferrite (α) and austenite (γ) phases in the heat-treated samples. It was observed that higher annealing temperatures and longer time periods produced more γ phase around the grain boundary. The γ phase is presumed to be the austenite retained after the annealing processes.



Figure 1. Coupons cut from the extruded bars. Note that the inner portion is the NFA, and the outer rim is the carbon steel can.

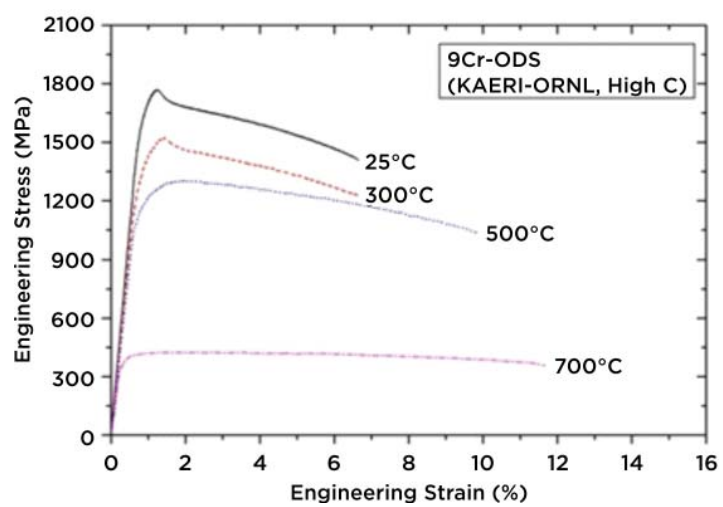


Figure 2. Engineering stress-strain curves for the 9Cr NFA at various temperatures.

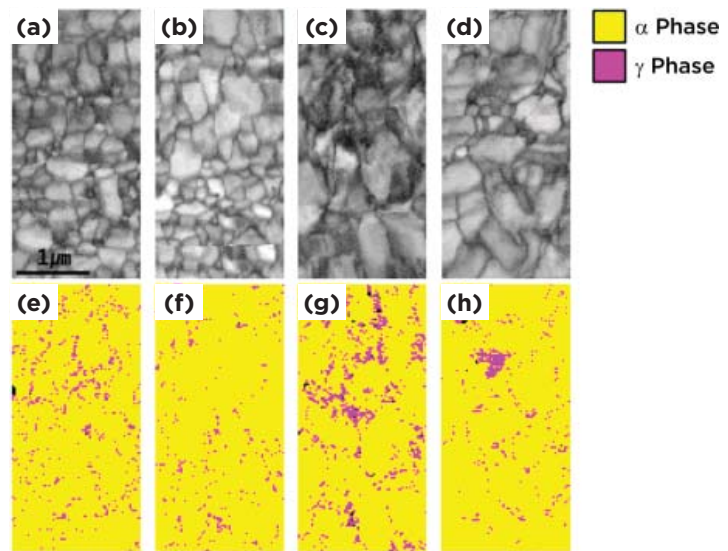


Figure 3. The α and γ phases are identified by EBSD phase maps. The band contrast maps of samples are suggested for the alloy after annealing at: (a) 900°C for 6 hours (b) 1050°C for 1 hour (c) 1050°C for 10 hours (d) 1050°C for 100 hours. The corresponding phase maps are displayed in (e), (f), (g), and (h), respectively.

The research team performed SEM analysis on polished specimens of 9YWT-PM1 and 9YWT-PM2 to investigate the grain structure. Backscattered electron (BSE) images, shown in Figure 4, revealed that the microstructures of both ODS 9Cr alloys contain uniform distributions of ultra-small grains (<300 nm). These results indicated that ball milling effectively distributed the Y_2O_3 powder in the pre-alloyed iron alloy powder. Furthermore, based on past studies of 14YWT NFA heats, the observation of uniform ultra-small grain size microstructures is consistent with the formation of a homogeneous distribution of nano-size oxide particles during extrusion.

Researchers performed detailed microstructural examination for the as-extruded 9Cr nanostructured ferritic alloy using X-ray diffraction (XRD) and field emission transmission electron microscopy (FE-TEM). The grains in the alloy have highly preferred orientations of {110} and {222} for ferrite and austenite, respectively. As shown in Figure 5, the nanoparticles within the grain are evenly scattered, with diameters of about 2 nm. Particles bigger than 10 nm rarely exist in the matrix and at the grain boundary. The 2-nm nanoparticles are fully coherent with the matrix. The size of the nanoparticles increased to around 5 nm after annealing at high temperatures, as shown in Figure 5.

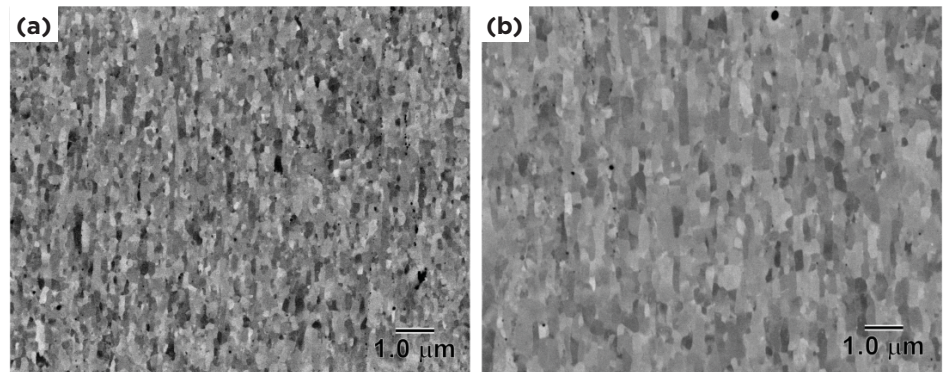


Figure 4. SEM BSE micrographs showing the ultra-fine grain structure of the extruded 9Cr NFAs: (a) 9YWT-PM1 (0.12% C) and (b) 9YWT-PM2 (0.05% C).

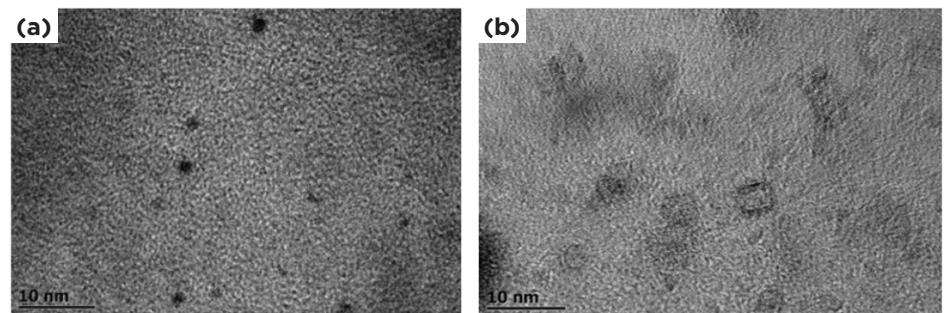


Figure 5. TEM micrograph showing nanoparticles (a) formed in as-extruded 9Cr NFA (with high carbon) and (b) after annealing at 1050°C for 10 hours.

Planned Activities

The research activities in the second project year (December 2011–November 2012) will focus on post-extrusion process optimization and microstructural and mechanical characterizations. The research team will:

- Apply various heat treatment schedules and perform basic characterization for each intermediate product. This subtask will be repeated until the entire process and microstructure are optimized for high fracture toughness and ductility.
- In parallel with the above task, carry out computational simulation for phase transformation and stability. The simulation results will be used as a guideline for further development and optimization.
- As more heat treatments are attempted, continue the study of thermomechanical stability of nanoparticles using various techniques, including high-resolution FE-TEM analysis. High-temperature annealing treatments are expected to coarsen the nanoparticles, and their stability in the austenitic phase is in question.
- Perform microstructural characterization for dual-phase structure and distribution as well as grain structure using SEM/EBSD and TEM for the composite microstructures after partial phase transformation.
- Start high-temperature mechanical tests, including uniaxial tensile, creep, and fracture, for the optimized material. Preliminary mechanical tests such as tensile tests will be carried out on intermediate materials produced during process development.

Atomic Ordering in Alloy 690 and its Effect on Long-Term Structural Stability and Stress-Corrosion Cracking Susceptibility

PI (U.S.): Michael Kaufman, Colorado School of Mines

PI (ROK): YoungSuk Kim, Korea Atomic Energy Research Institute

Collaborators: University of Michigan, University of North Texas

Program Area: Reactor Concepts RD&D

Project Start Date: October 2011

Project End Date: September 2014

The objective of this project is to determine the effects of atomic ordering in Alloy 690 under pressurized water reactor (PWR) operating conditions on mechanical integrity and susceptibility to intergranular stress–corrosion cracking (SCC). Nickel-based Alloy 690 is being considered as a possible replacement for Alloy 600 in reactor structural components due to its improved resistance to primary water SCC. However, thermally treated Alloy 690 subjected to 20% to 30% cold working has demonstrated crack growth rates as high as those of Alloy 600 during testing in high-temperature deaerated primary water. Alloy 690 is prone to multiple atomic ordering, including Ni₂Cr type ordering at 420°C and Fe₃Ni and Ni₃Fe type ordering at lower temperatures. Such ordering is likely under light water reactor operating conditions and would adversely affect the long-term structural stability and mechanical properties of this alloy.

To obtain a fundamental understanding of the SCC mechanisms, the project team will prepare eight samples of Alloy 690, four at each allowable extreme of iron content. Each set of samples will be subjected to either solution annealing or thermal treatment at 700°C, with and without 20% cold working. The eight samples will then be aged at 360°C to 550°C for up to 14,000 hours and characterized to investigate the degree of atomic ordering and its effect on mechanical properties. PWR primary water SCC tests will also be conducted as a function of aging. To evaluate the correspondence between atomic ordering and aging temperature and time, the team will analyze materials in the nano-scale ordered phase using electron microscopy and neutron analytical techniques. Key activities are as follows:

- Year 1: Prepare eight kinds of Alloy 690 samples, age at 360°C–550°C, and characterize.
- Year 2: Analyze nano-scale ordered phases to understand the effects of short-range ordering (SRO) and long-range ordering (LRO) phases on mechanical properties.
- Year 3: Evaluate SCC resistance of aged Alloy 690 to understand the effects of cold working, iron content, and thermal treatment.

Development of Microcharacterization Techniques for Nuclear Materials

This project will systematically investigate small-scale materials testing of structural materials for nuclear application, evaluating the full potential of these methods and standardizing the techniques for irradiated materials. The goal is to develop micro/nano-scale mechanical testing techniques (tensile, compressive, and creep) for irradiated materials that will allow researchers to assess mechanical property changes on the macro scale.

Degradation of materials properties under neutron irradiation is a key issue limiting the lifetime of nuclear reactors. Evaluating the property changes of materials due to irradiation and understanding the role of microstructural changes on mechanical properties are required to ensure reliable long-term reactor operation and to develop high-dose concepts. Researchers have been conducting post-irradiation mechanical testing on bulk specimens for decades, but the task remains time- and cost-intensive. It is also challenging, given the need to handle large quantities of radioactive materials. While ion beam irradiation does not result in activation of the materials, the irradiated volume is often too small for conventional mechanical testing. Small-scale materials testing has recently been applied to nuclear materials and shows potential to address these issues. While initial studies are promising, this technique is far from being fully developed or standardized. Developing these techniques as part of an international collaboration is significant, as it is a step towards global acceptance of a more standardized and unified approach in mechanical testing for nuclear materials. The project consists of the following major tasks:

- Fabricate micro/nano-scale testing samples and conduct initial multiscale testing of the unirradiated materials.
- Perform ion beam irradiation of the materials.
- Conduct materials testing of the ion beam irradiated samples and compare with modeling results.
- Conduct small-scale materials testing on materials irradiated in a reactor.

PI (U.S.): Peter Hosemann, University of California, Berkeley

PI (ROK): Chansun Shin, Korea Atomic Energy Research Institute

Collaborators: Los Alamos National Laboratory

Program Area: Reactor Concepts RD&D

Project Start Date: October 2011

Project End Date: September 2014

Verification and Validation of High-Fidelity Multi-Physics Simulation Codes for Advanced Nuclear Reactors

PI (U.S.): Changho Lee, Argonne National Laboratory

PI (ROK): Hyun Chul Lee, Korea Atomic Energy Research Institute

Collaborators: None

Program Area: Reactor Concepts
RD&D

Project Start Date: October 2011

Project End Date: September 2014

The objective of this project is to systematically verify and validate multi-physics simulation codes and high-fidelity whole-core neutron transport codes for very high-temperature reactors (VHTRs) and light water reactors (LWRs). The research team will expand upon and reorganize a suite of advanced simulation methods and codes developed under previous I-NERI projects to address both VHTR and LWR core types. Researchers will focus on developing benchmark models for verification and validation of the neutronics code, both with and without feedback from the thermo-fluid components, and will attempt uncertainty evaluations on the experimental data used to develop the benchmark problems. The work scope will include generating improved cross-section libraries for the targeted reactor types and performing detailed comparisons of predicted reactor parameters against both Monte Carlo solutions and experimental measurements. The team will also verify and validate the two thermo-fluid tools against benchmark problems and relevant experiments for phenomena important to the VHTR and LWR. Parametric studies will help determine the optimized level of geometry representation and model complexity within the limits of existing computational machines. Researchers will assess the accuracy of coupled simulations using code-to-code benchmark problems and comparisons of results against available experimental measurements.

The R&D plan consists of the following three primary tasks:

- Verification and validation of the DeCART neutronics code for VHTRs
- Verification and validation of the DeCART and PROTEUS neutronics codes for LWRs
- Verification and validation of the multi-physics simulation code suites DeCART/CORONA and DeCART/STAR-CCM+

Development of Diagnostics and Prognostics Methods for Sustainability of Nuclear Power Plant Safety Critical Functions

The objective of the project is to develop and demonstrate advanced technologies for condition monitoring, diagnosis, remote sensing, and safety actuation during beyond-design-basis events in operating nuclear plants and next-generation reactors. Design of self-powered sensors that function under loss of power, along with sensor networks that optimize fault monitoring, is key to providing plant information during extreme conditions. Effective mitigation of a beyond-design-basis accident is receiving increased scrutiny in light of the recent accident at the Fukushima Daiichi nuclear power plant. The accident highlighted the need to monitor core and coolant system conditions and communicate sensor measurements and other information during severe accident conditions.

Even though prognosis during accident situations is not always feasible, predicting or estimating impending changes in the performance of safety-related equipment is of high importance. This project will focus on implementing a variety of monitoring methods using low-frequency and wide-band data and developing self-powered sensors, a sensor network strategy, and data communication and control. The U.S. and Korean collaborators will develop and integrate monitoring and diagnostics methods and demonstrate techniques and measurement strategies for selected safety-related equipment. Using dynamic simulation of a typical nuclear plant's operations, the team will generate data needed to validate the proposed technical approach.

The project consists of four key tasks. Technologies and algorithms will be demonstrated throughout by application to selected components.

- Review operability of safety-critical functions and components in light water reactors.
- Develop algorithms for plant monitoring, diagnostics, and prognostics.
- Develop low-energy, self-powered process sensors and networks, and determine optimal placement strategies.
- Develop plant simulation models for data generation.

PI (U.S.): Belle R. Upadhyaya,
University of Tennessee

PI (ROK): Jung-Taek Kim, Korea
Atomic Energy Research Institute

Collaborators: Chungnam National
University, Kyung-Hee University, Pacific
Northwest National Laboratory

Program Area: Reactor Concepts
RD&D

Project Start Date: October 2011

Project End Date: September 2014

Fully Ceramic Microencapsulated Replacement Fuel for Light Water Reactor Sustainability

PI (U.S.): Lance Snead, Oak Ridge National Laboratory

PI (ROK): Won-Jae Lee, Korea Atomic Energy Research Institute

Collaborator: Ultra Safe Nuclear Corporation, Inc.

Program Area: FCR&D

Project Start Date: October 2011

Project End Date: September 2014

This project supports the introduction of a robust, accident-tolerant fuel that is compatible with currently operating light water reactors (LWRs). Specifically, the team will further investigate fully ceramic micro-encapsulated (FCM) fuel, a promising concept under Department of Energy development. The FCM fuel is a TRISO-based dispersion fuel consisting of ceramic-coated microspheres of low-enriched uranium embedded in a dense, uniform silicon carbide (SiC) matrix fuel pellet. Pellets can be stacked in non-zirconium cladding and fabricated into fuel assemblies compatible with existing LWR designs. The Fukushima nuclear accident has demonstrated the vulnerability of conventional uranium oxide (UO_2) LWR fuels to severe damage during station blackout events. The ceramic microspheres and ceramic compacting matrix provide additional barriers to the release of fission products.

The goal of this project is to establish FCM fuel as a feasible replacement for UO_2 ceramic fuel in the existing LWR fleet. To be viable one-for-one replacements, the FCM fuel pins must behave in essentially the same manner as UO_2 in terms of power generation, thermal-hydraulics, and neutronics. The FCM fuel must also achieve comparable levels of linear fissile density and reactivity behavior throughout its operational life in the reactor. To accomplish this, the project team will introduce high-fissile-density materials and investigate special packing techniques. Given the existing database of properties for the relevant materials, the team will evaluate performance at the fuel assembly and full-core levels, in addition to the customary neutronic and thermal-hydraulic analysis. The project consists of the following key elements:

- Selection of FCM fuel rod and assembly designs and preliminary neutronic exploration of LWR cores
- Modeling and preliminary thermal-hydraulic assessment of reference FCM cores
- Reactor systems modeling and preliminary safety assessment of FCM fueled cores
- FCM fuel qualification – manufacturing, irradiation, and performance analysis





Appendix I: Acronyms and Initialisms

Symbols and Numerals

Å	Angström
µg	Microgram
µm	Micrometer
3-D	Three-Dimensional

A

ACR	Advanced CANDU Reactor
AECL	Atomic Energy of Canada Limited
Ag	Silver
ANL	Argonne National Laboratory
ANRE	Agency of Natural Resources and Energy
APS	Advanced Photon Source
APT	Atom Probe Tomography
ARC	Advanced Reactor Concepts (program)

B

b	barns (10^{-24} cm 2)
BFS	Big Physical Stand (facility)
Bi	Bismuth
BSE	Backscattered Electron

C

C	Celsius
CASL	Consortium for Advanced Simulation of Light Water Reactors
Ce	Cerium
CEA	Commissariat à l'énergie atomique
CEN	Comité Européen de Normalisation
CERN	European Organization for Nuclear Research
Cf	Californium
CFD	Computational Fluid Dynamics
CG	Coarse-Grained
Cl	Chlorine

CLS	Canadian Light Source
cm	Centimeter
Cm	Curium
CMFD	Coarse-Mesh Finite-Difference
Co	Cobalt
Cr	Chromium
Cs	Cesium
Cu	Copper
CWF	Ceramic Waste Form

D

DOE	Department of Energy
dpa	Displacements per Atom

E

EBR-II	Experimental Breeder Reactor-II
EBSDD	Electron Backscatter Diffraction
ECAP	Equal Channel Angular Processing
EDS	Energy Dispersive X-ray Spectroscopy
ENDF	Evaluated Nuclear Data File
ER	Electrorefiner
Eu	Europium
EU	European Union
eV	Electron Volts

F

F	Flourine
fcc	Face-Centred Cubic
FCM	Fully Ceramic Microencapsulated (fuel)
FCR&D	Fuel Cycle Research and Development (program)
Fe	Iron
FE-TEM	Field Emission Transmission Electron Microscope/Microscopy
FFTF	Fast Flux Test Facility
FIB	Focused Ion Beam

F-M	Ferretic-Martensitic	ILS	Integrated Laboratory-Scale (experiment)
FY	Fiscal Year	IMF	Inert Matrix Fuel
G			
g	Gram(s)	INL	Idaho National Laboratory
GELINA	Geel Linear Accelerator	IPPE	Institute of Physics and Power Engineering
Gen IV	Generation IV	IRMM	Institute for Reference Materials and Measurements
GETMAT	Generation IV and Transmutation Materials (Euratom program)	ISO	International Organization for Standardization
GIF	Generation IV International Forum	ITU	Institute for Transuranium Elements
Gr.	Grade		
GWD/T	Gigawatt – Days per Metric Ton		
H			
H	Hydrogen	JEFF	Joint Evaluated Fission and Fusion
He	Helium	JENDL	Japanese Evaluated Nuclear Data Library
HELIOS	Heinz Electronic Library Interactive Online System	JRC	Joint Research Centre
HFEF	Hot Fuels Examination Facility		
Hf	Hafnium		
HLM	Heavy Liquid Metal	K	Potassium
HLW	High-Level Waste	KAERI	Korea Atomic Energy Research Institute
HTGR	High-Temperature Gas-Cooled Reactor	KAIST	(formerly the Korea Advanced Institute of Science and Technology)
HTTR	High-Temperature Test Reactor	k_{eff}	k-effective (neutron multiplication factor)
HT-UPS	High-Temperature Ultrafine Precipitate-Strengthened (steel)	keV	Kiloelectron Volt(s)
I			
IAEA	International Atomic Energy Agency	kg	Kilogram(s)
IFNEC	International Framework for Nuclear Energy Cooperation	KMC	Kinetic Monte Carlo
IHECSBE	International Handbook of Evaluated Criticality Safety Benchmark Experiments	kW	Kilowatt(s)

L

LANL	Los Alamos National Laboratory
LANSCE	Los Alamos Neutron Science Center
LAS	Low-Alloy Steel
Li	Lithium
LRO	Long-Range Ordering
LWR	Light Water Reactor
LWRS	Light Water Reactor Sustainability (program)

M

m	Meter(s)
M	Molar
MA	Minor Actinide
MC	Monte Carlo
MEST	Ministry of Education, Science and Technology
MeV	Megaelectron Volt(s)
MEXT	Ministry of Education, Culture, Sports, Science, and Technology
mg	Milligram(s)
MIR	Matched Index of Refraction
mm	Millimeter(s)
Mn	Manganese
Mo	Molybdenum
MOC	Method of Characteristics
MONNET	Mono Energetic Neutron Tower
MOX	Mixed Oxide
MST	Ministério da Ciência e Tecnologia
MV	Megavolt

N

n_TOF	Neutron Time-of-Flight (facility)
Na	Sodium
Nd	Neodymium
NE	Office of Nuclear Energy
NEA	Nuclear Energy Agency (of OECD)
NEAMS	Nuclear Energy Advanced Modeling and Simulation (program)
NFA	Nanostructured Ferritic Alloy
NGNP	Next Generation Nuclear Plant
Ni	Nickel
nm	Nanometer(s)
Np	Neptunium
NRCan	Department of Natural Resources Canada

O

O	Oxygen
ODS	Oxide Dispersion-Strengthened
OECD	Organisation for Economic Co-operation and Development
ORELA	Oak Ridge Electron Linear Accelerator
ORNL	Oak Ridge National Laboratory

P

pcm	Percent Millirho
PCT	Product Consistency Test
PI	Principal Investigator
PIV	Particle Image Velocimeter
Pm	Promethium
PMR	Prismatic Modular Reactor
Pu	Plutonium
PWR	Pressurized Water Reactor

R

R&D	Research and Development
RCH	Rotating Cylinder Hull
RD&D	Research, Development and Demonstration
ROK	Republic of Korea
RPCM	Resonance Parameter Covariance Matrix

S

s	Second(s)
S	Sulfur
SAGD	Steam Assisted Gravity Drainage
SAP	Silicon-Aluminum-Phosphate
SCC	Stress-Corrosion Cracking
SEM	Scanning Electron Microscope/Microscopy
SFR	Sodium-Cooled Fast Reactor
SiC	Silicon Carbide
SIMS	Secondary Ion Mass Spectrometry
Sm	Samarium
SMR	Small Modular Reactor
Sn	Tin
SND	Standard Neutron Detector
SOEC	Solid Oxide Electrolysis Cell
SOFC	Solid Oxide Fuel Cell
SRO	Short-Range Ordering

T

Ta	Tantalum
TEM	Transmission Electron Microscope/Microscopy
TKE	Total Kinetic Energy
Ti	Titanium
TRISO	Tristructural-Isotropic
TRU	Transuranic

U

U	Uranium
UFG	Ultrafine-Grained
URL	Underground Research Laboratory

V

VERDI	Velocity for Direct Particle Identification
VHTCR	Very High-Temperature Reactor Critical Assembly
VHTR	Very High-Temperature (Gas-Cooled) Reactor

W

WKB	Wentzel-Kramers-Brillouin
WNR	Weapons Neutron Research (facility)
wt%	Weight Percent

X

XRD	X-ray Diffraction
-----	-------------------

Y

Y	Yttrium
---	---------

Z

ZIT	Zinc/Titanium
ZPPR	Zero Power Plutonium Reactor
Zr	Zirconium



The background image shows a coastal industrial facility at night. A large white bridge spans the water in the upper left. In the foreground, a beach with scattered rocks is visible, reflecting the warm lights from the industrial buildings. The buildings are illuminated with numerous bright lights, and a road or walkway leads towards them. In the distance, a range of hills or mountains is visible under a dark sky.

Appendix II: Index of I-NERI Projects

2007

- 2007-004-K** Development and Characterization of New High-Level Waste Forms for Achieving Waste Minimization from Pyroprocessing

2008

- 2008-001-C** Upgrading of the Athabasca Oil Sands for the Production of Diesel and Gasoline
- 2008-001-K** Advanced Multi-Physics Simulation Capability for Very High-Temperature Gas-Cooled Reactors
- 2008-002-K** Experimental and Analytic Study on the Core Bypass Flow in a Very High-Temperature Reactor
- 2008-003-K** Nuclear Data Uncertainty Analyses to Support Advanced Fuel Cycle Development

2009

- 2009-001-K** ZPPR-15 and BFS Critical Experiments Analysis for Generation of Physics Validation Database of Metallic-Fueled Fast Reactor Systems
- 2009-002-K** Enhanced Radiation Resistance Through Interface Modification of Nanostructured Steels for Gen IV In-Core Applications

2010

- 2010-001-E** Measurements of Fission Fragment Mass Distributions and Prompt Neutron Emission as a Function of Incident Neutron Energy for Major and Minor Actinides
- 2010-002-E** Spherical Particle Technology Research for Advanced Nuclear Fuel/Target Applications
- 2010-003-E** Irradiation and Testing of Advanced Oxide Dispersion-Strengthened and Ferritic-Martensitic Steels
- 2010-004-E** Development of a Standard Neutron Detector for the Energy Range up to 20 MeV and Its Application
- 2010-005-E** Interoperability of Material Databases
- 2010-006-E** State-of-the-Art Post-Irradiation Examination of Advanced Nuclear Fuels
- 2010-001-K** Investigation of Electrochemical Recovery of Zirconium from Spent Nuclear Fuels

- 2010-002-K** Science-Based Approach to Nickel Alloy Aging and Its Effect on Cracking in Pressurized Water Reactors
- 2010-003-K** Low-Loss Advanced Metallic Fuel Casting Evaluation
- 2010-004-K** Development and Characterization of Nanoparticle-Strengthened Dual-Phase Alloys for High-Temperature Nuclear Reactor Applications

2011

- 2011-001-E** Development of a 2E-2V Instrument for Fission Fragment Research
- 2011-001-K** Atomic Ordering in Alloy 690 and Its Effect on Long-Term Structural Stability and Stress-Corrosion Cracking Susceptibility
- 2011-002-K** Development of Microcharacterization Techniques for Nuclear Materials
- 2011-003-K** Verification and Validation of High-Fidelity Multi-Physics Simulation Codes for Advanced Nuclear Reactors
- 2011-004-K** Development of Diagnostics and Prognostics Methods for Sustainability of Nuclear Power Plant Safety Critical Functions
- 2011-005-K** Fully Ceramic Microencapsulated Replacement Fuel for Light Water Reactor Sustainability

